MEHTOD FOR IMPROVING THERMODYNAMIC PERFORMANCE OF VAPOUR COMPRESSION REFRIGERATION SYSTEM UGING NANOFLUID

A Major Dissertation submitted

in partial fulfillment of the requirements for the award of the degree of

Master of Technology

In

Thermal Engineering

By

Rahul Kumar Jaiswal

Roll No. **2K12/THE/28**

Session **2012-15**

Under the Guidance of

Prof. Dr.R.S.Mishra

Department of Mechanical Engineering

Delhi Technological University

Delhi-110 042

STUDENT'S DECLARATION

I hereby certify that the work which is being presented in the manor project entitled **"MEHTOD FOR IMPROVING THERMODYNAMIC PERFORMANCE OF VAPOUR COMPRESSION REFRIGERATION SYSTEM UGING NANOFLUID"** in partial fulfillment of the requirements for the award of the degree of Master of Engineering in Thermal Engineering, submitted to the Department of Mechanical Engineering, is an authentic record of my own work carried under the supervision of Prof. Dr.R.S.Mishra Department of Mechanical Engineering , Delhi Technological University, Delhi.

I have not submitted the matter embodied in this major project as whole or in part, for the award of any other degree.

Rahul Kumar Jaiswal
Roll No. 2K12/THE/28
M.Tech.(Thermal Engg.)
Session 2012-15

Date: _____

CERTIFICATE

This is to certify that the Major Project Thesis entitled "**MEHTOD FOR IMPROVING THERMODYNAMIC PERFORMANCE OF VAPOUR COMPRESSION REFRIGERATION SYSTEM UGING NANOFLUID**" which is being submitted by Shri RAHUL KUMAR JAISWAL, is the authentic record of student's own work carried by him out under my guidance and supervision for partial fulfillment of the award of the degree of Master of Technology in Thermal Engineering, Department of Mechanical Engineering, Delhi Technological University, Delhi.

Prof. Dr.R.S.Mishra

Professor

Department of Mechanical Engineering

Delhi Technological University, Delhi

ACKNOWLEDGEMENT

It is distinct pleasure to express my deep sense of gratitude and indebtedness to my learned supervisor Prof Dr. R.S.Mishra, Department of Mechanical Engineering, Delhi Technological University, Delhi, for his invaluable guidance, encouragement and patient review. His continuous inspiration only has made me complete this major project.

I am again thankful to Prof Dr. R.S.Mishra, Department of Mechanical Engineering, Delhi Technological University, Delhi, for his kind approval for the equipment and infrastructure required for completion of this project and the input provided about the topic during his theory lecture in the previous semester.

I am thankful to my family members, all teachers, classmates and friends for their unconditional support and motivation during this project. It is a great opportunity for me to extend my heartiest felt gratitude to everybody who helped me throughout the course of this minor project in anyway.

Rahul Kumar Jaiswal
Roll No. 2K12/THE/28
M.Tech. (Thermal Engg.)
Session 2012-15

ABSTRACT

In this research nanoparticle based refrigerant has been used to increase the heat transfer performance of base refrigerant in the vapour compression refrigeration system. Many types of solid and oxide materials could be used as the nanoparticles to be suspended into the conventional/non conventional refrigerants. In this project work, the effect of the suspended copper oxide (CuO), Titanium Oxide (TiO_2), Aluminum Oxide (Al_2O_3), into the eco friendly refrigerant (i.e. R134a, R407c and R404A) is used for enhancing the thermal performance of vapour compression refrigeration system. Comparison was made between utility of eco friendly refrigerant mixed with nanoparticle and used in the primary circuit of VCRS. That eco friendly nanorefrigerant is used in primary circuit of VCRS along with mixing of nanoparticle with R718 in the secondary evaporator circuit. The performance of VCRS is evaluated using (i) pure refrigerant (w/o nano particle) in the primary circuit and R718 in the secondary circuit (ii) Eco friendly refrigerant in primary circuit and nanofluid (nanoparticle mixed with R718 in the evaporator secondary circuit (iii) nanorefrigerant (nanoparticle mixed into pure refrigerant) in primary circuit and R718 in secondary circuit of VCRS. Experiment was conducted to verify theoretically computed value and it was observed that the experimental value matches well with theoretical calculated value of VCRS for case (i) as mentioned above. Computational simulation was also carried out to compare for above mentioned three cases and it was observed that the performance enhancement is ranging between 8 to 19 % for case(ii) with different types of nanoparticle while for case (iii) the enhancement value ranges between 2.6 to 35 % with different types of nanoparticle.

CONTENTS

LIST OF TABLES

LIST OF FIGURES

NOMENCLATURE USED

COP	Coefficient of performance
COPt	Global coefficient of performance
Cp	Specific heat (J/kg K)
D	Diameter (m)
h	Specific enthalpy (J/kg)
k	Thermal conductivity (W/m K)
L	Length (m)
M	Mass flow rate (kg/s)
N	Compressor speed (r.p.m.)
P	Power consumption (W)
p	Pressure (Pa)
Q	Volumetric rate of flow (m3/s)
q	Heat transfer rate (W)
q”	Heat Flux (W/m2)
r	Radius (m)
S	Area (m2)
T	Temperature (K)
t	Time (s)
U	Overall heat transfer coefficient (W/m2 K)
VG	Geometric compressor volume (m3)
v	Velocity (m/s)
x	Refrigerant quality
X n,o	nanoparticle/oil suspension concentration

Suffixes

air	Environment
avg	Brine/nanofluid
C	Compressor
e	Evaporation
i	Inner
in	Input
k	Condensation
l	Liquid
M	Metal
o	Outer
out	Output
r	Refrigerant

sat	Saturated
V	Vapor
w	Water
nf	Nanofluid
m	Base fluid
p	Nanoparticle
ϕ	volume fraction
n	nanoparticle
o	Lubricating oil
f	Saturated liquid
G	Saturated vapour
nb	Nucleate boiling
wn	Nanoparticle concentration in nanoparticle oil suspension

Greek symbols

α	Heat transfer coefficient (W/m^2 K)
λ	Phase change latent heat (J/kg)
μ	Dynamic viscosity (Pa s)
η_v	Compressor volumetric efficiency
η_{is}	Compressor isentropic efficiency
η_G	Global electromechanical compressor efficiency
ρ	Density (kg/m^3)
σ	Surface tension (N/m)

CHAPTER 1

INTRODUCTION

1.1 Introduction of Nanofluid

Ultrahigh-performance cooling is one of the most vital needs of many industrial technologies. However, inherently low thermal conductivity is a primary limitation in developing energy-efficient heat transfer fluids that are required for ultrahigh-performance cooling. Modern nanotechnology can produce metallic or nonmetallic particles of nanometer dimensions. Nanomaterials have unique mechanical, optical, electrical, magnetic, and thermal properties. Nanofluids are engineered by suspending nanoparticles with average sizes below 100 nm in traditional heat transfer fluids such as water, oil, refrigerant and ethylene glycol. A very small amount of guest nanoparticles, when dispersed uniformly and suspended stably in host fluids, can provide dramatic improvements in the thermal properties of host fluids. Nanofluids (nanoparticle fluid suspensions) is the term coined by Choi [1] to describe this new class of nanotechnology-based heat transfer fluids that exhibit thermal properties superior to those of their host fluids or conventional particle fluids suspensions.

Nanofluid technology, a new interdisciplinary field of great importance where nanoscience, nanotechnology, and thermal engineering meet, has developed largely over the past decade. The goal of nanofluids is to achieve the highest possible thermal properties at the smallest possible concentrations (preferably <1% by volume) by uniform dispersion and stable suspension of nanoparticles (preferably <10 nm) in host fluids. To achieve this goal it is vital to understand how nanoparticles enhance energy transport in liquids. Since Choi [1] conceived the novel concept of nanofluids in the spring of 1993, talented and studious thermal scientists and engineers in the rapidly growing nanofluids community have made scientific breakthrough not only in discovering unexpected thermal properties of nanofluids, but also in proposing new mechanisms behind enhanced thermal properties of nanofluids, developing unconventional models of nanofluids, and identifying unusual opportunities to develop next-generation coolants such as smart coolants for computers, Industrial appliances and safe coolants for nuclear reactors. As a result, the research topic of nanofluids has been receiving increased attention worldwide. The recent growth of work in this rapidly

Emerging area of nanofluids is most evident from the exponentially increasing number of publications.

1.2 Utility of nanofluid

Heat transfer is one of the most important processes in many industrial and consumer products. The inherently poor thermal conductivity of conventional fluids puts a fundamental limit on heat transfer. Therefore, for more than a century since Maxwell [2], scientists and engineers have made great efforts to break this fundamental limit by dispersing millimeter- or micrometer-sized particles in liquids. However, the major problem with the use of such large particles is the rapid settling of these particles in fluids. Because extended surface technology has already been adapted to its limits in the designs of thermal management systems, technologies with the potential to improve a fluid's thermal properties are of great interest once again. The concept and emergence of nanofluids is related directly to trends in miniaturization and nanotechnology. Maxwell's concept is old, but what is new and innovative in the concept of nanofluids is the idea that particle size is of primary importance in developing stable and highly conductive nanofluids.

1.3 Development of the concept of nanofluid

In the development of energy-efficient heat transfer fluids, the thermal conductivity of the heat transfer fluids plays a vital role. Despite considerable previous research and development efforts on heat transfer enhancement, major improvements in cooling capabilities have been constrained because traditional heat transfer fluids used in today's thermal management systems, such as water, oils, and ethylene glycol, have low thermal conductivities, also pure refrigerant orders-of-magnitude smaller than those of most solids. Due to increasing global competition, a number of industries have a strong need to develop advanced heat transfer fluids with significantly higher thermal conductivities than are presently available. It is well known that at room temperature, metals in solid form have orders of magnitude higher thermal conductivities than those

of fluids. For example, the thermal conductivity of copper at room temperature is about 700 times greater than that of water and about 3000 times greater than that of engine oil, as shown in Table 1.1. The thermal conductivity of metallic liquids is much greater than that of nonmetallic liquids. Therefore, the thermal

Conductivities of fluids that contain suspended solid metallic particles could be expected to be significantly higher than those of conventional heat transfer fluids.

Table 1.1 Thermal Conductivity of Various Materials

Type	Material	Thermal conductivity (W/m.K)
Metallic solids	Silver	429
	Copper	401
	Aluminum	237
Nonmetallic solids	Diamond	3300
	Carbon nanotube	3000
	Silicon	148
	Alumina (Al_2O_3)	40
Metallic liquids	Sodium at 644 K	72.3
Nonmetallic liquids	Water	0.613
	Ethylene glycol	0.253
	Engine oil	0.145

Note:- All the property of nanoparticle is taken at 300 K unless mentioned.

Modern nanotechnology has enabled the production of metallic or nonmetallic nanoparticles with average crystallite sizes below 100 nm. The mechanical, optical, electrical, magnetic, and thermal properties of nanoparticles are superior to those of conventional bulk materials with coarse grain structures. Recognizing an excellent opportunity to apply nanotechnology to thermal engineering, Choi conceived the novel concept of nanofluids by hypothesizing that it is possible to break down these century-old technical barriers by exploiting the unique properties of nanoparticles. Nanofluids are a new class of nanotechnology-based heat transfer fluids engineered by dispersing nanometer-sized particles with typical length scales on the order of 1 to 100 nm (preferably, smaller than 10 nm in diameter) in traditional heat transfer fluids. At the 1995 annual winter meeting of the American Society of Mechanical Engineers (Choi,

1995) Choi presented the remarkable possibility of doubling the convection heat transfer coefficients using ultrahigh-conductivity nanofluids instead of increasing pumping power by a factor of 10.

1.4 Importance of Nanosize

As noted above the basic concept of dispersing solids in fluids to enhance thermal conductivity is not new; it can be traced back to Maxwell. Solid particles are added because they conduct heat much better than do liquids. The major problem with the use of large particles is the rapid settling of these particles in fluids. Other problems are abrasion and clogging. These problems are highly undesirable for many practical cooling applications. Nanofluids have pioneered in overcoming these problems by stably suspending in fluids nanometer-sized particles instead of millimeter- or micrometer-sized particles. Compared with microparticles, nanoparticles stay suspended much longer and possess a much higher surface area. The surface/volume ratio of nanoparticles is 1000 times larger than that of microparticles. The high surface area of nanoparticles enhances the heat conduction of nanofluids since heat transfer occurs on the surface of the particle. The number of atoms present on the surface of nanoparticles, as opposed to the interior, is very large. Therefore, these unique properties of nanoparticles can be exploited to develop nanofluids with an unprecedented combination of the two features most highly desired for heat transfer systems: extreme stability and ultrahigh thermal conductivity. Furthermore, because nanoparticles are so small, they may reduce erosion and clogging dramatically. Other benefits envisioned for nanofluids include decreased demand for pumping power, reduced inventory of heat transfer fluid, and significant energy savings.

Because the key building block of nanofluids is nanoparticles (1000 times smaller than microparticles), the development of nanofluids became possible simply because of the advent of nanotechnology in general and the availability of nanoparticles in particular. Researchers in nanofluids exploit the unique properties of these tiny nanoparticles to develop stable and high-thermal-conductivity heat transfer fluids. Stable suspension of

small quantities of tiny particles makes conventional heat transfer fluids cool faster and thermal management systems smaller and lighter.

It should be noted that in today's science and technology, size matters. Size is also an important physical variable in nanofluids because it can be used to tailor nanofluid thermal properties as well as the suspension stability of nanoparticles. Maxwell's concept is old, but what is new and innovative with the concept of nanofluids is the idea of using nanometer-sized particles (which have become available to investigators as well as commercially only recently) to create stable and highly conductive suspensions, primarily for suspension stability (gravity is negligible) and for dynamic thermal interactions.

1.5 Making of Nanofluid

Materials for base fluids and nanoparticles are diverse. Stable and highly conductive Nanofluids are produced by one- and two-step production methods. Both approaches to creating nanoparticle suspensions suffer from agglomeration of nanoparticles, which is a key issue in all technology involving nanopowders. Therefore, synthesis and suspension of nearly non agglomerated or mono dispersed nanoparticles in liquids is the key to significant enhancement in the thermal properties of nanofluids.

1.5.1. Material for Nanoparticles and Fluids

Modern fabrication technology provides great opportunities to process materials actively at nanometer scales. Nano structured or nanophase materials are made of nanometer-sized substances engineered on the atomic or molecular scale to produce either new or enhanced physical properties not exhibited by conventional bulk solids. All physical mechanisms have a critical length scale below which the physical properties of materials are changed. Therefore, particles smaller than 100 nm exhibit properties different from those of conventional solids. The noble properties of nanophase materials come from the relatively high surface area/volume ratio, which is due to the high proportion of constituent atoms residing at the grain boundaries. The thermal, mechanical, optical, magnetic, and electrical properties of nanophase materials are

superior to those of conventional materials with coarse grain structures. Consequently, research and development investigation of nanophase materials has drawn considerable attention from both material scientists and engineers.

Nanoparticle material types

Nanoparticles used in nanofluids have been made of various materials, such as oxide ceramics (Al_2O_3, CuO), nitride ceramics (AlN, SiN), carbide ceramics (SiC, TiC), metals (Cu, Ag, Au), semiconductors (TiO_2,SiC), carbon nanotubes, and composite materials such as alloyed nanoparticles $Al_{70}Cu_{30}$ or nanoparticle core–polymer shell composites. In addition to nonmetallic, metallic, and other materials for nanoparticles, completely new materials and structures, such as materials "doped" with molecules in their solid–liquid interface structure, may also have desirable characteristics. 30

Host liquid types

Many types of liquids, such as water, ethylene glycol, refrigerant and oil, have been used as host liquids in nanofluids.

1.5.2. Method of Nanoparticle Manufacture

Fabrication of nanoparticles can be classified into two broad categories: physical Processes and chemical processes Kimoto [3]. Currently, a number of methods exist for the manufacture of nanoparticles. Typical physical methods include inert-gas condensation (IGC), developed by Granqvist and Buhrman (1976), and mechanical grinding. Chemical methods include chemical vapor deposition (CVD), chemical precipitation, micro emulsions, thermal spray, and spray pyrolysis. The current processes for making metal nanoparticles include IGC, mechanical milling, chemical precipitation, thermal spray, and spray pyrolysis.

1.5.3 Dispersion of Nanoparticles in Liquids

Stable suspensions of nanoparticles in conventional heat transfer fluids are produced by two methods, the two-step technique and the single-step technique. The two-step method first makes nanoparticles using one of the above-described nanoparticle

processing techniques and then disperses them into base fluids. The *single-step method* simultaneously makes and disperses nanoparticles directly into base fluids. In either case, a well-mixed and uniformly dispersed nanofluid is needed for successful production or reproduction of enhanced properties and interpretation of experimental data. For nanofluids prepared by the two-step method, dispersion techniques such as high shear and ultrasound can be used to create various particle–fluid combinations.

Most nanofluids containing oxide nanoparticles and carbon nanotubes reported in the open literature are produced by the two-step process. If nanoparticles are produced in dry powder form, some agglomeration of individual nanoparticles may occur due to strong attractive Van Der Waals forces between nanoparticles. This undesirable agglomeration is a key issue in all technology involving making nanofluids using the two-step processes has remained a challenge because individual particles quickly agglomerate before dispersion, and nanoparticle agglomerates settle out in the liquids. Well-dispersed stable nanoparticle suspensions are produced by fully separating nanoparticle agglomerates into individual nanoparticles in a host liquid. In most nanofluids prepared by the two-step process, the agglomerates are not fully separated, so nanoparticles are dispersed only partially. Although nanoparticles are dispersed ultrasonically in liquid using a bath or tip sonicator with intermittent sonication time to control overheating of nanofluids, this two-step preparation process produces significantly poor dispersion quality. Because the dispersion quality is poor, the conductivity of the nanofluids is low. Therefore, the key to success in achieving significant enhancement in the thermal properties of nanofluids is to produce and suspend nearly mono dispersed or nonagglomerated nanoparticles in liquids.

A promising technique for producing nonagglomerating nanoparticles involves

Condensing nanophase powders from the vapor phase directly into a flowing

Low-vapor-pressure fluid. . The direct evaporation–condensation process yielded a uniform distribution of nanoparticles in a host liquid.

1.6 Synthesis of Nanofluid

There are several factors of interest when considering a given synthetic approach such as nanoparticle material, concentration size and shape of nanoparticle in base fluid, all these parameter play major role in design and synthesis of nanofluid. The complex correlation between all these parameter on the performance of nanofluid in shown in Fig. 1.1. Here we can see that all parameter for example when we increase the concentration of nanoparticle in base fluid the all 4 thermo physical of nanofluid will be change.

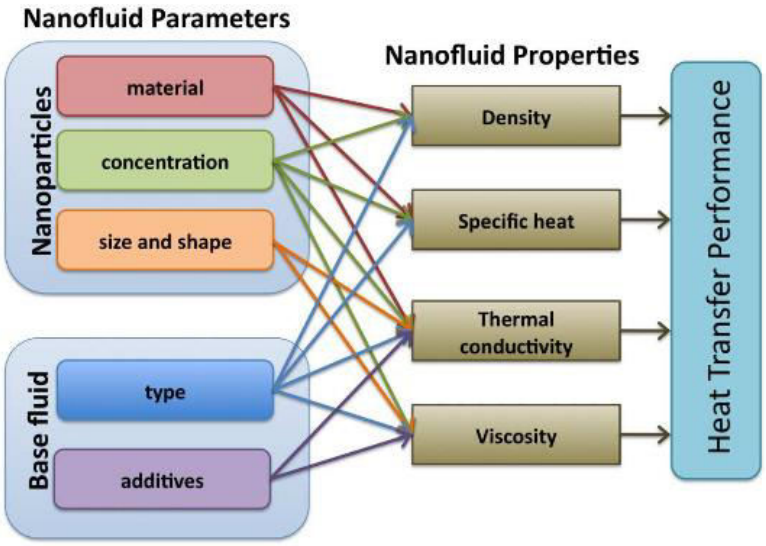

Fig. 1.1 Complexity and multi-variability of nanoparticle suspensions

1.7 Application of nanofluid

Nanofluids are a new type of heat transfer fluid engineered by uniform and stable suspension of nanometer-sized particles into liquids. Most nanofluids are very dilute suspensions of nanoparticles in liquids and contain a very small quantity, preferably less than 1% by volume, of nanoparticles. The average size of nanoparticles used in nanofluids may vary from 1 to 100 nm (preferably <10 nm). Because nanoparticles are

so small, they remain in suspension almost indefinitely and dramatically reduce erosion and clogging compared with the suspension of larger particles. Also, their larger surface area may improve heat transfer. Due to these dramatically thermal properties of nanofluid there are many application of nanofluid have been justified till now. Some of these are given below.

1.7.1 Cooling application

Crystal Silicon Mirror Cooling

One of the first applications of research in the field of nanofluids is for developing an advanced cooling technology to cool crystal silicon mirrors used in high-intensity x-ray . Because an x-ray beam creates tremendous heat as it bounces off a mirror, cooling rates of 2000 to 3000 W/cm^2 should be achievable with the

Advanced cooling technology. Lee and Choi carried out analysis to estimate the performance of microchannel heat exchangers with water, liquid nitrogen, and nanofluids as the working fluid. For an optimized channel width that minimizes the thermal resistance of a microchannel heat exchanger, performance of a nanofluid-cooled microchannel heat exchanger has been compared with that of water-cooled and liquid-nitrogen-cooled microchannel heat exchangers. The results show that nanofluids can remarkably reduce the thermal resistances and increase the power densities, so they demonstrated the superiority of a nanofluid-cooled silicon microchannel heat exchanger. The benefits of using nanofluids as a room-temperature coolant are clear, including dramatic enhancement of cooling rates while operating the advanced cooling system at room temperature.

Electronic cooling

Many of researcher used gold nanofluids as the working fluid for a conventional meshed circular heat pipe. Monodispersed gold nanoparticles of various sizes (2 to 35 and 15 to 75 nm) were synthesized by the reduction of aqueous hydrogen tetra chloroaurate ($HAuCl_4$) with tri sodium citrate and tannic acid. The heat pipe was designed as a heat spreader for a CPU in a notebook or desktop PC. A 200-mesh wire screen was used in

the heat pipe being tested. They measured the thermal resistance of the meshed heat pipe with nanofluids and DI water. The thermal resistance of the meshed heat pipe with nanofluids is in the range 0.17 to 0.215° C/W, lower than that with DI water. The results show that at the same charge volume, there is a significant reduction (by as much as 37%) in the thermal resistance of heat pipe with nanofluid compared with DI water.The results also show that the thermal resistance of a vertical meshed heat pipe varies with the size of gold nanoparticles and that monodispersed nanoparticles are better than aggregated nanoparticles. The work clearly shows the advantages of a *conventional* circular heat pipe with nanofluids over that with DI water.

Vehicle cooling

Many researcher have been studied the suspension of nanoparticle into the radiator of vehicle and found that by using of nanofluid in radiator coolant we can enhance the fluid heat transfer property of and so that efficient cooling of vehicle engine may be possible. Also some experiment has been done for rotary blade coupling (RBC) of a power transmission system of a real-time four-wheel-drive vehicle. It adopts advanced RBC, where a high local temperature occurs easily at high rotating speed. RBC design is so precise that if the local temperature is higher than 266°F, excessive thermal stress may damage its rotating components. As a result, the power cannot be transmitted to the rear wheels, affecting vehicle performance severely. Moreover, the damaged RBC is not repairable and should be replaced. Therefore, it is imperative to improve the heat transfer efficiency to contain excessive thermal stress on the components of the power transmission system. Experiment result show the temperature distribution of the RBC exterior at four different rotating speeds (400, 800, 1200, and 1600 rpm), simulating the conditions of a real car at various rotating speeds. The results show that CuO nanofluids have the lowest temperature distribution at both high and low rotating speed and accordingly, the best heat transfer effect.

Transformer Cooling

The power generation industry is interested in transformer cooling application of nanofluids for reducing transformer size and weight. The ever-growing demand for

greater electricity production will require upgrades of most transformers at some point in the near future at a potential cost of millions of dollars in hardware retrofits. If the heat transfer capability of existing transformers can be increased, many of the upgrades may not be necessary the heat transfer properties of transformer oils can be improved by using nanoparticle additives The increased thermal transport of transformer oils translates into either a reduction in the size of new transformers at the same level of power transmitted or an increase in the performance of existing transformers. Keeping at the cutting edge of nanotechnology remains a top task for many companies and laboratories. Specifically, nanofluid-based transformer oil is likely to be the next-generation cooling fluid in transformers. The first key element in nanofluid technology is uniform dispersion of nonagglomerated nanoparticles. Homogeneity of the dispersion may be overcome by special mechanical dispersing techniques and the creative use of chemical dispersants. However, this goal is still challenging.

Space and Nuclear System Cooling

The ability to greatly increase the CHF, the upper heat flux limit in nucleate boiling systems, is of paramount practical importance to ultrahigh-heat-flux devices that use nucleate boiling, such as high-power lasers and nuclear reactor components. Therefore, nanofluids have opened up exciting possibilities for raising chip power in electronic devices or simplifying cooling requirements for space applications. Most of all, leading nuclear researchers are very much interested in the use of nanofluids with dramatically increased CHF values because it could enable very safe operation of commercial or military nuclear reactors.

Defense Applications

A number of military devices and systems, such as high powered military electronics, military vehicle components, radars, and lasers, require high-heat-flux cooling, to the level of thousands of W/cm^2. At this level, cooling with conventional heat transfer fluids is difficult. Some specific examples of potential military applications include power electronics and directed-energy weapons cooling. Since directed-energy weapons involve heat sources with high heat fluxes (>500 to 1000 W/cm^2), cooling of the direct-

energy weapon and associated power electronics is critical and is further complicated by the limited capability of current heat transfer fluids. Nanofluids also provide advanced cooling technology for military vehicles, submarines, and high-power laser diodes.
It appears that nanofluid research for defense applications considers multifunctional nanofluids with added thermal energy storage or energy harvesting through chemical reactions.

1.7.2 Tribological Applications

Nanofluid technology can help develop better oils and lubricants. Recent nanofluid Activity involves the use of nanoparticles in lubricants to enhance tribological properties of lubricants, such as load-carrying capacity and antiwear and friction-reducing properties between moving mechanical components. In lubrication application it has been reported that surface-modified nanoparticles stably dispersed in mineral oils are very effective in reducing wear and enhancing load-carrying capacity.

1.7.3 Biomedical Applications

Nanofluids was originally developed primarily for thermal management applications such as engine, microelectronics, and photonics. However, nanofluids can be formulated for a variety of other uses for faster cooling. Nanofluids are now being developed for medical applications, including cancer therapy. Traditional cancer treatment methods have significant side effects. Iron-based nanoparticles can be used as delivery vehicles for drugs or radiation without damaging nearby healthy tissue by guiding the particles up the bloodstream to a tumor with magnets. Nanofluids could also be used for safer surgery by cooling around the surgical region, thereby enhancing a patient's chance of survival and reducing the risk of organ damage.

Other possible areas for the application of nanofluids technology include cooling a new class of super powerful and small computers and other electronic devices for use in military systems, airplanes, or spacecraft as well as for large-scale cooling. In the future, nanofluids could be used to maintain a high temperature gradient in thermoelectric that

would convert waste heat to useful electrical energy. In buildings, nanofluids could increase energy efficiency without the need to use a more powerful pump, so saving energy in a HVAC system and providing major environmental benefits. In the renewable energy industry, nanofluids could be utilized to enhance heat transfer from solar collectors to storage tanks and to increase the energy density. To this must be added cooling for major process industries, including materials, chemical, food and drink, oil and gas, paper and printing, and textiles.

1.8 Vapor Compression Refrigeration

Vapour compression refrigeration cycle is most commonly used for HVAC system of Automobile, hotel, public buildings, theaters, private residences, and many industrial appliances. Vapour compression refrigeration cycle have four main process as below.

1. Isobaric Expansion
2. Isentropic Compression
3. Isobaric Condensation
4. Throttling (Expansion)

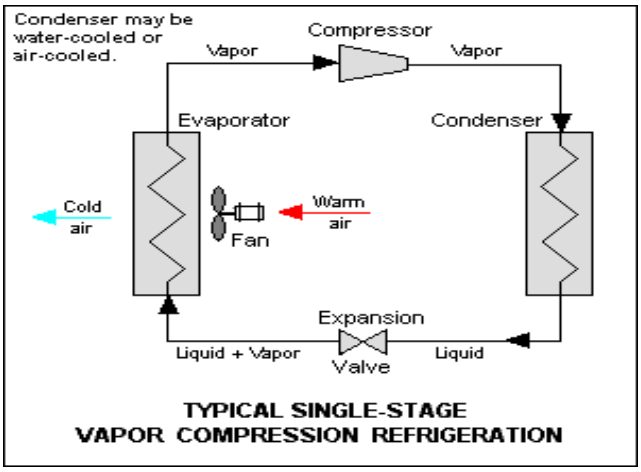

Fig. 1.2 Component of vapour compression cycle (Source www.wikipedia.org)

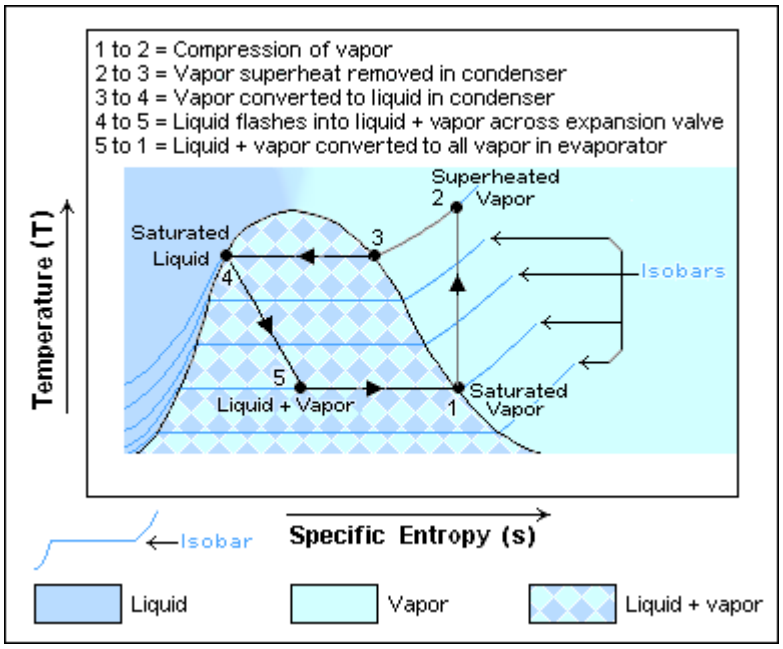

Fig 1.3 Temperature–Entropy diagram of vapour compression cycle
(Source www.wikipedia.org)

As shown in Fig. 1.2 and 1.3 heat absorbed by refrigerant at constant pressure in the evaporator and then refrigerant goes to compressor where isentropic compression takes place and high temperature liquid then goes to condenser and heat rejection takes place at constant pressure in the condenser refrigerant converted in to liquid phase and then throttling (constant enthalpy) process in the expansion device.

Thus heat transfer from low temperature zone to high temperature takes place.

CHAPTER 2

LITERATURE REVIEW AND RESEARCH OBJECTIVES

A few studies have been illustrated as a part of literature review related to theoretical study and experimental investigation of refrigeration systems based on first law and second law analysis with different pairs of refrigerants, nanoparticle behaviour and application of nanofluid in vapour compression refrigeration system.

.Jwo et al. [4] investigated the replacement of polyester lubricant and R-134a refrigerant with mineral lubricant and hydrocarbon refrigerant. The mineral lubricant contains Al_2O_3 nanoparticles to improve the lubrication and performance of heat-transfer. Their studies show that the R-134a at 60% and Al_2O_3 0.1 wt % nanoparticles were optimum .Under these conditions, the consumption of power was reduced by 2.4%, and the C.O.P. was increased by 4.4%.

Peng et al. [5] investigated with an experiment that nucleates boiling heat transfer property of refrigerant/oil mixture containing diamond nano particles. The refrigerant used was R113 and the oil was VG68. They found out that the nucleate pool boiling heat transfer coefficient of R113/oil mixture with diamond nanoparticles is larger than the R113/oil mixture. They also proposed a general correlation for calculating nucleate boiling coefficient heat transfer of mixed refrigerant/oil with nanoparticles, which fully satisfies their experimental results.

Henderson et al. [6] conducted an experimental analysis on the flow boiling heat transfer coefficient of R134a (refrigerant) based nanofluids in a horizontal tube. They found excellent dispersion of CuO nanoparticle with R134a and POE oil and the heat transfer coefficient increases more than 100% over baseline R134a/POE oil results.

Bobbo et al. [7] conducted a study on the influence of dispersion of single wall carbon nanohorns (SWCNH) and Ti_2O_3 on the tribological properties of POE oil together with the effects on the solubility of R134a at different temperatures. They showed that the tribological behavior of the base lubricant can be either improved or worsen by adding nanoparticles. On the other hand the nanoparticle dispersion did not affect significantly the solubility.

Bi et al. ([8] conducted an experimental study on the performance of a domestic refrigerator using Ti_2O_3 -R600a nanorefrigerant as working fluid. They showed that the

Ti_2O_3-R600a system worked normally and efficiently in the refrigerator and an energy saving of 9.6%. They too cited that the freezing velocity of nano refrigerating system was more than that with pure R600a system. The purpose of this article is to report the results obtained from the experimental studies on a vapour compression system.

Lee et al. [9] investigated the friction coefficient of the mineral oil mixed with 0.1 vol.% fullerene nanoparticles, and the results indicated that the friction coefficient decreased by 90% in comparison with raw lubricant, which lead us to the conclusion that nanoparticles can improve the efficiency and reliability of the compressor.

Wang and Xie [10] found that Ti_2O_3 nanoparticles could be used as additives to enhance the solubility between mineral oil and hydrofluorocarbon (HFC) refrigerant. The refrigeration systems using the mixture of R134a and mineral oil appended with nanoparticles Ti_2O_3, posses to give best performance by returning more vol of lubricant oil return to the compressor, and had the similar performance compared to the systems using polyol-ester (POE) and R134a. In the present study the refrigerant selected is R600a and the nanoparticle is alumina. Isobutane (R600a) is more widely adopted in domestic refrigerator because of its better environmental and energy performances. In this paper, a new refrigerator test system was built up according to the National Standard of India. A domestic R600a refrigerator was selected. Al_2O_3-R600a nano-refrigerant was prepared and used as working fluid. The energy consumption test and freeze capacity test were conducted to compare the performance of the refrigerator with nano-refrigerant and pure refrigerant so as to provide the basic data for the application of the nanoparticles in the refrigeration system.

Heris et al.[11] in their experiment they have examined the convective heat transfer coefficient through a circular tube maintaining temperature of tube wall for boundary condition for nanofluids consisting containing Al_2O_3 and CuO oxide nanoparticles in water considering water as a base fluid. In the experiment they have chosen a tube having 6 mm diameter and length 1meter copper tube. Thickness of copper tube is taken 0.5 mm and a another outer stainless steel tube having 32 mm diameter. In their experiment nanofluid flow inside the copper tube and saturated steam in the annuli section of the steel tube makes constant wall temp. The fluid after then

goes to a heat exchanger where water was used for cooling the test chamber. The experimental result concluded that homogeneous model (single phase correlation of nanofluid) was not able to calculate enhancement of coefficient of heat transfer of nanofluid. The experimental result shows that the heat transfer coefficient predicted for CuO/water and Al_2O_3 /water of homogeneous model were very close to each other but when they increase the vol. % concentration of nanoparticle much higher coefficient of heat transfer observed for Al_2O_3 /water. They have concluded that the coefficient of heat transfer of nanofluid depend upon many factor such as nanoparticle diameter and thermal conductivity of nanoparticle, movement of nanoparticle suspension process of nano particle etc.

Y. He et al. [12] conduct an experiment to find out the behavior of nanofluid under laminar and turbulent flow. Their experiment consist a a heating and cooling unit, a flow loop and a measurement unit. The test section consist a straight vertically oriented copper tube having 1834 mm length and 6.35 outer 3.97 mm inner diameter. In the experiment they heated the tube with help of 2 silicon rubber flexible heater. For the constant heat flux condition in the test section they provided a thermally insulated layer. For measurement the pressure drop 2 pressure transducer ware used. They have experimented the effect of Reynolds number nanoparticle size, concentration of nanopraticle in the base fluid. They concluded that suspension of nanoparticle into the host fluid the enhancement of thermal conductivity of base fluid may achieved and as well we go for decreasing particle size and increasing concentration the enhancement increases. Thus the nanoparticle concentration and particle size paly major role in enhancement of thermal conductivity of base fluid in both turbulent and laminator flow. They have also concluded that the pressure drop by using nanofluid were close to the base fluid.

Kulkarni et al., [13] investigated the heat transfer performance also fluid dynamics performance of nanofluids using SiO_2 nanoparticle suspended in the ration of 60:40 weight % in to the EG/water mixture. A test section they have taken for this experiment having copper tube 3.14 mm inside and 4.76 mm outer diameter and 1m length. To measure the wall temperature they fitted 6 no. of thermocouple on surface of

the copper tube along the length, the outlet and inlet temperature measurement they used 2 thermocouple at the outlet and inlet section respectively. To isolate the thermal heat transfer two plastic fitting ware provided at the inlet and outlet section respectively. To obtain the constant heat flux four strip heater were used. The whole test section was insulated with 10 cm fiber glass to reduce the heat loss from the test section to the ambient. To maintain the constant inlet temperature of fluid four shell and tube type heat exchanger with counter flow were used. In their experiment they have investigated the effect of enhancement of convective heat transfer of nanofluid with diameter of nanoparticle 20nm, 50nm and 100nm in the turbulent region by increasing volume fraction of nanoparticle and pressure drop recorded when they increase the concentration of nanoparticle in the nanofluid.

Hwang et al., [14] investigated the convective heat transfer coefficient of Al_2O_3 /water based nanofluid. In their experiment nanofluid considered flowing through circular tube having 1.812 mm inside diameter and maintaining constant heat flux for fully developed laminar regime. Al_2O_3 /water based nanofluids with various volume % concentration 0.01% to 0.3% are manufactured with two-step method. They have also obtained the thermo physical property of nanofluid such as density, viscosity, heat capacity and thermal conductivity. They have concluded that the convective heat transfer coefficient enhancement occurs with 0.01 and 0.3 vol % concentration of nanoparticle in fully developed laminar regime and heat transfer enhancement about 8 % obtained under the same Reynolds number of base fluid. They also concluded that enhancement in heat transfer coefficient were much higher that the thermal conductivity enhancement at the same vol % concentration of nanoparticle.

Sharma et al.,[15] investigated to evaluate friction factor and heat transfer coefficient with a inserted twisted tape in the flow region of tube with Al_2O_3 nanofluid they have consider a test section of L/D ration 160 and 1.5m length. For uniform heating test section were wrapped with 1 KW .The aluminum strip having 0.018mm width and 1mm thick are used. Test section is subjected to 180° twist holding both end of test section in lathe machine obtaining 5, 10 and 15 twist ratio. Their result show enhancement in heat transfer coefficient with Al_2O_3 nanoparticle into the base fluid

compare to the base water. The heat transfer coefficient was 23.7 % higher that the water at Reynolds number 9000.

Yu et al., [16] investigated the heat transfer coefficient of silicon carbide nanoparticle having diameter 170nm and 3.7 vol % suspended into the pure water and found that an increment in heat transfer coefficient about 50-60 % compared to host fluid. Their test section was stainless steel tube with 4.76 mm outside diameter and 2.27 inside diameter. Their test rig have heat exchanger flow meter horizontal tube, pre heater as a closed loop system. They concluded that enhancement is 14-32 % higher that the predicted value for single phase turbulent correlation of heat transfer. Also they found that the pressure loss is little lower than the Al_2O_3 water nanofluid.

Torii and Yang [17] investigated the heat transfer coefficient of suspended diamond nanoparticle into the host fluid by maintaining constant heat flux. Their test section contain a flow loop, a digital flow meter, a pump, a reservoir and a tank. The test is prepared stainless steel tube having 4.3 mm outer diameter 4.0 mm inner diameter and 1000 mm length. The whole is heated with a dc electrode heater considering joule heating. They reported that (i) the heat transfer performance of nanofluid increases with the suspension of diamond nano particle into the water compared to pure water. (ii) Reynols number variation influence the enhancement occurs in heat transfer coefficient.

Rea et al., [18] investigated the heat transfer coefficient and viscous pressure loss for Al_2O_3 /water and zirconia-water nanoparticle based nanofluid flowing loop. The stainless steel vertical heated test section considered having outer diameter of 6.4 mm, an inner diameter of 4.5 mm and 1.01 m length. The test section 8 T type thermocouples sheathed and insulated electrically and soldered onto the outside wall of the tube along axial direction 5, 16, 30,44, 58, 89 and 100 cm from heated inlet section of the test facility. to measure the fluid temperatures Two same T-type thermocouples were inserted into the flowing passage of the channel after and before of the test section. They observed that the heat transfer coefficients increased 17% and 27%, in fully developed region compare to base water. The heat transfer of zirconia–water nanofluid increases by approx 2% at 1.32 vol.% in the inlet region and 3% at 1.32 vol %

in the fully developed region. The observed pressure loss for nanofluids was higher than the base water having good agreement with predicted model for laminar flow.

Murshed et al.[19] carried out experiments with spherical and rod-shaped TiO_2nanoparticles. The spherical particles were 15 nm in diameter and the rod-shaped particles were 10 nm in diameter and 40 nm in length. The base fluid was deionized water. The measurement method was transient hot wire. It should be mentioned here that they used oleic acid and cetyltrimethyl ammonium bromide (CTAB) surfactants (0.01 to 0.02 vol %). They maintained a nearly neutral (pH 6.2 to 6.8) suspension. For the first time, a nonlinear correlation between the volume fraction and conductivity enhancement was observed here at lower concentrations. This is interesting with respect to the temperature effect and pure metallic particles. They found that the conductivity enhancement was higher for rod-shaped particles than for spherical particles. Enhancement up to 29.7% was found with 5% spherical particles and up to 32.8% with rod-shaped particles. They attributed this to the higher shape factor (n =6) of the rods than of the spheres (n =3) in the Hamilton–Crosser [20] model.

Xuan and Li [21] were first to show a significant increase in the turbulent heat transfer coefficient. They found that at fixed velocities, the heat transfer coefficient of nanofluids containing Cu nanoparticles at 2.0 vol% was improved by as high as 40% compared to the host water. The Dittus–Boelter correlation failed to obtain the improved experimented heat transfer behavior of nanofluids. Recent unpublished work shows that the effect of particle size and shape and dispersion becomes predominant in enhancing heat transfer in nanofluids. Even greater heat transfer effects are expected for nanofluids produced by the one-step process. Therefore, there is great potential to “engineer” ultra-energy-efficient heat transfer fluids by choosing the nanoparticle material as well as by controlling particle size, shape, and dispersion.

Mahbubul and Saadah [22] investigated the thermal performance of Al_2O_3/R134a nanorefrigerant C.O.P. of nanorefrigerant increased about 15% and thermal conductivity about 28.8 %, dynamic viscosity about 13.68 % and density of nanorefrigerant about 11 % compare to the pure refrigerant . In their study they have considered uniformly mass flux of nanorefrigerant in a horizontal smooth tube.

Faulkner et al. [23] conducted fully developed laminar convection heat transfer tests and made the startling discovery that water-based nanofluids containing CNTs provide significant enhancements to the overall heat transfer. First, the heat transfer coefficient of the nanofluids increase with Reynolds number. The heat transfer coefficient of the nanofluid were roughly twice those of plain water at the upper end of the Reynolds number range tested, and it appears that this enhancement will continue to increase with larger Reynolds numbers. Second, nanofluids outperform water, but nanofluids with low particle concentrations (1.1 vol %) perform better than those with higher concentrations (2.2 and 4.4 vol%). This is an unexpected and, indeed, counterintuitive result. This negative concentration dependence of the heat transfer enhancement could be due partially to the interaction between particles. Faulkner et al. proposed that the pseudo turbulence induced by rolling and tumbling CNT agglomerates in a microchannel results in micro scale mixing, which enhances the laminar heat transfer coefficient. Since heat transfer applications operate over a wide range of Reynolds numbers and heat fluxes, additional work is needed to develop nanofluids that can provide the most significant benefit to specific heat transfer applications.

Wen and Ding [24] were first to study the laminar entry flow of nanofluids and showed a substantial increase in the heat transfer coefficient of water-based nanofluids containing γ-Al_2O_3 nanoparticles in the entry region and a longer entrance length for the nanofluids than water. Also in 2006 they have studied the laminar entry flow of water-based nanofluids containing multiwalled carbon nanotubes (CNT nanofluids). For nanofluids containing only 0.5 wt% Carbon nano tubes, the maximum convective heat transfer coefficient enhancement reaches above 350% at Re equal to 800. Such a higher enhancement could not be considered purely for thermal conductivity enhancement. They proposed possible mechanisms such as thickness of thermal boundary layer, particle rearrangement, due to the presence of carbon nanotubes, and very high aspect ratio of Carbon nano tubes.

Lee et al. [25]. They measured thermal conductivities of nanofluid at temperatures between 21 and 55°C, and the results were nothing less than miraculous.

Over this small 34° C rise in temperature, the thermal conductivity enhancement was more than three times higher. With Al_2O_3, the enhancement increased from 2% to 10.8% at a 1% particle volume fraction and it went from 9.4% to 24.3% at a 4% particle-volume fraction. The same increase for CuO–water nanofluids was 6.5% to 29% for a 1% particle-volume fraction and 14% to 36% for a 4% particle fraction. This puts the entire phenomenological concept regarding nanofluids completely in perspective. In fact, all the theories proclaimed before this work was published crumpled at this observation because none of them could predict such a strong temperature effect. The other important observation from the preceding result is that at elevated temperatures, neither Al_2O_3 nor CuO-based nanofluids comply with the Hamilton–Crosser model. This is because the model is completely insensitive to temperature variations between 21 and 55°C. This clearly indicates that agreement of the Al_2O_3 nanofluids with the Hamilton–Crosser model.

Joaquin Navarro et al [26] in his investigation performance analysis of vapour compression refrigeration cycle (system) using R1234yf as a replacement of R134a. In their work, they the performance of vapour compression refrigeration system using both the refrigerant R1234yf and R134a with presence of internal heat exchanger also without internal heat exchanger under a large range of operating condition. Experimental result is obtained with varying evaporator temperature and condenser temperature and use of internal heat exchanger. From their result C.O.P and cooling capacity decreased 13 and 6 % respectively when R134a is replaced by R1234yf. However the presence of internal heat exchanger can help to control the reduction about 6 and 2 % respectively. The experimental result agreed with the mathematical analysis of the system considering pressure drop negligible.

2.2 Conclusion from Literature Review and research gap Identified

The study of above literatures and many others not mentioned in the description Concluded that Lots of researches have been done and going on based on the performance evaluation of various metallic/ nonmetallic nanoparticle suspended into the conventional fluid (w/o refrigerant) to enhance the heat transfer property of base fluid. Also some theoretical analysis of suspension of nanoparticle Al_2O_3 in conventional refrigerant has been done. On the other hand the performance of vapour compression cycle based chiller facility using nanorefrigerant yet to be analyzed with different type, concentration and diameter of nanoparticle. Thermal performance of nanorefrigerant (nanoparticle mixed into pure refrigerant) with different type, concentration and diameter of nanoparticle are yet to be analyzed and also performance enhancement of vapour compression refrigeration system using nanofluid (nanoparticle mixed in water) in secondary circuit and eco friendly refrigerant in primary circuit is yet to be analyzed. Also find out the various parameter witch effect the performance enhancement of VCRS.

2.3 Objectives of research

- Thermodynamic analysis of simple vapour compression system using Eco friendly refrigerant without nanoparticle suspension.
- Validation of theoretical result with experimental observation without nanoparticle suspension into pure refrigerant.
- Development of computational model for vapour compression refrigeration system using nanoparticle based nanorefrigerant in the primary circuit of VCRS.
- Development of computational model for vapour compression refrigeration system using nanofluid (nanoparticle mixed with R718) and eco friendly refrigerant (without nanoparticle mixing)in primary circuit.

CHAPTER 3

THERMODYNAMIC MODEL FORMULATION

3.1 Introduction

In this paper to evaluate the performance parameter of VCRS using nanorefrigerent following model and formulation for each component of VCRS is used as shown in following Fig.3.1

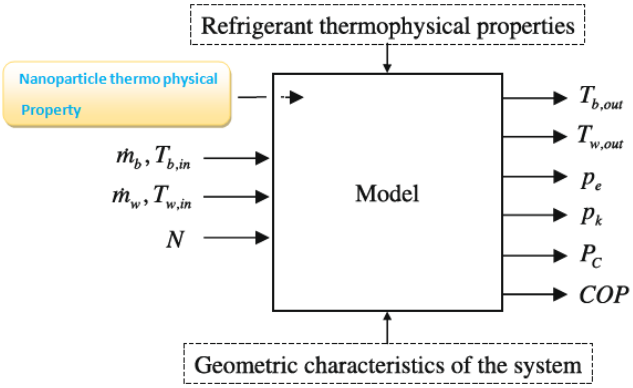

Fig. 3.1. Vapour compression refrigeration system Model

In this model we have taken only five variable and nanoparticle physical property with geometric parameter of the complete system (assumed) as input variable for the VCRS. These variables, together with the thermo physical properties of the refrigerant, nanoparticle and geometric characteristics of the VCRS (vapour compression refrigeration system) are used to obtain the evaporation and condensing pressure and brine, water outlet temp. Power consumption, energy efficiency and exergy efficiency of VCRS. Thus we will be able to evaluate the performance of VCRS by changing the operating parameter on the system performance so that we can optimize the performance of the VCRS.

The Schematic structure of the model proposed for this investigation is presented in Fig. 3.1 where it can be seen that the model input variable are brine inlet temperature in the evaporator, water inlet temperature in the condenser, compressor speed, types of refrigerant, mass flow rate of brine, water and geometric parameter of the heat exchanger (Evaporator and Condenser) and used to evaluate the performance of VCRS

without nanofluid. When we go to compute the performance of VCRS using nano fluid an additional input parameter is required i.e. type of nanoparticle, diameter of nanoparticle, thermo physical property of nanofluid/nanoparticle (thermal conductivity, specific heat, density). The proposed model is basically a VCRS based chiller machine in which two concentric tube (copper) heat exchanger is used for evaporating and condensing operation. In this model refrigerant is supposed to flow in inner side of the evaporator tube and brine in annuli side as shown in fig 3.2. And water flow in inner side of the condenser tube and refrigerant in the annuli side as shown in fig 3.2. The input parameter taken initially to compute the performance of VCRS using nanofluid and without nanofluid is given below.

Input variable	
Type of Refrigerant	R$='R134a',R407c,R404A
RPM of compressor	N=2900 {rpm}
Brine inlet Temperature	Tb_in =25+273.15 {K}
Water inlet Temperature	Tw_in=25+273.15 {K}
Mass flow rate of brine	m_b=0.006 {kg/s}
Mass flow rate of water	m_w=0.006 {kg/s}
Air Temperature	T_air=30+273.15 {K}
Inlet pressure of brine	Pb_in=2{bar}
Inlet pressure of water	Pw_in=2{bar}
Air Pressure	P_air=1.01325 {bar}
Acceleration due to gravity	g=9.81{m/s2}
Ambient Temperature	T_ambient=298{K}
Inside dia. of brine tube in evaporator	D_bie=0.013875 {m}
Inside dia. of refrigerant tube in evaporator	D_rie=0.007525 {m}
Outside dia. of refrigerant tube in evaporator	D_roe=0.009525 {m}
Geometric Parameter	
Inside dia. of brine tube in evaporator	D_bie=0.013875 {m}
Inside dia. of refrigerant tube in evaporator	D_rie=0.007525 {m}
Outside dia. of refrigerant tube in evaporator	D_roe=0.009525 {m}

Length of tube in evaporator	L_e=0.76 {m}
Surface area of evaporator	S_e=3.14*(D_roe)*L_e {m2}
Geometric compressor volume	V_g =5.79E-06 {m3}
Inside dia. of refrigerant tube in condenser 3-4	D_rik=0.013875 {m}
Inside radius of refrigerant tube in condenser 3-4	r_rik=D_rik/2 {m}
Inside dia. of water tube in condenser 3-4	D_wik=0.007525 {m}
outside dia. of water tube in condenser 3-4	{D_wok=0.009525 {m}}
outside radius of water tube in condenser 3-4	r_wok=D_wok/2 {m}
Length of tube in condenser 3-4	L_k=1.05 {m}
outside dia. of water tube in condenser 3-4	D_wok=0.00508 {m}
Surface area of condenser 3-4	S_k=3.14*(D_wok)*L_k {m2}
Inside dia. of refrigerant tube in condenser 2-3	D_ri23=0.007525 {m}
Inside radius of refrigerant tube in condenser 2-3	r_ri23=D_ri23/2 {m}
Outside dia. of refrigerant tube in condenser 2-3	D_ro23=0.009525 {m}
Outside radius of refrigerant tube in condenser 2-3	r_ro23=D_ro23/2 {m}
Length of tube in condenser 2-3	L_23=0.6 {m}
Surface area of condenser 2-3	S_23=3.14*D_ro23*L_23 {m2}
Inside dia. of Capillary Tube	D_cap=0.0006 {m}
Fouling in the tubes	R_TFO=0.000086 {m2 K/W}

Using these inputs and the main characteristics of the compressor and heat exchangers, the model compute the operating pressures (without considering pressure drops), secondary fluids output variables and the energy performance. The property of nanorefrigerant/refrigerant and the thermo-physical properties of secondary fluids are evaluated by using Engineering equation solver *(EES).*

Vapor compression system modeling

The model contain of a set of below equations based on physical laws showing the main parts of the system, as shown Properly (Schematically) in Fig. 3.2.. The

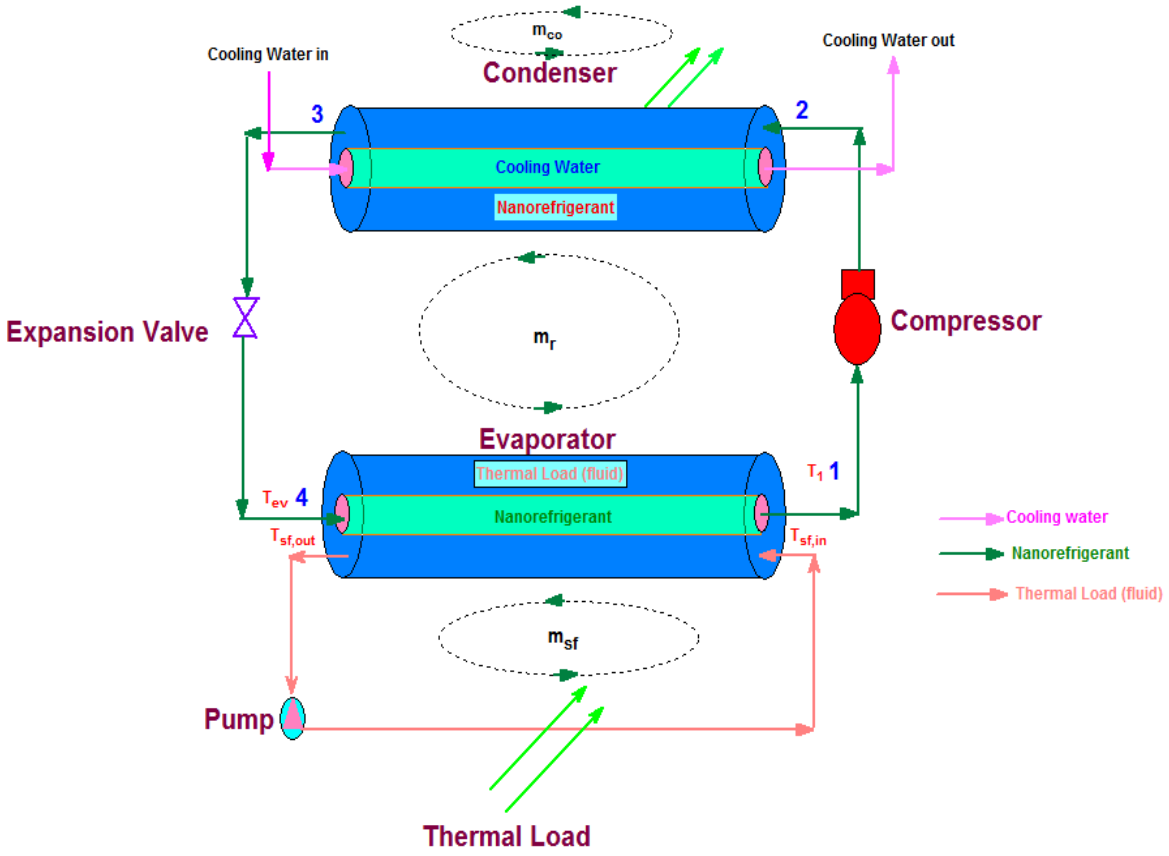

Fig.3.2. Schematic diagram of vapour compression refrigeration system model

Nanorefrigerant/refrigerant states are numbered in Fig. 3.3. To compute nanorefrigerant/refrigerant mass flow rate *(m_r)* Eq. (1) is used, where the compressor volumetric efficiency (η_v) is shown as a function of operating pressure and compressor speed (*N*) as shown in Eq. (2). For simplicity, *(ρ_1)* is the nanorefrigerant/refrigerant density taken is the one corresponding to the saturated condition.

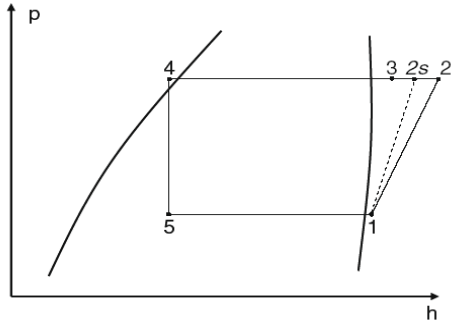

Fig. 3.3. Vapor compression cycle

Vapor at the evaporating pressure and V_g is the geometric compressor volume.

$$m_r = \eta_v \cdot \rho_1 \cdot V_g \cdot N \quad (1)$$

.

$$\eta_v = 1 + C - C \cdot \left[\frac{P_k}{P_e}\right]^{\left[\frac{1}{n_1}\right]} \quad (2)$$

$$C = \frac{V_{suction}}{V_{discharge}}$$

Where,

P_k & P_e is the condenser pressure and evaporator pressure.

$V_{Suction}$ & $V_{Discharge}$ is the suction volume and discharge volume of compressor.

n_1 is the index of expansion.

3.2 Evaporator Formulation

The evaporator is computed with the help of energy balance equation of heat exchanger i.e. Eq. (3)

$$m_r \cdot (h_1 - h_5) = m_b \cdot Cp_b \cdot (Tb_{in} - Tb_{out}) \quad (3)$$

Where, h_1 is enthalpy at state one and h_5 is at state 5 of refrigerant, see Fig. 3.4. Cp_b is the Specific heat of brine. Tb_{in} and Tb_{out} is the inlet and outlet Temperature of the brine.

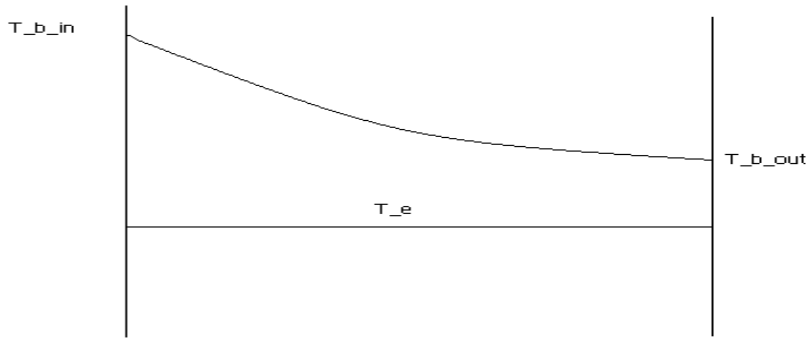

Fig. 3.4 Temperature variation in evaporator

The logarithmic mean temperature difference and global heat transfer coefficient, with LMTD correction factor = 1

$$\dot{m}_r \cdot (h_1 - h_5) = U_e \cdot S_e \cdot \left[\frac{Tb_{in} - T_e - (Tb_{out} - T_e)}{\ln\left(\frac{Tb_{in} - T_e}{Tb_{out} - T_e}\right)} \right] \quad (4)$$

Here, U_e is the global evaporator heat transfer coefficient and S_e is the evaporator surface area. T_e is the evaporator Temperature. The evaporator global heat transfer coefficient *(Ue)* computed using Eq. *(5)* as below.

$$U_e = \frac{1}{r_o} \cdot \left[\frac{1}{\alpha_b \cdot r_o} + \frac{\ln\left(\frac{r_o}{r_i}\right)}{K_M} + \frac{1}{\alpha_{lv} \cdot r_i} + R_{TFO} \right]^{-1} \quad (5)$$

Where,

K_M is metal (copper) thermal conductivity.

r_o & r_i is the inside and outside radius of the copper tube.

α_{lv} is the heat transfer coefficient for the nanorefrigerent/refrigerant.

$R_{T\,Fo}$ is fouling resistance in heat exchanger tube and its value is taken = 0.000086 m^2.

The coefficient of heat transfer for the brine (α_b) is computed using Zukauskas' correlation [27].

$$\alpha_b = \frac{K_b}{D_o} \cdot C_1 \cdot Re_b^{\,m_1} \cdot Pr_b^{\,0.36} \cdot \left[\frac{\mu_b}{\mu_{bM}}\right]^{0.25} \qquad (6)$$

Where,

K_b is the thermal conductivity of brine.

D_O is the outer diameter of copper tube.

Re_b is the Reynold's No. of brine.

Pr_b is the Prandle No. of brine.

C_1 and m_1 is a correlation coefficient and value taken 0.683 and 0.466 respectively.

μ_b viscosity of brine.

μ_{bM} viscosity of brine at metal temperature.

And the refrigerant/nanorefrigerant heat transfer coefficient (α_{lv}) is modeled With the Chen's correlation [28].

$$\alpha_{lv} = sf \cdot \alpha_{nb} + F \cdot \alpha_{conv} \qquad (7)$$

Where,

α_{nb} is the nucleated boiling coefficient taken by Stephan and Abdelsalam[29].

α_{conv} is the convective heat transfer coefficient , obtained using the Dittus–Boelter correlation[30].

sf is the suppression factor.

F is Enhancement factor.

The values of these parameters are obtained using the following equations:

$$\alpha_{nb} = 207 \cdot \frac{K_r}{BD} \cdot \left[\frac{q'' \cdot BD}{K_r \cdot T_e}\right]^{0.674} \cdot \left[\frac{\rho_G}{\rho_{l,r}}\right]^{0.581} \cdot Pr_r^{0.533} \quad (8)$$

$$BD = 0.51 \cdot \left[\frac{2 \cdot \sigma}{g_g \cdot (\rho_{l,r} - \rho_G)}\right]^{0.5}$$

Where,

BD is the bubble departure diameter computed from above equation

σ is the surface tension of refrigerant.

Kr is the thermal conductivity of refrigerant/nanorefrigerant in liquid phase in evaporator.

q" is the heat flux (W/m2) supplied in the evaporator

Te is the evaporator temperature

Prr is the prandle number of the refrigerant in the evaporator

ρ_g & ρ_{Lr} is the density of refrigerant in gas and liquid phase in evaporator.

$$\alpha_{conv} = 0.023 \cdot Re^{0.8} \cdot Pr^{0.4} \cdot \frac{K_L}{D_i} \quad (9)$$

$$sf = 0.927 \cdot \left[\left(\frac{1 - x}{x}\right)^{0.8} \cdot \left(\frac{\rho_G}{\rho_{l,r}}\right)^{0.5}\right]^{0.319}$$

$$F = 53.64 \cdot \left[\frac{q''}{G_r \cdot h_{fg}}\right]^{0.314} \cdot X_{tt}^{-0.839}$$

$$G_r = \rho_r \cdot v_r$$

Where,

D_i is the tube inner diameter.

X_{tt} is the Martinelli's Parameter.

x *or* X_v is the quality of refrigerant.

h_{fg} is the latent heat of evaporation

Gr is mass flux of refrigerant (Kg/m2-s)

Vr is the velocity of nanorefrigerant/refrigerant

$$X_{tt} = \left[\frac{1 - X_v}{X_v}\right]^{0.9} \cdot \left[\frac{\rho_v}{\rho_L}\right]^{0.5} \cdot \left[\frac{\mu_L}{\mu_v}\right]^{0.1}$$

3.3 Compressor Formulation

The compressor performance is computed from the isentropic efficiency *(η_{is})* and the pressures (Low and High) in the compressor. So that , with the help of refrigerant state at the evaporator outlet and the refrigerant state at the compressor discharge is obtained using Eq.*(10)* from the isentropic compression process work and the isentropic efficiency of the compression,

$$h_2 = h_1 + \frac{h_{2s} - h_1}{\eta_{is}} \quad (10)$$

$$\eta_{is} = 0.156323 + 0.0000912 \cdot N + 0.004302 \cdot P_k + 0.09151 \cdot P_e \quad (11)$$

Where, η_{is} is the compression isentropic efficiency and it can be obtained from gathered empirical data, as a function of operating pressures, yielding Eq. *(11):*

To find out compressor power consumption, the model if supposed to use of a global electromechanical efficiency eq. (12) as a function of *N*,

$$\eta_g = 0.00002805 \cdot N^2 + 0.02593961 \cdot N + 6.4965 \quad (12)$$

As in Eq. (2) the efficiencies obtained by Eq. (11) and (12) Show a significant relationship between variables with a satisfactory level of 99%. The correlations used to obtain isentropic and electromechanical efficiency of the compressor in the system, and similar relations must be obtained from experimental results for second compressor. The heat transfer from the refrigerant/nanorefrigerant in the compressor discharge line to the inlet of the condenser has been modeled, due considering the length of that line in the chiller facility, using eq. (13:

$$\dot{m}_r \cdot (h_2 - h_3) = U_{23} \cdot S_{23} \cdot \left[\frac{T_2 - T_{air} - (T_3 - T_{air})}{\ln\left(\frac{T_2 - T_{air}}{T_3 - T_{air}}\right)} \right] \quad (13)$$

U_{23} is the universal heat transfer coefficient used in Eq. (13) is obtained by:

$$U_{23} = \frac{1}{r_o} \cdot \left[\frac{1}{\alpha_i \cdot r_i} + \frac{\ln\left(\frac{r_o}{r_i}\right)}{K_M} + \frac{1}{\alpha_o \cdot r_o} \right]^{-1} \quad (14)$$

With the help of a modified version of the Gnielinski's correlation (14a) for the refrigerant flowing inside the tubes, α_i.

If Re < 10000 then use,

$$\alpha_i = \frac{K_v}{2 \cdot r_i} \cdot \left[\frac{\frac{Fric}{8} \cdot (Re - 1000) \cdot Pr}{1 + 12.7 \cdot \left(\frac{Fric}{8}\right)^{0.5} \cdot (Pr^{(2/3)} - 1)} \right] \cdot \left[\frac{\mu_v}{\mu_{vM}} \right]^{0.11} \quad (14a)$$

Or, If Re >10000 then use,

$$\alpha_i = \left[\frac{K_v}{2 \cdot r_i} \right]^{0.027} \cdot Re^{(4/5)} \cdot Pr^{(1/3)} \cdot \left[\frac{\mu_v}{\mu_{vM}} \right]^{0.14} \quad (14b)$$

Where,

$$Fric = \frac{1}{(0.79 \cdot \ln(Re) - 1.64)^2}$$

and the heat transfer coefficient (natural-convection) is obtained by,

$$\alpha_o = \frac{K_{air}}{D_o} \cdot (Nul^{10} + Nutt^{10})^{\left[\frac{1}{10}\right]} \quad (15)$$

Where,

$$Nul = 2 \cdot \frac{fc}{\ln\left[1 + \frac{2 \cdot fc}{NuT}\right]}$$

$$Nutt = 0.103 \cdot Ra^{(1/3)}$$

Being

$$NuT = 0.7772 \cdot 0.103 \cdot Ra^{0.25}$$

$$F = 1 - \frac{0.13}{NuT^{0.16}}$$

$$Ra = g \cdot \frac{1}{T_{air}} \cdot (T_M - T_{air}) \cdot \frac{(2 \cdot r_o)^3}{\frac{\mu_{air} \cdot K_{air}}{\rho_{air} \cdot \rho_{air} \cdot Cp_{air}}} \qquad (16)$$

3.4 Condenser Formulation

The condenser behavior is modeled by considering heat exchanger into two zone first is *the superheated vapor zone* and second is *the condensing zone*, here it is assume that no sub-cooling at the outlet of the condenser, as it has been consider in the assumptions. The overall heat exchanger is computed with two energy balance equation one using the heat flow in secondary fluid and another is the heat flow in the primary circuit (nanorefrigerant/refrigerant) with LMTD correction factor considering equal to 1 for simplifying the equation. As below,

$$m_r \cdot (h_3 - h_{Vsat}) = m_w \cdot Cp_w \cdot (Tw_{out} - Tw_m) \qquad (17)$$

$$m_r \cdot (h_3 - h_{Vsat}) = U_v \cdot S_v \cdot \left[\frac{T_k - Tw_m - (T_3 - Tw_{out})}{\ln\left(\frac{T_k - Tw_m}{T_3 - Tw_{out}}\right)} \right] \qquad (18)$$

Where U_K is the average heat transfer coefficient obtained by eq. (19),

$$U_k = \frac{U_v \cdot S_v + U_{vl} \cdot (S_k - S_v)}{S_k} \quad (19)$$

being,

S_K is the heat exchanger overall heat transfer area.

S_V is the superheated vapor zone theoretical heat transfer area computed from eq. (20).

$$S_{vL} = S_k - S_v \quad (20)$$

$$m_r \cdot (h_{Vsat} - h_{Lsat}) = m_w \cdot Cp_w \cdot (Tw_m - Tw_{in}) \quad (21)$$

$$m_r \cdot (h_{Vsat} - h_{Lsat}) = U_{vl} \cdot S_{vL} \cdot \left[\frac{T_k - Tw_m - (T_k - Tw_{in})}{\ln\left(\frac{T_k - Tw_m}{T_k - Tw_{in}}\right)} \right] \quad (22)$$

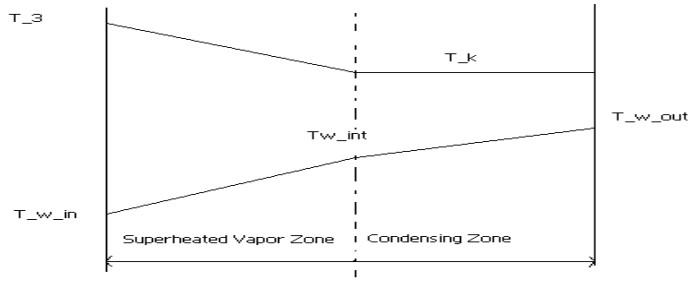

Fig. 3.5. Temperature variation in condenser is shown

For the calculation of the partial coefficient of heat transfer, U_V and U_{VL}, the convective heat transfer coefficient in the water side is obtained using Eq. *(14)*. For the calculation of the convective heat transfer coefficient for the refrigerant one can distinguish

between the convective heat transfer coefficient can be obtain by eq. (23) in the superheated vapor zone,

$$\alpha_v = \frac{K_v}{D_o} \cdot C_1 \cdot Re^{m_1} \cdot Pr^{0.36} \cdot \left[\frac{\mu_v}{\mu_{vM}}\right]^{0.25} \quad (23)$$

Where, C_1 and m_1 depend on the value of Reynolds number ,

$$[C_1, m_1] = \begin{cases} [0.9, 0.4] & Re \le 100 \\ [0.683, 0.466] & 100 < Re \le 1000 \\ [0.4, 0.6] & 1000 < Re \le 200000 \\ [0.022, 0.84] & Re > 200000 \end{cases}$$

and the convective heat transfer coefficient in the condensing zone, obtained using eq.(24),

$$\alpha_k = 0.729 \cdot \left[\frac{g \cdot \rho_L \cdot (\rho_L - \rho_V) \cdot \lambda_{k,mod} \cdot K_l^3}{\mu_l \cdot T_{abs} \cdot 2 \cdot r_o}\right]^{0.25} \quad (24)$$

Here λ_K mod is the modified latent heat with considering effects of thermal advection,

$$\lambda_{k,mod} = \lambda_k \cdot (1 + 0.68 \cdot j_a) \quad (25)$$

here,

$$\lambda_k = h_3 - h_{Vsat}$$

and J_a represent the Jacobsen's number computed by eq.(26).

$$j_a = \frac{Cp_L \cdot T_{abs}}{\lambda_k} \quad (26)$$

And

$$T_{abs} = \left| T_k - T_M \right| \quad (27)$$

3.5 Nanofluid/Nanorefrigerant property calculation

Suspension of nanoparticle into pure refrigerant can be achieved by two methods.

1. Direct suspension of nanoparticle into base refrigerant through appropriate method and procedure and then calculate the thermo physical property of nanorefrigerant with the help of following equation and that property is used to compute the performance of vapour compression refrigeration system (VCRS). To compute the performance of VCRS with nanoparticle based nanorefrigerant we use thermo physical property of nanorefrigerant instead of pure refrigerant as below.

Thermal conductivity of nanorefrigerant

Thermal conductivity of nanorefrigerant is computed by using Sitprasert correlation [31] This relation consider the effect of temperature dependence interfacial layer of nanofluid as below,

$$K_{r,n} = \frac{(K_p - k_l)\cdot\phi\cdot k_l\cdot(2\cdot\beta_1^{\,3} - \beta^3 + 1) + (K_p + 2\cdot k_l)\cdot\beta_1^{\,3}\cdot(\phi\cdot\beta^3\cdot(k_l - K_r) + K_r)}{\beta_1^{\,3}\cdot(K_p + 2\cdot k_l) - ((K_p - k_l)\cdot\phi\cdot(\beta_1^{\,3} + \beta^3 - 1))} \quad (28)$$

K r,n is the thermal conductivity of nanorefrigerant.

ϕ is the volume % suspension of nanoparticle into the pure refrigerant.

Kp is the thermal conductivity of nanoparticle.

Kl is the interfacial thermal conductivity can be obtained using eq. (29)

$$\beta = 1 + \frac{t}{r_p}$$

$$\beta_1 = 1 + \frac{t}{2 \cdot r_p}$$

$$t = 0.01 \cdot (T_e - 273) \cdot r_p^{0.35}$$

$$k_l = C \cdot K_r \cdot \frac{t}{r_p} \quad (29)$$

Where t is the interfacial layer thickness

Kr is the thermal conductivity of pure refrigerant at liquid face

r_p is the radius of nanoparticle in nanometer

C is constant its value 30 for Al_2O_3, CuO and TiO_2 100 for Cu

Viscosity of nanorefrigerant

The viscosity of nanorefrigerant is computed using Brinkman correlation[32]

$$\mu_{r,n} = \mu_r \cdot \frac{1}{(1 - \phi)^{2.5}}$$

Where μ r,n is the viscosity of nanorefrigerant

μ r is the viscosity of liquid pure refrigerant

Density of nanorefrigerant

The density of nanorefrigerant is calculated using Pak and Cho [33]

$$\rho_{n,r} = \phi \cdot \rho_p + (1 - \phi) \cdot \rho_r$$

Where $\rho_{n,r}$ is the density of nanorefrigerant

ρ_p is the nanoparticle density

ρ_r is the density of liquid refrigerant

Specific heat of nanorefrigerant

Specific heat of nano refrigerant is computed using Pak and Cho[33]

$$Cp_{r,n} = (1 - \phi) \cdot Cp_{r,l} + \phi \cdot Cp_p$$

Where Cp r,n is the specific heat of nanorefrigerant

Cp r,l id the specific heat of liquid pure refrigerant

Cp p is the nano particle specific heat

And other parameter/property of nanorefrigerant is calculated using following equation.

$$Re_{r,n} = G_n \cdot \frac{D_i}{\mu_{r,n}}$$

$$Re_r = G_r \cdot \frac{D_i}{\mu_r}$$

$$Pr_{r,n} = Cp_{r,n} \cdot \frac{\mu_{r,n}}{K_{r,n}}$$

$$Pr_r = Cp_{r,l} \cdot \frac{\mu_r}{K_r}$$

$$\alpha_{conv,r,n} = N_{u,r,n} \cdot \frac{K_{r,n}}{D_i}$$

$$\alpha_{conv,r} = N_{u,r} \cdot \frac{K_r}{D_i}$$

$$\alpha_{LV,nr} = F_n \cdot \alpha_{conv,r,n} + S_n \cdot \alpha_{nb,r,n}$$

$$\alpha_{nb,r,n} = 207 \cdot \frac{K_{r,n}}{BD_n} \cdot \left[\frac{q'' \cdot BD_n}{K_{r,n} \cdot T_e}\right]^{0.674} \cdot \left[\frac{\rho_{G,n}}{\rho_{l,r,n}}\right]^{0.581} \cdot Pr_{r,n}^{0.533}$$

$$BD_n = 0.51 \cdot \left[\frac{2 \cdot \sigma}{g_g \cdot (\rho_{l,r,n} - \rho_{G,n})}\right]^{0.5}$$

$$F_n = 53.64 \cdot \left[\frac{q''}{G_n \cdot h_{fg}}\right]^{0.314} \cdot X_{tt,n}^{-0.839}$$

$$G_n = \rho_{n,r} \cdot v_r$$

$$X_{tt,n} = \left[\frac{1 - x}{x}\right]^{0.9} \cdot \left[\frac{\rho_{G,n}}{\rho_{l,r,n}}\right]^{0.5} \cdot \left[\frac{\mu_{r,n}}{\mu_{G,n}}\right]^{0.1}$$

$$S_n = 0.927 \cdot \left[\left(\frac{1 - x}{x}\right)^{0.8} \cdot \left(\frac{\rho_{G,n}}{\rho_{l,r,n}}\right)^{0.5}\right]^{0.319}$$

Where Re r,n is the Reynold number of nanorefrigerant

Pr,n Prandle number of nanorefrigerant

Gr is the mass flux of nanorefrigerant

Xtt,n is the martinelli parameter of nanorefrigerant

X is the vapour quality of nanorefrigerant

BDn is the bubble diameter of nanorefrigerant

Sn is suppression factor of of nanorefrigerant

q" is the heat flux received by the nanorefrigerant in the evaporator

Vr is the velocity of nanorefrigerant in the evaporator

All these property are used to compute the performance of VCRS using nanorefrigerant in the above equation from (1) to (28). Thus we can find out the performance of VCRS using nanorefrigerant in primary circuit. In this project work first method (direct suspension of nanoparticle into the base refrigerant is proposed and effect of various input parameter of the proposed model on the performance of VCRS is computed using nanofluid (nanorefrigerant) and without nanofluid are shown in result and discussion chapter.

2. In second method of suspension of nanoparticle into pure refrigerant can be achieved followed by two procedures as given below.
    I. Suspension of nanoparticle into the compressor oil of VCRS a little higher Volume % concentration as compare to pure refrigerant as proposed in first method (direct suspension) is considered and we know that during operation of VCRS some amount of compressor oil goes into the pure refrigerant. Thus nanoparticle suspension into pure refrigerant can be achieved.

According to this procedure we have to calculate thermo physical property of nanorefrigerant/oil in different way as below.

Firstly thermo physical property of nanoparticle oil mixture is calculated and these data is used to calculate the property of nanorefrigerant.

The following formulations are used to calculate the thermo physical properties of nanolubricant.

Thermo physical property of nanolubricant

Specific heat of nanolubricant

Specific heat of nanolubricant is computed using Pak and Cho, [33] correlation as below

$$Cp_{n,o} = (1 - \phi_n) \cdot Cp_o + \phi_n \cdot Cp_n \quad (30)$$

Where Cpn,o is the specific heat of nanolubricant

Cpo is the specific heat of lubricant/oil

Cpn is the specific heat of nanoparticle

Φn is the volume fraction of nanoparticle in the nanoparticles/oil suspension

Thermal conductivity of nanolubricant

Thermal conductivity of nanolubricant is calculated using Hamilton and Crosser, [34] equation

$$K_{n,o} = K_o \cdot \left[\frac{K_n + 2 \cdot K_o - 2 \cdot \phi_n \cdot (K_o - K_n)}{K_n + 2 \cdot K_o + \phi_n \cdot (K_o - K_n)} \right] \quad (31)$$

Being Kn,o is the thermal conductivity of nanolubricant

Ko is the thermal conductivity of lubricant/oil

Viscosity of nanolubricant

Viscosity of nanolubricant is calculated with the help of Brinkman correlation [32]

$$\mu_{n,o} = \mu_o \cdot \frac{1}{(1 - \phi_n)^{2.5}} \quad (32)$$

Where μ n,o is the viscosity of nanolubricant

μ o is the viscosity of lubricant/oil

Density of nanolubricant,

Density of nanolubricant can be calculated using following equation

$$\rho_{n,o} = (1 - \phi_n) \cdot \rho_o + \rho_n \cdot \phi_n \quad (33)$$

Volume fraction of nanoparticle in the nanoparticle/oil suspension

$$\phi_n = \omega_n \cdot \left[\frac{\rho_o}{\omega_n \cdot \rho_o + (1 - \omega_n) \cdot \rho_n} \right] \quad (34)$$

ω_n is the mass fraction of nanoparticle in nanolubrical/oil suspension and can be calculated using following equation

$$\omega_n = \frac{m_n}{m_n + m_o} \quad (35)$$

$$\sigma_{n,o} = \sigma_o$$

Where m n is the mass nanoparticle and m o is the mass of lubricant/oil and $\sigma_{n,o}$, σ_o is the surface tension of nanolubricant and lubricant/oil respectively

Calculation of thermo physical properties refrigerant/oil mixture

Specific heat of the refrigerant/oil mixture

$$Cp_{r,n,o,f} = (1 - X_{n,o}) \cdot Cp_{r,f} + X_{n,o} \cdot Cp_{n,o} \quad (36)$$ (Jensen and Jackman, [35])

Where Cp r,n,o,f is the specific heat of refrigerant/oil mixture

Cp r,f is the specific heat of pure refrigerant

Xn,o is the nanoparticle/oil suspension concentration

Viscosity of the refrigerant/oil mixure

$$\mu_{r,n,o,f} = \exp\left(X_{n,o} \cdot \ln(\mu_{n,o}) + (1 - X_{n,o}) \cdot \ln(\mu_{r,f})\right) \quad (37)$$

(Kedzierski and Kaul, [36])

Where μ r,n,o,f is the viscosity of refrigerant oil mixture

μ r,f is the viscosity of pure refrigerant

μ n,o is viscosity of nano/oil mixture calculated by eq. (32)

Thermal conductivity of the refrigerant/oil mixture

$$K_{r,n,o,f} = K_{r,f} \cdot (1 - X_{n,o}) + K_{n,o} \cdot X_{n,o} - (0.72 \cdot X_{n,o} \cdot (1 - X_{n,o}) \cdot (K_{n,o} - K_{r,f})) \quad (38)$$

(Baustian et. al, [37])

Kr,n,o,f is the thermal conductivity of refrigerant/oil mixture

K n,o is the thermal conductivity of nano/oil mixture can be calculated by eq. (31)

Density of the refrigerant/oil mixture

$$\rho_{r,n,o,f} = \left[\frac{X_{n,o}}{\rho_{n,o}} + \frac{1 - X_{n,o}}{\rho_{r,f}} \right]^{-1} \quad (39)$$

$\rho_{r,n,o,f}$ is the density of refrigerant/oil mixture

$\rho_{r,f}$ is the pure refrigerant density

$\rho_{n,o}$ is the density of nano/oil mixture can be calculated using equation (33)

Nanoparticle/oil suspension concentration

$$X_{n,o} = \frac{m_{n,o}}{m_{n,o} + m_r} \quad (40)$$

m n,o is the mass of nano/oil mixture

mr is the mass of pure refrigerant

Surface tension of refrigerant/oil mixture

$$\sigma_{r,n,o} = \sigma_r + (\sigma_{n,o} - \sigma_r) \cdot X_{n,o}^{0.5} \quad (41)$$ (Jensen and Jackman, [35])

$\sigma_{r,n,o}$ Is the surface tension refrigerant/oil mixture

$\sigma_{n,o}$ Is the surface tension of nano/oil

Based on the above formulation we can calculate the thermo physical property of nano/oil mixture as well as refrigerant/oil mixture with nanoparticle and that property are used to calculate the thermo physical property of VCRS and we can find out the performance parameter of VCRS using nanoparticle suspended into pure refrigerant through compressor oil.

Based upon all the formulation given above set of linear and non linear equation is prepared in the engineering equation solver to calculate the operating performance of VCRS.

In this modeling of VCRS all the property are taken in S.I. unit , temperature in °K, energy in Joule (J) specific property mass basis and pressures in bar.

CHAPTER 4

EXPERIMENTATION

4.1 Introduction

In this chapter the experimental procedure for operating the test rig has been developed as shown in Fig 4.1. For the development of experimental test rig the various components has been used for vapor refrigeration system, the configuration of the components and system is as per computational design input. Following components and instruments has been used for development of test rig.

Fig.4.1 Vapour compression refrigeration system model

Compressor

A hermetically sealed model no. KCE419HAG B130, serial – DBKA 36610 reciprocating compressor is used. The low pressure and temperature vapor refrigerant from evaporator is drawn into the compressor through inlet or suction valve, where it is compressed to a high pressure and temperature. This high pressure and temperature vapor refrigerant is discharged into the condenser through the delivery or discharge valve as shown in Fig 4.2.

SPECIFICATION

Power Input	245 watts
Input Current	1.6 amps
Displacement	5.79
Weight	10.2 kg
Oil Charge	510
Wiring	RSIR

Fig.4.2 hermetically sealed reciprocating compressor

Pressure Gauge

Pressure gauges are mounted at salient point in the setup to measure pressure. In this setup following two types of pressure gauges are used (Fig 4.3).

- Suction pressure gauge. (Range -30 to 24.6 kg/cm2)
- Discharge pressure gauge. (Range 0 to 35 kg/cm2)

As Shown in Fig 4.3.

Fig 4.3 Pressure gauge

Fig.4.4 Temperature meter

Temperature meter

In the setup there are four temperature meters is used to measure brine, water inlet & outlet temperature and is to be used to find out the result as shown in Fig. 4.4.

Range	-50°c to 80°c
Accuracy	+-1
Resolution	0.1
Using environment	20 to 85% RH
Power supply	Battery LR$$,1.5V

Watt meter

A wattmeter is used in the experimental setup to determine the load of setup which is used to calculate the performance of experimental setup as shown in Fig. 4.5.

Range 0-500 watt

Fig 4.5 Watt meter

Hand Shut Off Valve

Hand shut off valve are provided to stop or allow the refrigerant flows as desired to run the setup in vapor compression cycle as shown in Fig. 4.6.

Fig.4.7 Flow meter/Rota meter

Fig.4.6 Hand Shut Off Valve

Flow meter / Rota meter

It is fitted in liquid line in between dryer & expansion valve (capillary tube) to determine the mass flow rate of refrigerant during experiment for calculations as shown in Fig. 4.7 (Range 0.1 to 1 LPM).

Fig 4.8 Drier

Fig.4.9 Capillary tube

Drier

It is fitted between the condenser outlet and evaporator inlet. It contain silica gel to observe the moisture from the refrigerant acts as a drier as shown in Fig. 4.8.

Capillary tube

It is placed between condenser outlet and evaporator inlet. Capillary tube is used to reduce the pressure and boiling point of the refrigerant as shown in Fig. 4.9 It acts as a expansion device in the experimental setup.

Condenser and evaporator concentric tubes

In the Fig 4.10 shown the above pipe namely condenser having two concentric tube length 1.2 m and size of inner tube diameter is 3/8", outer tube diameter is 5/8'. The below pipe namely evaporator also having two concentric tube length 0.8 m and size of inner tube 3/8", outer tube 5/8'. Both the pipe are insulated with three layer of insulation first inner insulation with aluminum foil in the inner side then PVC black tape then KIMI foam.

Fig.4.10 Condenser and evaporator

Fig.4.11 Relay

Relay

Relay is used to start the compressor as shown in Fig. 4.11

4.2 Development of Experimental test Rig

Following procedure for the development of experimental test rig.

Procedural Steps of Experimental Setup

Selection of Refrigerant

- Selection of refrigerant is to be finalized (i.e. R-134a).

Selection of equipments

- A list of equipments & materials for Experimental Setup is to made.

Purchase of components & testing equipments

- Equipments & components of the experimental setup are to be purchased from the market.
- I purchase the materials as per our list.

Making of testing table

- Roughly placing the components in their suitable position make an idea of the testing table size for the experimental setup.
- The testing table of the required size is to be made for brazing the component as suitable position as required for the experimental setup.

Primary refrigeration circuit (i.e. mechanical refrigeration cycle)

- Compressor model no.KCE419HAG (i.e. R-134a).
- The condenser & evaporator concentric tube type is fabricated as per the required size.
- Flow of refrigerant in both condenser & evaporator is counter flow.
- In the evaporator Refrigerant flows inside the inner tube and water surrounding the inner tube and the condenser water flows inside the inner tube and refrigerant surrounding the inner tube.
- To prevent the heat loss the condenser and evaporator tubes are insulated.
- The pressure gauge and thermometer are mounted on the compressor discharge line which is connected to the condenser.
- Liquid indicator, drier, pressure gauge, thermometer, Rota meter are mounted on the liquid line after the condenser outlet.
- Condenser liquid line is connected from the condenser liquid line through capillary and pressure gauge and thermometer is mounted before the evaporator line after the capillary tube.
- Evaporator is connected to the suction of the compressor and pressure gauge, thermometer are mounted on the suction of compressor line.

Secondary refrigeration circuit (i.e. water circulation cycle)

- In the condenser water flows inside the inner tube and refrigerant surrounding the inner tube.
- Fresh water is taken for circulation in the inside tubes.

Electrical circuit

- The electrical component such as compressor, motor, m.c.b., volt meter, ammeter & wattmeter are connected in the experimental setup.

Leak testing

- The leakage is to check with dry Nitrogen, if leakage is found it is to be rectified after rectifying again leakage is to be checked and it is to be hold for 4 hours in the same and N2 should not be charge higher than its operating pressure.

Evacuating the refrigeration system

- After leak testing evacuate the refrigeration system with two stage rotary vacuum pump for minimum 8hr's up to 150 micron.
- After the completing the leakage the refrigerant system evacuated with 2 stage rotatory compressor vacuum pump for min 8 hrs.

Charge of refrigerant in the system

- Charge the refrigerant by weight & measure all the parameters like pressure, temperature & mass flow rate.

Testing of the refrigeration system

- Once the power supply is given the voltage, wattage & frequency are noted down.
- The pressure & temperature readings are noted after starting the compressor.
- The water supply to the condenser and the evaporator tubes are given and the flow rate is set as the given requirement.
- The refrigerant is charged as per the requirement of the experimental setup and all the parameter like pressure temperature and mass flow rate measure it.

- After reaching the steady state condition the reading are noted down and C.O.P. of the system is determine.
- The experimental C.O.P. is compared with the C.O.P. is determined from program.

CHAPTER 5

RESULT AND DISCUSSION

.

5.1 Solution Methodology

In this chapter we discussed about the solution methodology of the various formulation used for design components of the system, we use for solution of formulation of the components by EES (Engineering equation solver) in which we supply the initial conditions of the software before solving, there should be No. of equations is equal to No. of variables.

First all of write all the equation for design of the components of the system. Then we put inputs as per our model and for output we put some guess values in the software then solve the equations one after one components. First we design evaporator then compressor then condenser. For design evaporator we “comment” the other components and check the No. of equations is equal to No. of variables then solve the formulation, if there is some error while solving then we update our guess nearest values of our design.

For the design of the components set all the inputs like, size of the evaporator and condenser, mass flow rate of brine and water, compressor speed, Temperature of brine and water. So, as per our objective to constant our inputs data we use various nearest replacement of eco-friendly refrigerants on the same configuration then compare the outputs as per various refrigerants used like, R134a, R404a, R407c, R290.

5.2 Model Validation

In this section the validation of the model using experimental measurements of different steady states is presented. To this end, three sets of steady state experiments have been undertaken. Each set of experiments consists of a group of tests where the facility is working at a defined set of inputs Table 5.1. The experimental result validation is done without using nanofluid or nanorefrigerant.

The table is shown below from table 5.1 to 5.6 and graph Fig 5.1 to Fig 5.8 express result without using nanofluid.

Initial condition

Condenser and evaporator concentric tube type.

- Condenser outer tube diameter is 5/8” and inside tube diameter is 3/8”
- Evaporator outer tube diameter is 5/8” and inside tube diameter is 3/8”

S. No	m_b (kg/s)	m_w (kg/s)	Tb_{in} (°C)	Tw_{in} (°C)	N (rpm)	Condenser size (m)	Evaporator size (m)
1.	0.006	0.008	25	25	2900	1.2	0.8

Table 5.1 Inputs of the design and experimental test rig.

Prediction in comparison with Experimental Data

For the experiment we use refrigerant is R134a. In table 5.2 the initial input to for the computational and for test Rig. In table 5.3 is the computational or predict data, table 5.4 is the experimental data.

S. No	m_b (kg/s)	m_w (kg/s)	Tb_{in} (°C)	Tw_{in} (°C)	N (rpm)	Condenser size (m)	Evaporator size (m)
1.	0.006	0.008	25	25	2900	1.2	0.8
2.	0.008	0.008	25	25	2900	1.2	0.8
3.	0.006	0.006	25	25	2900	1.2	0.8

Table 5.2 Inputs for the test rig and computational.

S. No	Te (°C)	Tk (°C)	Tb_{out} (°C)	Tw_{out} (°C)	Pe (bar)	Pk (bar)	COP
1.	-1.501	48.25	12.9	37.01	2.774	12.62	2.978
2.	0.277	49.17	15.29	37.69	2.96	12.91	3.131
3.	-0.78	51.32	13.19	40.82	2.847	13.63	2.827

Table 5.3 Computational or predict data.

S. No	Te (°C)	Tk (°C)	Tb_{out} (°C)	Tw_{out} (°C)	Pe (bar)	Pk (bar)	COP
1.	-1.8	42.10	13.1	34.70	2.86	12.90	2.67
2.	-0.7	43.60	14.3	36.10	2.56	11.80	2.75
3.	1.1	46.30	16.4	35.20	2.80	12.64	2.84

Table 5.4 Experimental data.

A comparison between the measured and predicted values for the parameters in three sets is presented. It has been observed that the predicted values of the parameters are within the 20% of the measured values.

5.3 Parametric Study

The most widely used fluorocarbon refrigerants in the world. These include the environmentally friendly hydrocarbon (HFC) refrigerants R134a, R404A, R407C and R290. Table 5.5 shows the physical and environmental characteristics of these refrigerants as shown in fig 5.2.

Properties	R134A	R404A	R407C	R290
Molecular Weight (kg / Kmol)	102	97.6	86.20	44.1
B.P. at 1.013 bar (°C)	-26.1	-51.4	-43.6	-42.2
Critical temperature (°C)	101.1	72.15	85.8	96.68
Critical pressure (bar)	40.60	37.35	46.00	42.47
ODP	0	0	0	0
GWP_{100}	1300	3260	1800	3

Table 5.5 Physical and environmental characteristics of selected refrigerants

In a simple reciprocating system which can simulate the performance of actual system as closely as possible, has been used to compare the characteristics of various refrigerants R134a, R404A, R407C and R290.

Summary of relative Comparison of Refrigerants

Table 5.6 show the comparison between most commonly used refrigerant R134a, R404A, and R407cand R290. It can be seen from the table that R134a have highest C.O.P. than other refrigerant for the same geometry and input parameter of the VCRS. it is because compressor work reduces about 20-30 % than other refrigerant by using R134a in VCRS. Also working pressure ratio is little lower than the other refrigerant. So that R134a is most commonly used in HVAC and automobile AC system.

Parameters	***R134A***	***R404A***	***R407C***	***R290***
COP	2.978	2.638	2.574	2.959
Compressor work (W)	102	131.4	127.8	121.2
Refrigerating effect (W)	303.7	346.5	329	358.4
Mass flow rate (kg/s)	0.00236	0.0047	0.0027	0.00157
Condenser pressure (bar)	12.62	27	23.27	17.16
Evaporator pressure (bar)	2.774	5.788	4.208	9.148
Condenser Temperature (°C)	48.25	56.94	52.49	51.26
Evaporator Temperature (°C)	-1.501	-1.338	-2.272	-4.326
Brine outlet temperature (°C)	12.9	11.19	11.89	10.72
Water outlet temperature (°C)	37.01	39.16	38.47	39.23

Table 5.6 Comparison of performance parameters for different refrigerants

R407C exhibits a relatively high temperature glide compared to the other refrigerants, which have almost no glide. It also offer '0' ODP, low global warming potential. European market embraced R407C and currently offers a wide R407C AC product range. Further, a change to polyester lubricant is also required. R404A has been in the market place for more than 10 years

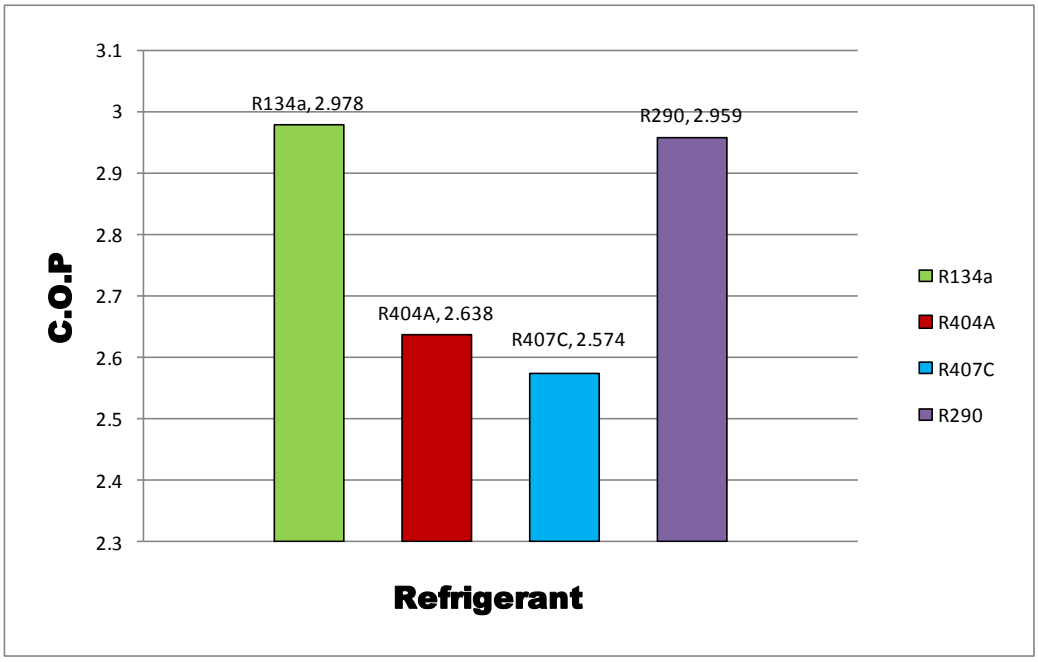

Fig 5.1 Comparison of COP of different refrigerants

Fig 5.1 show that C.O.P. value of R134a and R290 is quite similar but R404A and R407C have very less value of C.O.P than R134a and R290. Thus the R134 and R290 are more efficient considering 1st law of thermodynamics. But due to their different thermo physical property it is used in different application.

Fig 5.2 show the compressor work for different refrigerant respectively and it can be seen that compressor work is also high of R407C and R404A than the R134a and R290 so that its performance reduces 1st law of thermodynamics.

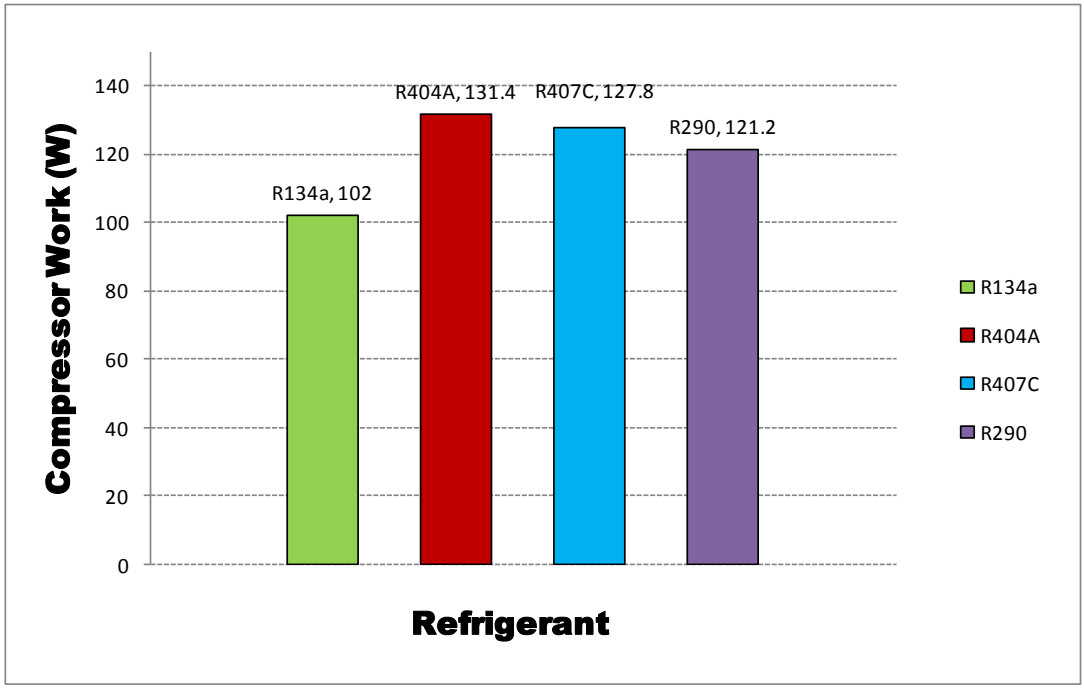

Fig. 5.2 Comparison of compressor work of different refrigerants

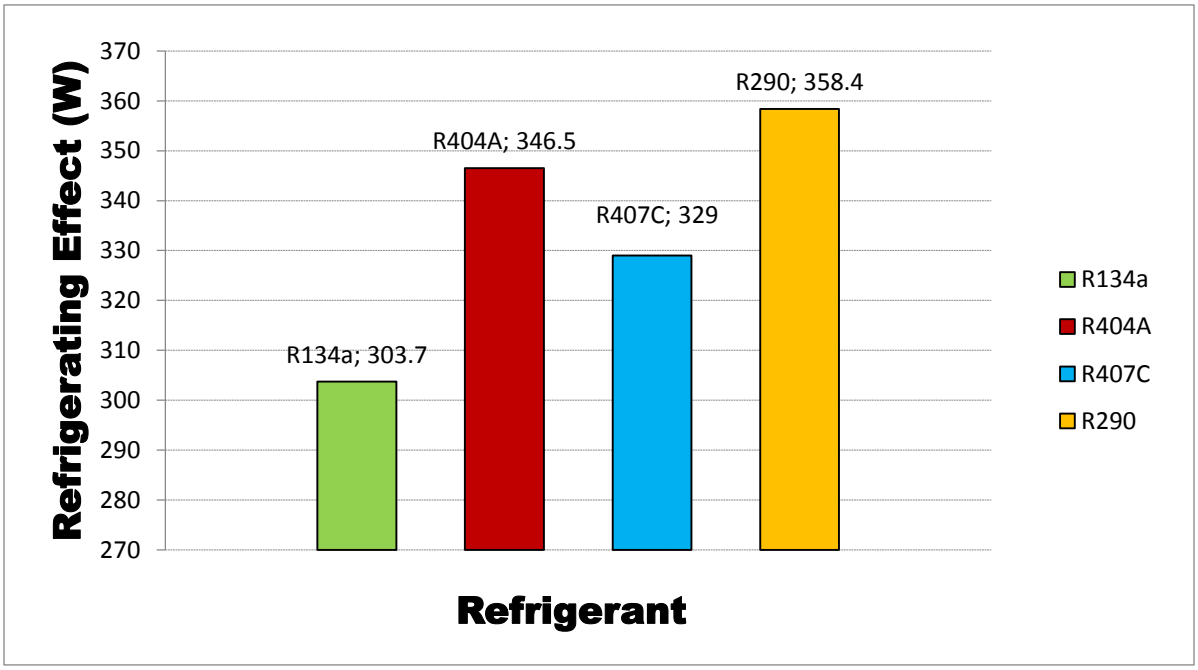

Fig. 5.3 Comparison of refrigerating effect of different refrigerants

Fig 5.3 show the refrigeration effect R134a, R290, R404A and R407C respectively and from the Fig shown it is very clear that refrigeration effect of R134a is less than the R290 but due to higher compressor work of R290 than R134a the C.O.P. value of R290

is lower than the R134.fig also show that refrigeration effect of R404A is higher than the R407C.

Characteristic performance curves

The characteristic performance curves of vapor-compression refrigeration systems are defined as a plot between the inputs of the system by using refrigerants R134a, R404A, R407C and R290 to the coefficient of performance (COP) of the system.

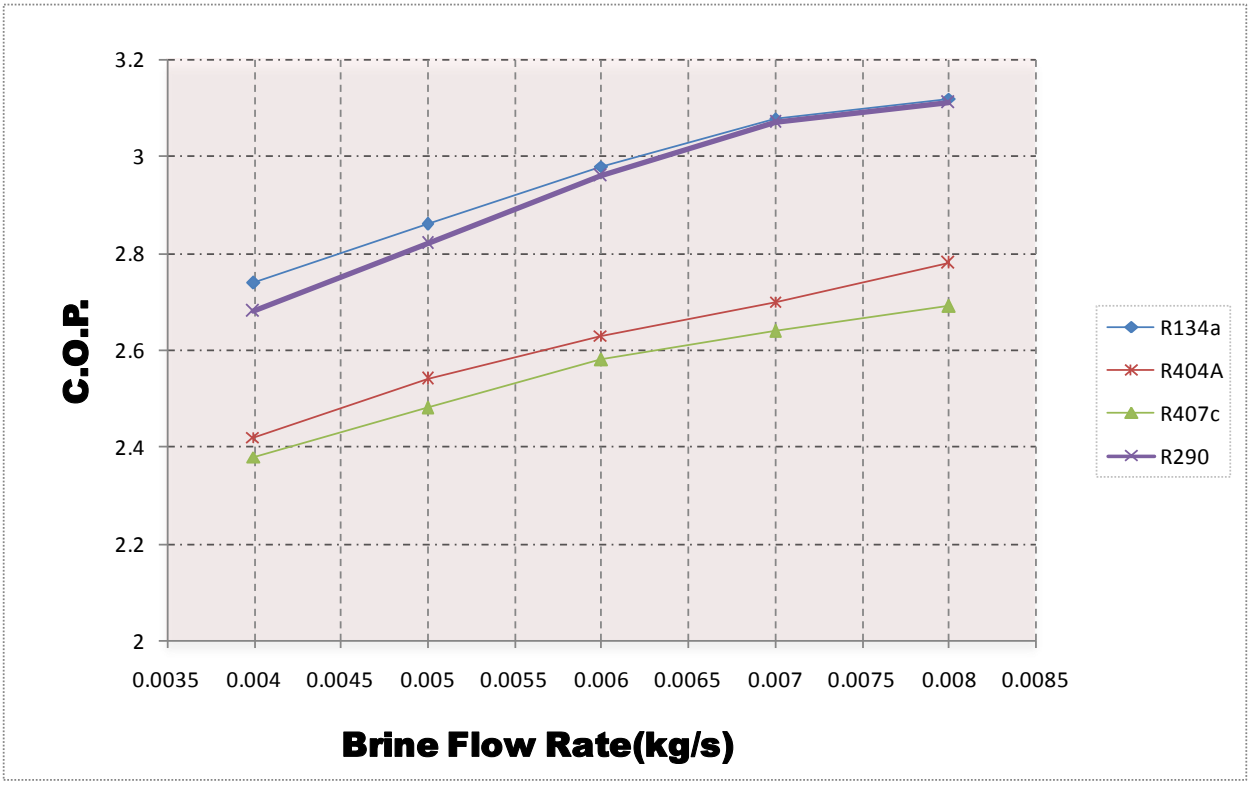

Fig. 5.4 Variation of C.O.P with brine flow rate of VCRS using different refrigerants

In Fig 5.4 the performance curve is shown between COP and Brine flow rate of different refrigerants. When brine mass flow rate 0.004 to 0.008 kg/s (100%) then change in COP for R134a is 14.10 %, R404a is 13.94%, R407c is 14.39% and R290 is 17.06%.

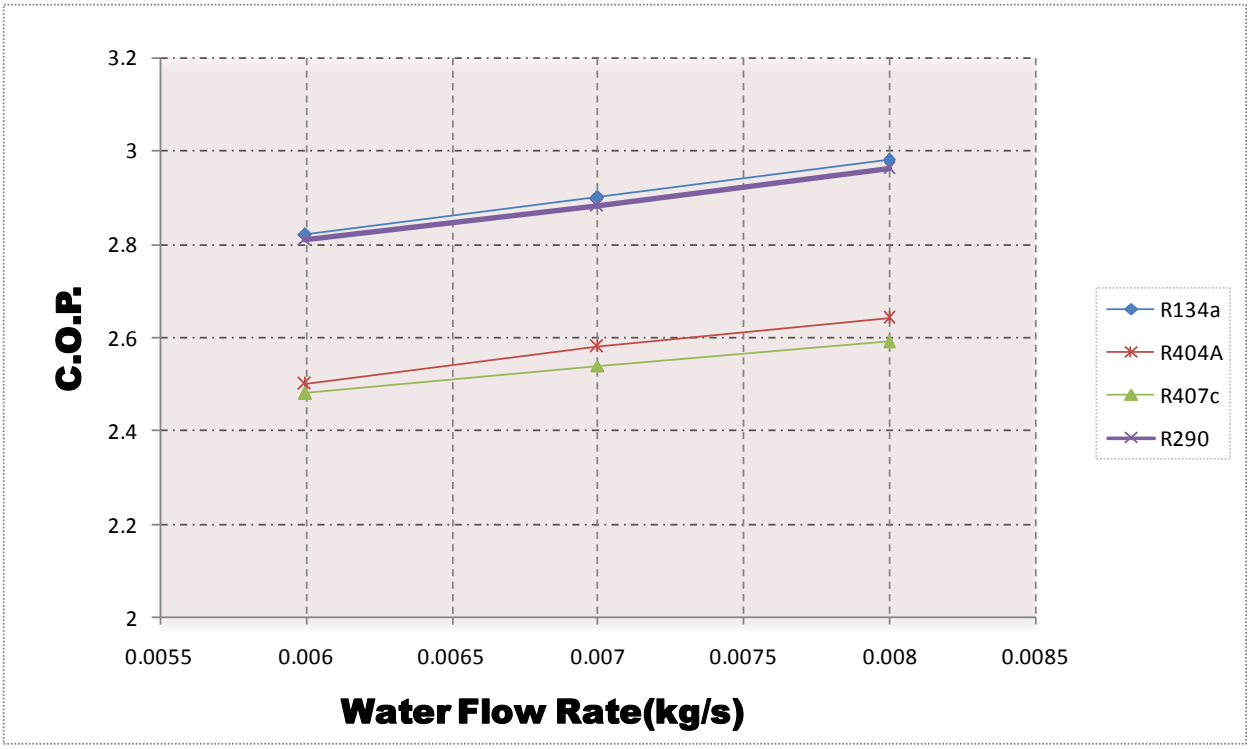

Fig. 5.5 Variation of C.O.P with condensing water flow rate of VCRS using different refrigerants

In Fig 5.5 the performance curve is shown between COP and Water flow rate of different refrigerants. When water mass flow rate 0.006 to 0.008 kg/s (33.3%) then change in COP for R134a is 5.54%, R404a is 5.65%, R407c is 3.58% and R290 is 5%.

In Fig 5.6 the performance curve is shown between COP and condensing water inlet temperature of different refrigerants. When condensing water inlet temperature 18 to 30 ^{o}C (66.67%) then change in COP for R134a is 20.27%, R404a is 16.13%, R407c is 12.50% and R290 is 16.32%.

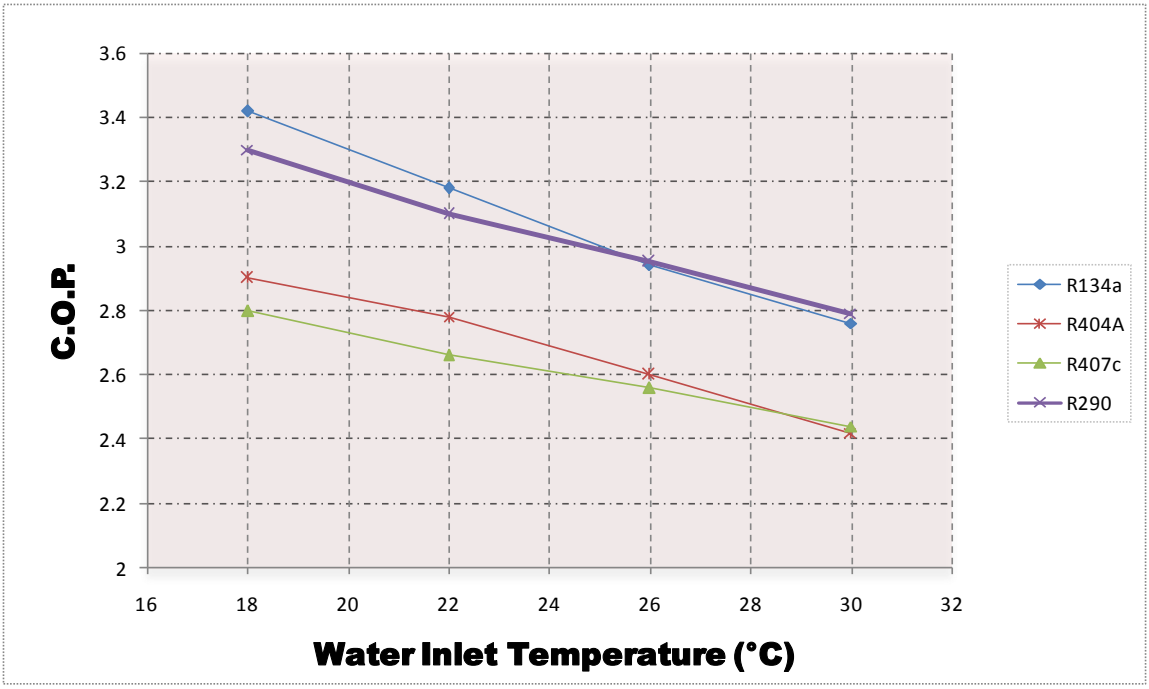

Fig. 5.6 Variation of C.O.P with condensing water inlet temperature of VCRS using different refrigerants

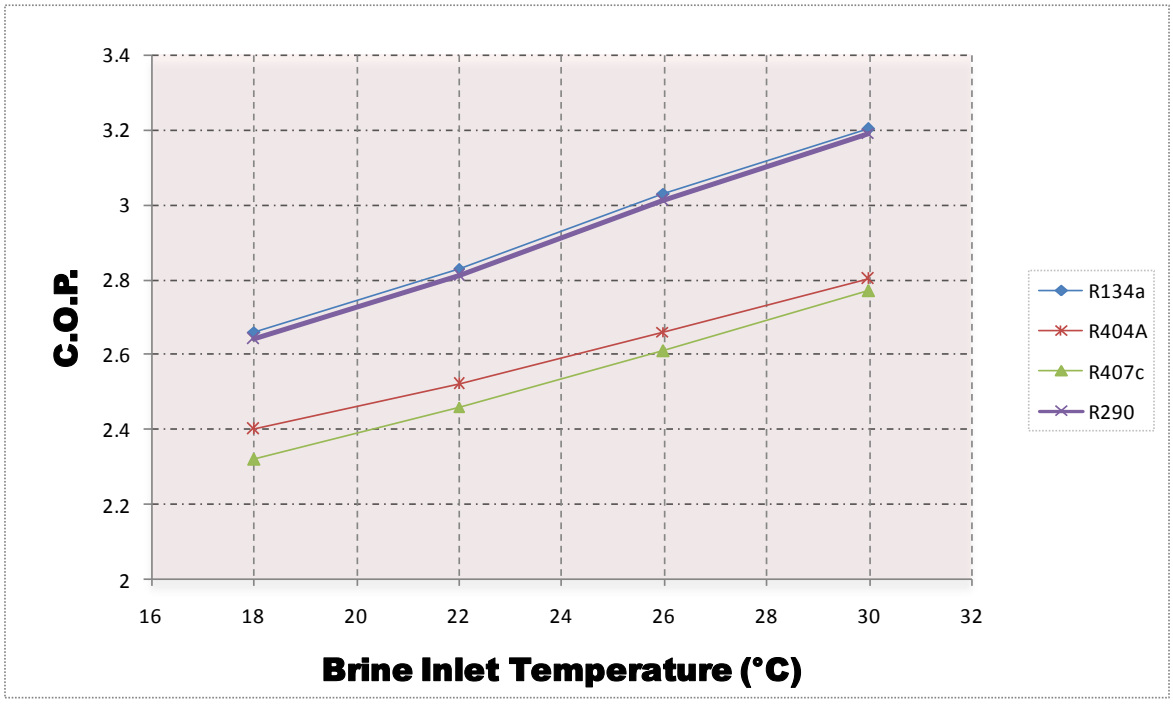

Fig. 5.7 Variation of C.O.P with Brine inlet temperature of VCRS using different refrigerants

In Fig 5.7 the performance curve is shown between COP and Brine inlet temperature of different refrigerants. When brine inlet temperature 18 to 30 ^{o}C (66.67%) then change in COP for R134a is 20.46%, R404a is 17.15%, R407c is 18.47% and R290 is 20.54%.

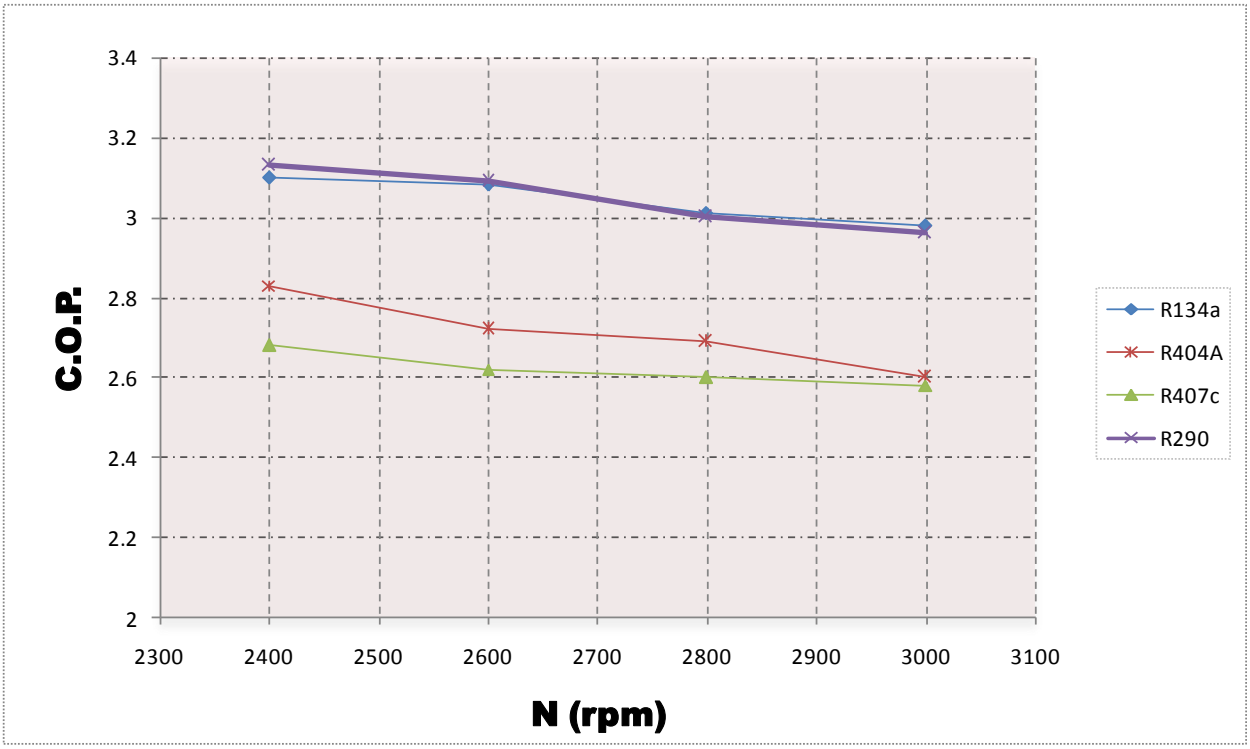

Fig.5.8 Variation of C.O.P with Compressor speed of VCRS using different refrigerants

In Fig 5.7 the performance curve is shown between COP and speed of the compressor N (rpm) of different refrigerants. When Compressor speed is from 2400 to 3000 rpm (25%) then change in COP for R134a is 5.55%, R404a is 7.38%, R407c is 5.08% and R290 is 6.98%.

5.4 Theoretical result of nanorefrigerant

A computational program has been developed to solve non linear equation of vapour compression refrigeration cycle for case (iii) mentioned in abstract. Considering same geometric parameter of the VCRS model theoretical analysis has been done using EES

software for nanorefrigerant flowing in primary circuit and R718 (water) flowing in secondary circuit of VCRS and results are given below.

5.4.1 Thermo physical property of nanorefrigerant

In this section variation of thermo physical property of base refrigerant using nanoparticle suspended into base refrigerant at 5 Vol % are shown below.

5.4.1(a) Thermal conductivity of nanorefrigerant using different nanoparticle and base refrigerant

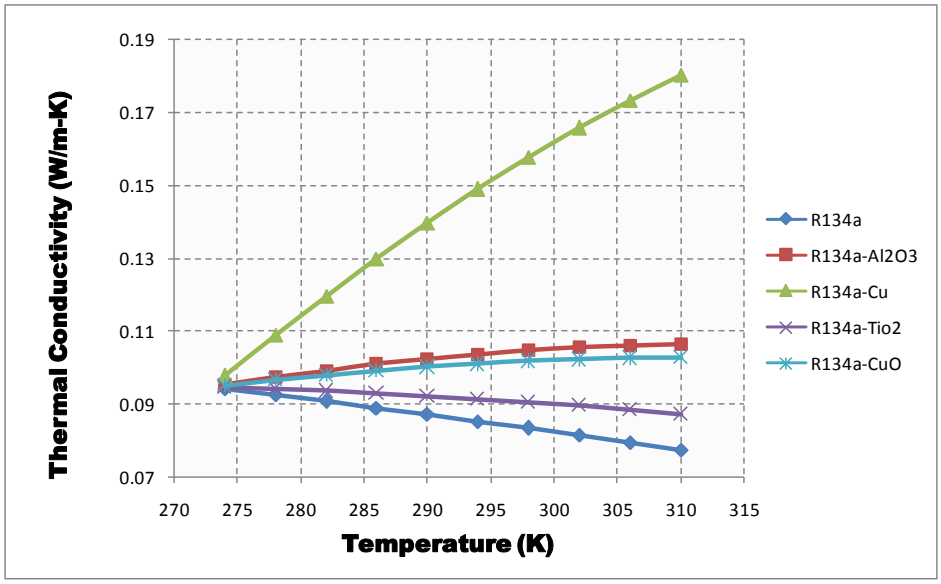

Fig.5.9 Variation of Thermal conductivity with Temperature of R134a using different nanoparticles

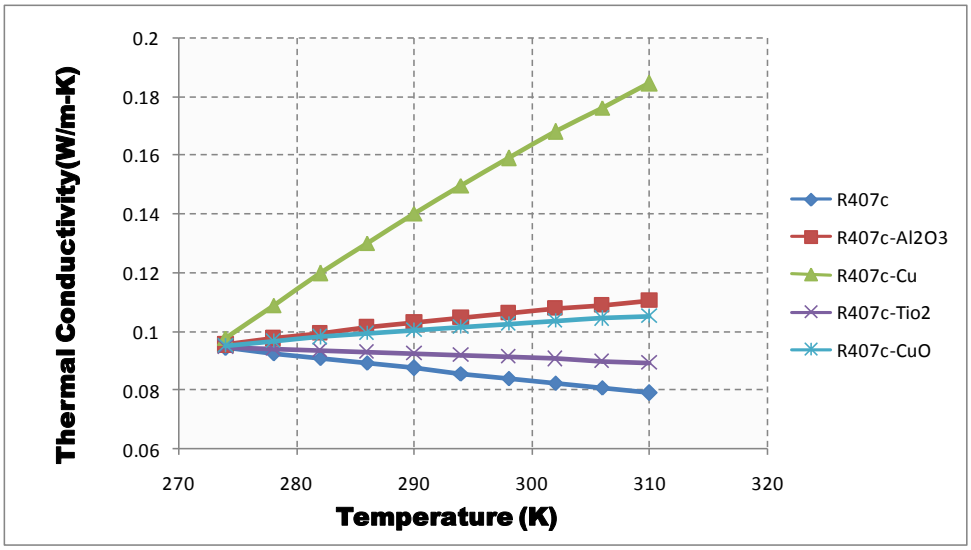

Fig.5.10 Variation of Thermal conductivity with Temperature of R407c using different nanoparticles

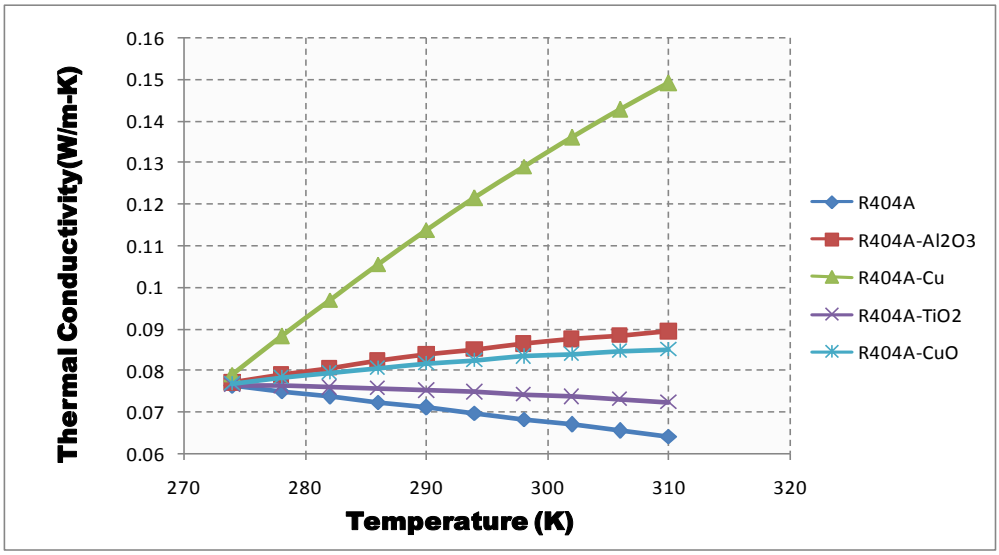

Fig.5.11 Variation of Thermal conductivity with Temperature of R404A using different nanoparticles

Fig. 5.9 to Fig. 5.11 show the enhancement in thermal conductivity of nanorefrigerant when different kind of nanoparticle is suspended into the host refrigerant. The enhancement factor varies from 0.06 to 2 for different nanoparticle.from the Fig we can see that cu nanoparticle have more EF at higher temperature which value is approx 2.

5.4.1(b) Density of nanorefrigerant with different nanoparticle and base refrigerant

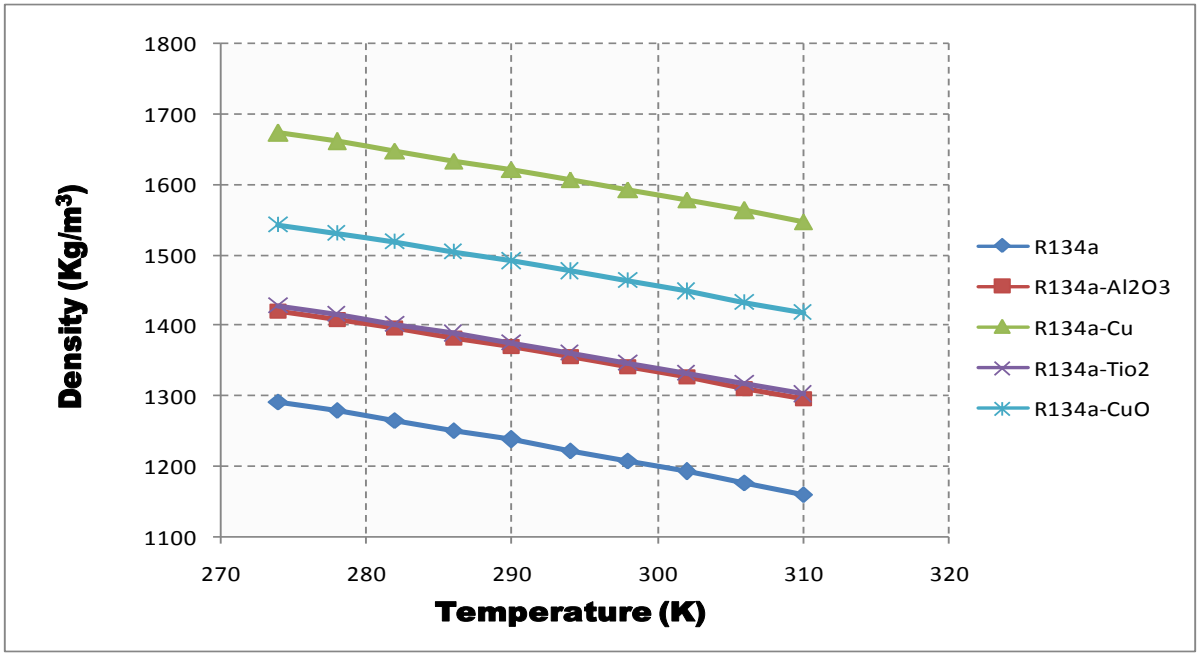

Fig.5.12 Variation of Density with Temperature of R134a using different nanoparticles

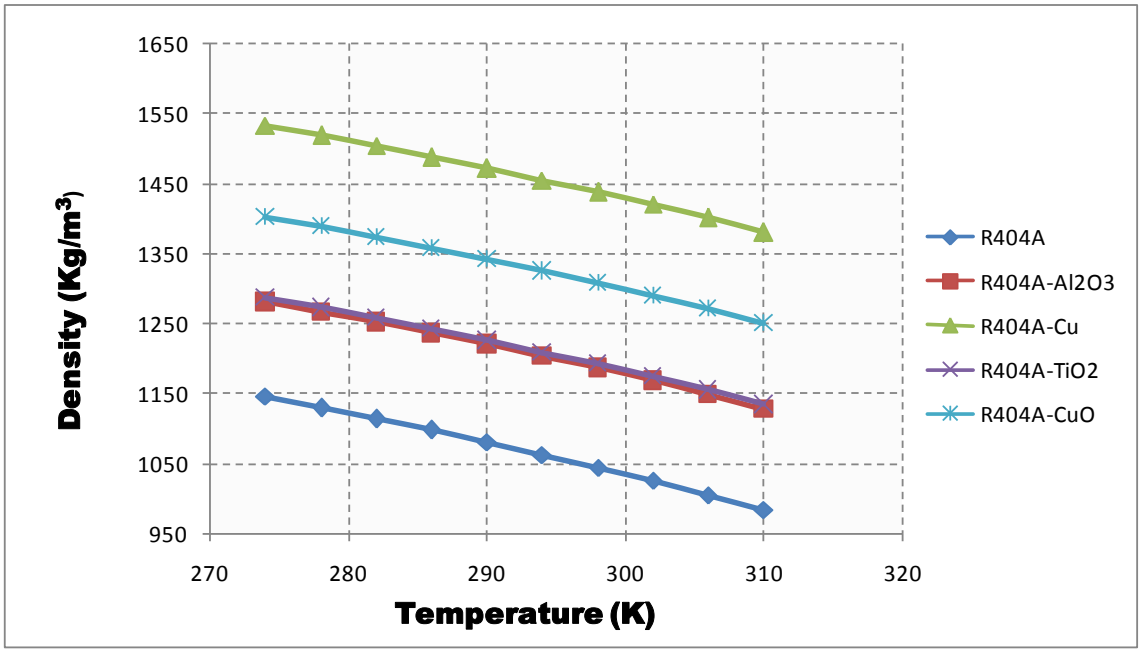

Fig.5.13 Variation of Density with Temperature of R404A using different nanoparticles

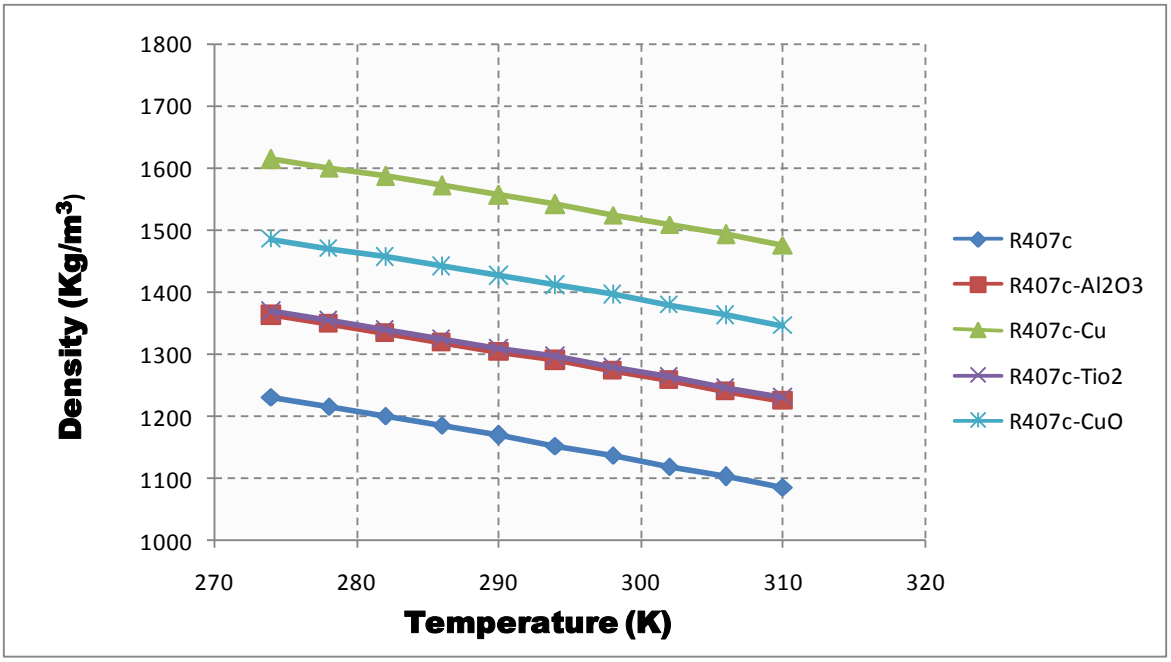

Fig.5.14 Variation of Density with Temperature of R407c using different nanoparticles

Fig. 5.12 to fig. 5.14 shows variation in density of nanorefrigerant subject to temperature variation. Fig shows that density variation of nanorefrigerant is similar to pure refrigerant as higher temperature low density and lower temperature high.

5.4.1(c) Dynamic viscosity of nanorefrigerant using different nanoparticle and base refrigerant

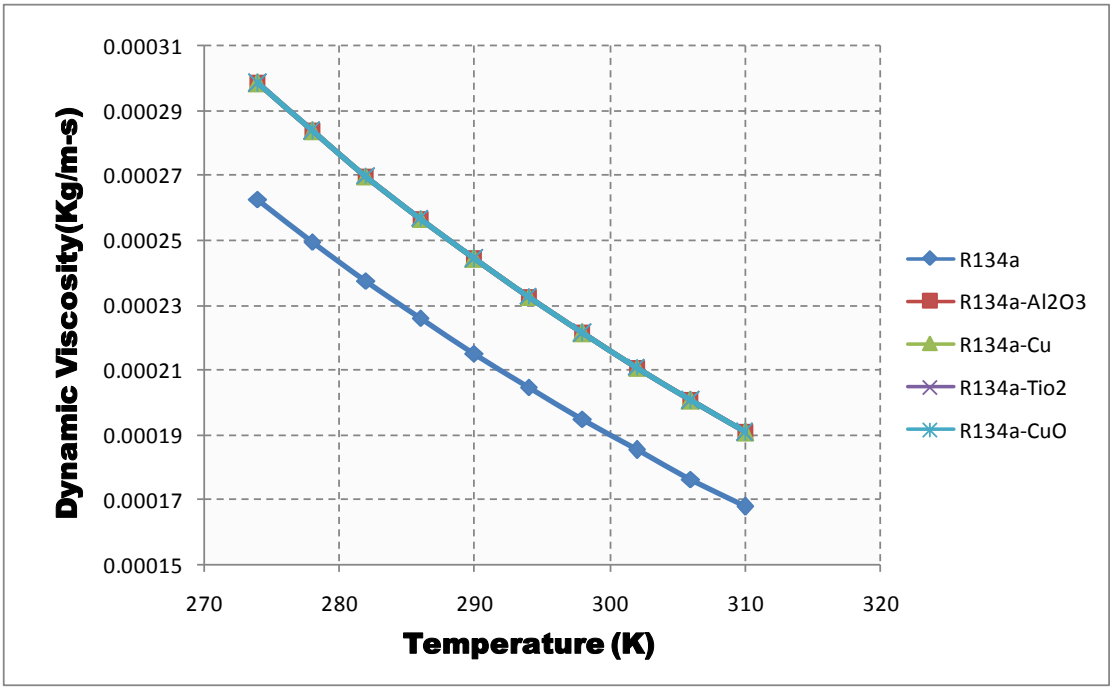

Fig.5.15 Variation of Dynamic viscosity with Temperature of R134a using different nanoparticles

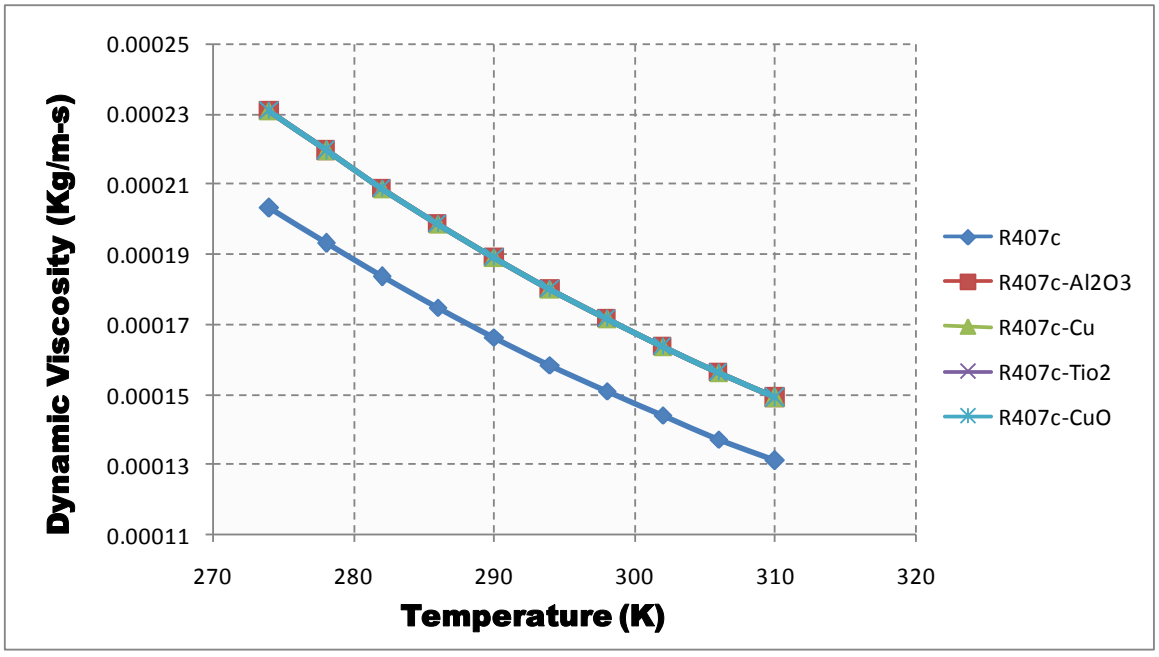

Fig.5.16 Variation of Dynamic viscosity with Temperature of R407c using different nanoparticles

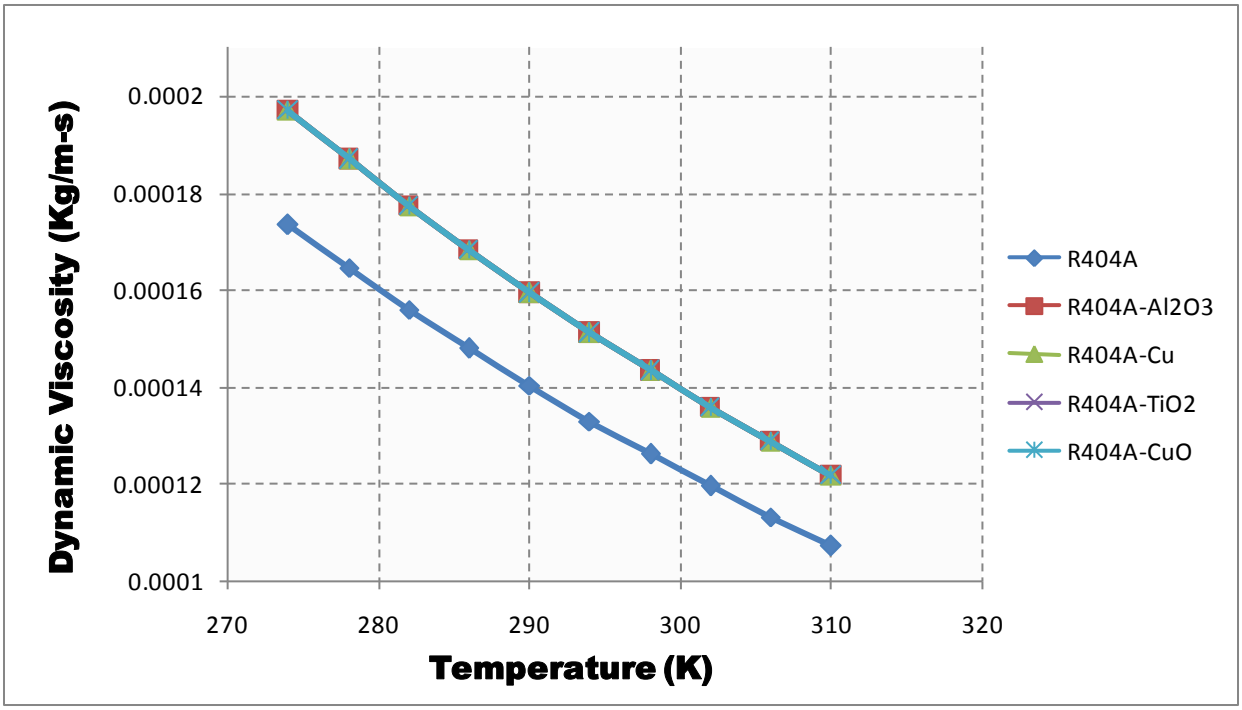

Fig.5.17 Variation of Dynamic viscosity with Temperature of R404A using different nanoparticles

Fig. 5.15 to fig. 5.17 shows variation in Dynamic viscosity of nanorefrigerant subject to temperature variation. Fig shows that Dynamic viscosity variation of nanorefrigerant is similar to pure refrigerant as higher temperature low viscosity and lower temperature high.

5.4.1(d) Specific heat of nanorefrigerant using different nanoparticle and base refrigerant

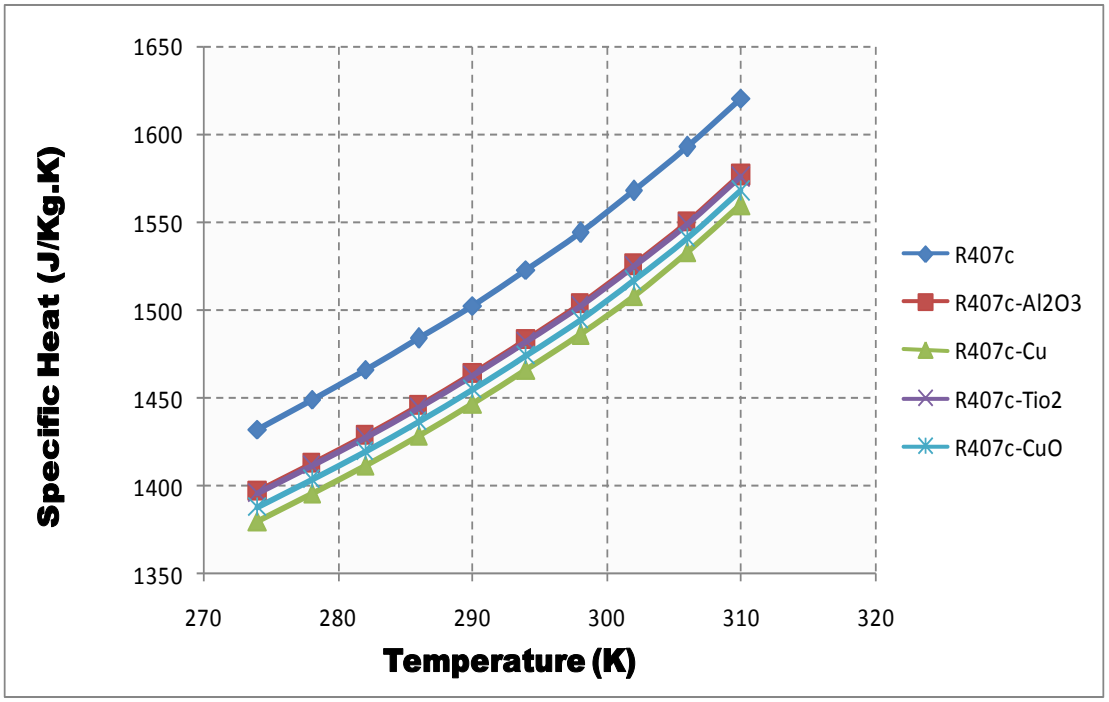

Fig.5.18 Variation of Specific heat with Temperature of R407c using different nanoparticles

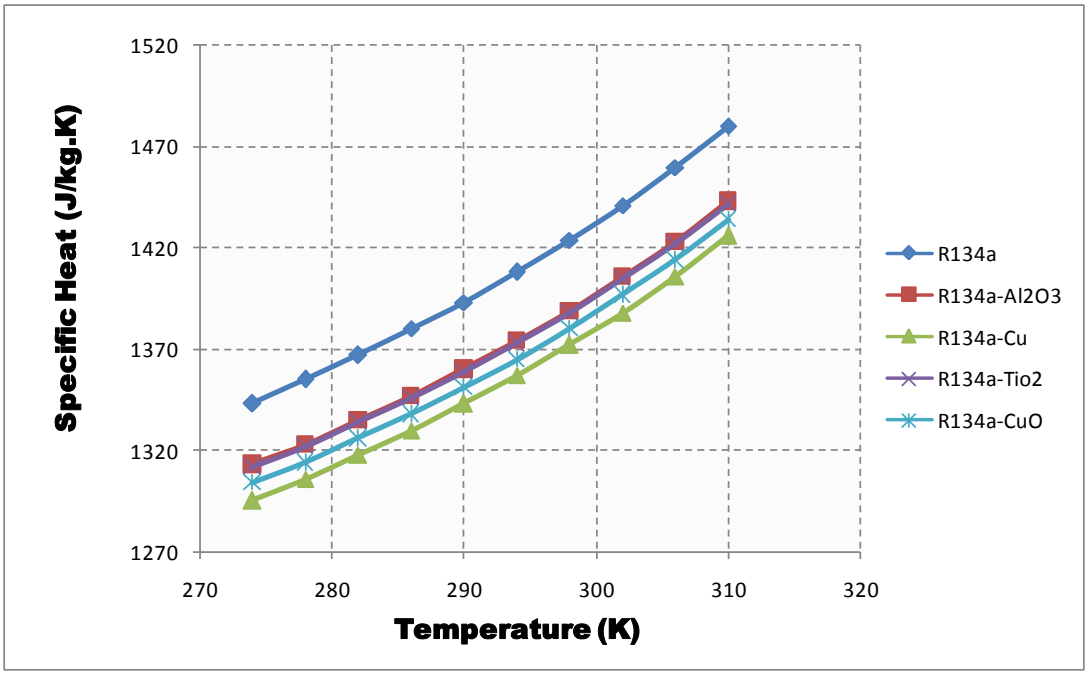

Fig.5.19 Variation of Specific heat with Temperature of R134a using different nanoparticles

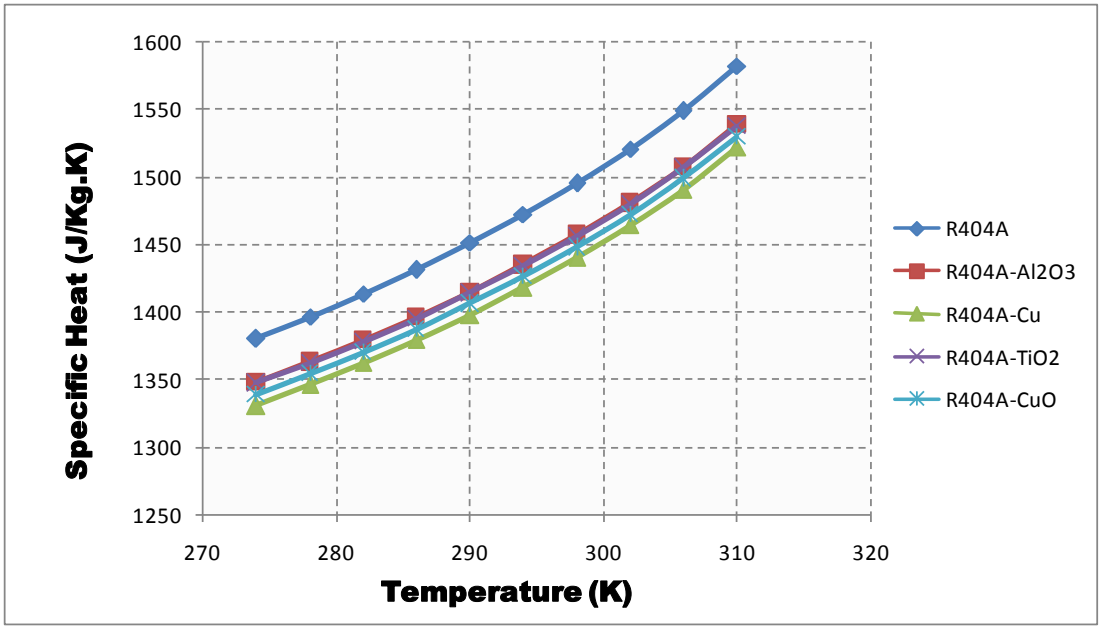

Fig.5.20 Variation of Specific heat with Temperature of R404A using different nanoparticles

Fig. 5.18 to fig. 5.20 shows variation in Specific heat of nanorefrigerant subject to temperature variation. Fig shows that Specific heat variation of nanorefrigerant is similar to pure refrigerant as higher temperature High Specific heat and lower temperature low. But when we go for higher vol % concentration of nanoparticle Specific heat will reduce.

5.4.2(a) Effect of volume fraction on Thermo physical property of nanorefrigerant with different nanoparticle and base refrigerant (at 280K temperature)

Density ratio shown Fig 5.21 is defined as the ratio of density of nanorefrigerant (nanoparticle mixed with pure refrigerant) to the density of pure refrigerant.

Thermal conductivity shown in Fig 5.2 is defined as the ratio of thermal conductivity of nanorefrigerant (pure refrigerant mixed with nanoparticle) to the thermal conductivity of pure refrigerant

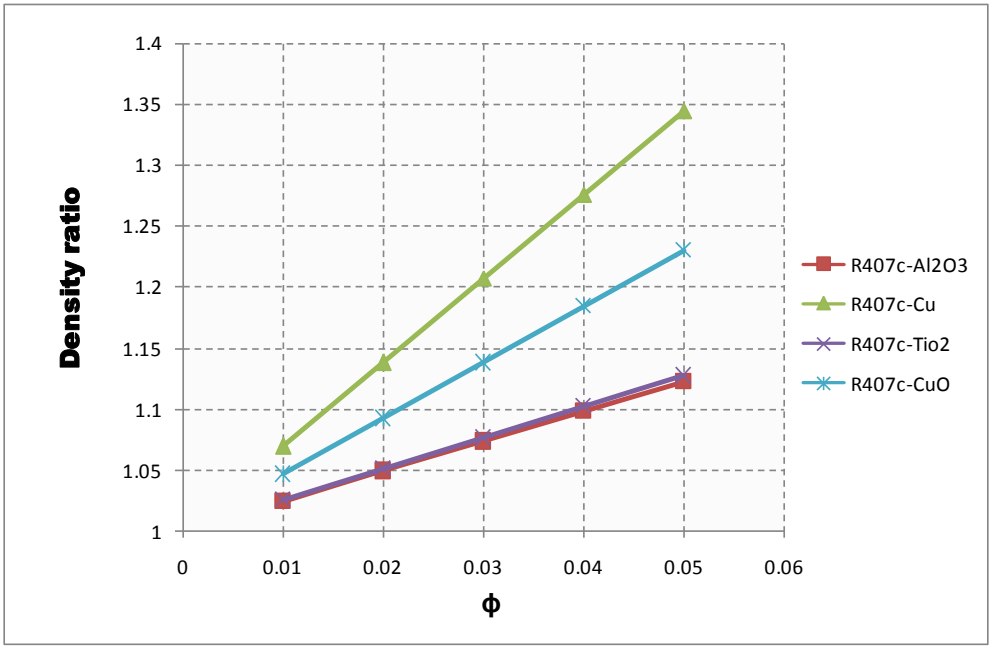

Fig.5.21 Variation of Density Ratio with volume fraction (ϕ) of R407c using different nanoparticles

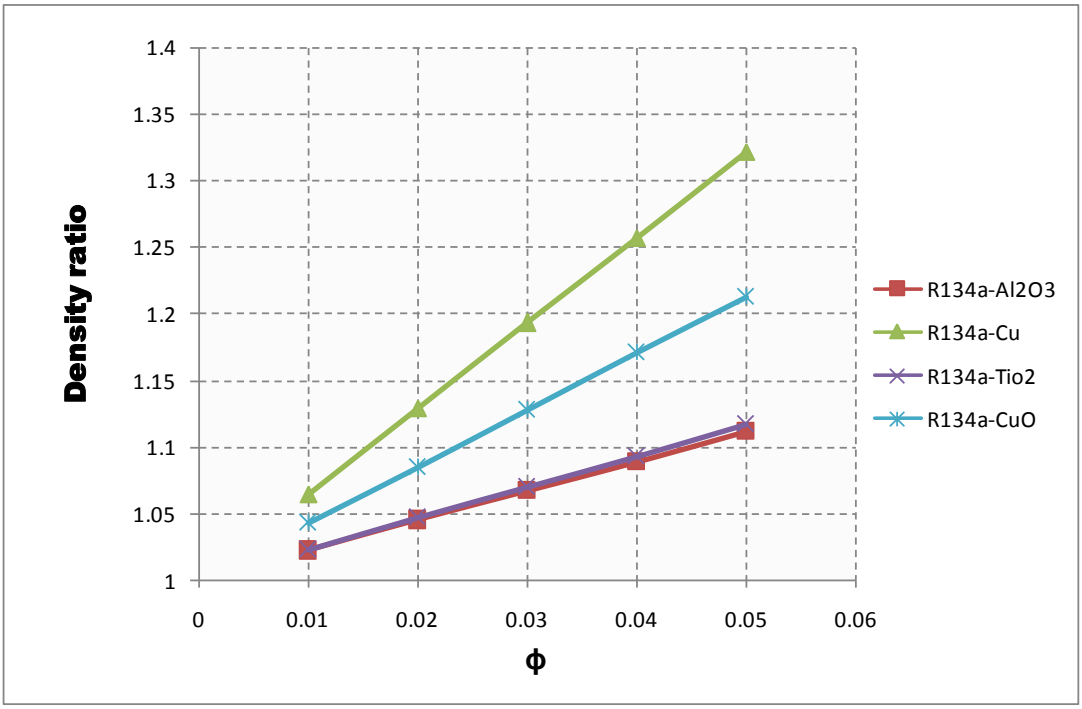

Fig.5.22 Variation of Density Ratio with volume fraction (ϕ) of R134a using different nanoparticles

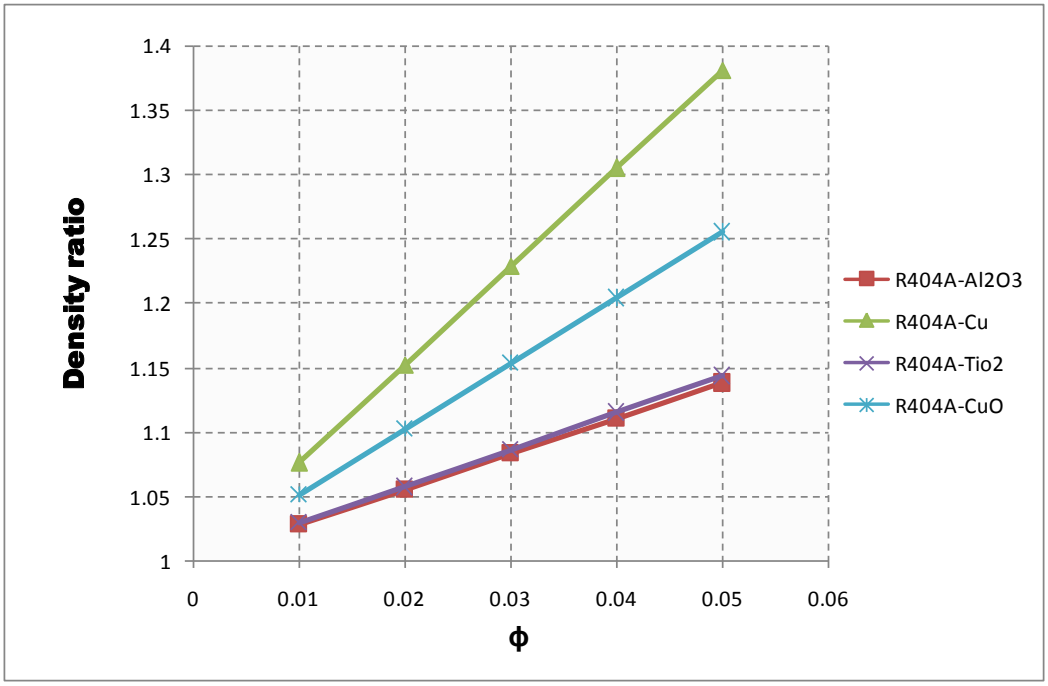

Fig.5.23 Variation of Density Ratio with volume fraction (ϕ) of R404A using different nanoparticles

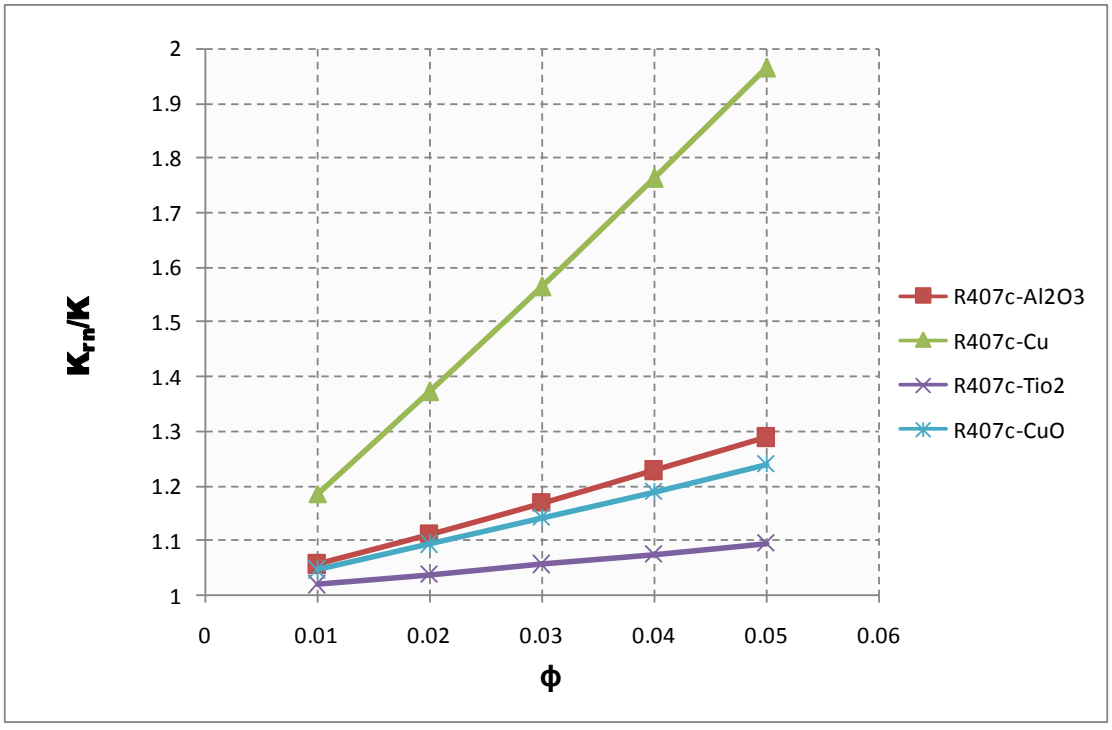

Fig.5.24 Variation of Thermal conductivity Ratio with volume fraction (ϕ) of R407c using different nanoparticles

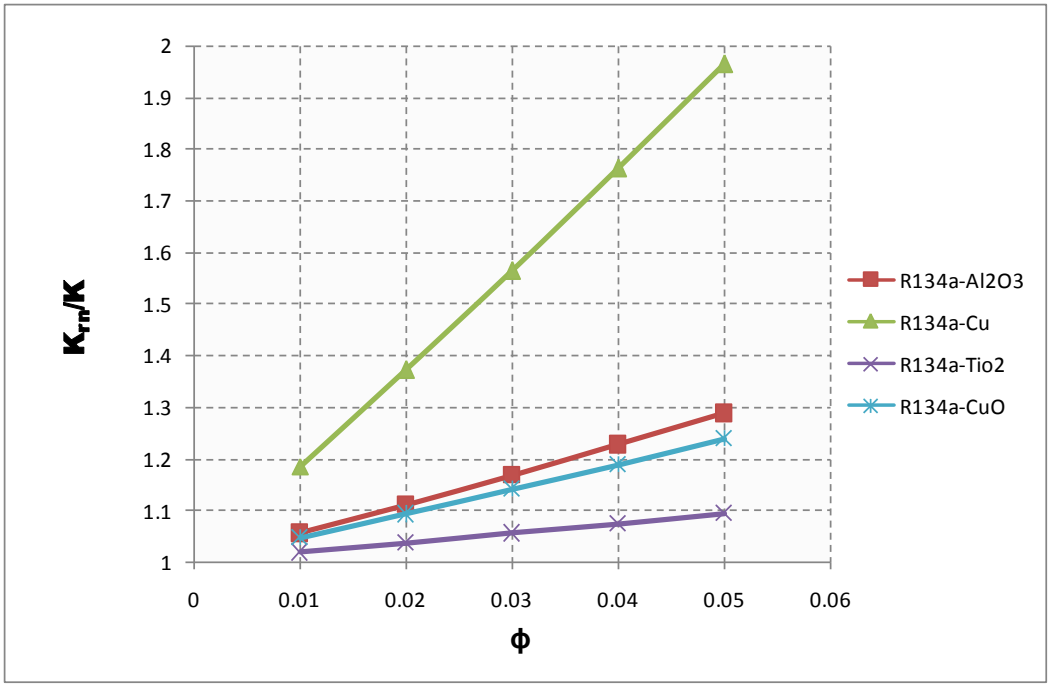

Fig.5.25 Variation of Thermal conductivity Ratio with volume fraction (ϕ) of R134a using different nanoparticles

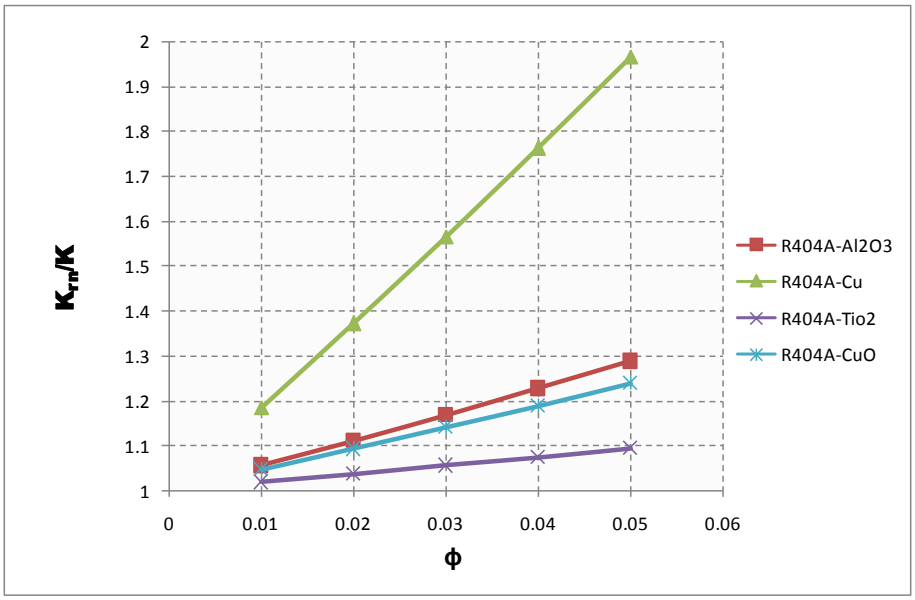

Fig.5.26 Variation of Thermal conductivity Ratio with volume fraction (ϕ) of R404A using different nanoparticles

Fig 5.24 to Fig. 5.26 Shows that conductivity ratio of pure refrigerant to nanorefrigerant increases with increasing concentration of nanoparticle into the host refrigerant. From

the fig we can see that Cu nanoparticle based nanorefrigerant have higher cond. Ratio than other nanoparticle and have approx two times higher than base refrigerant at 5 vol % concentration.

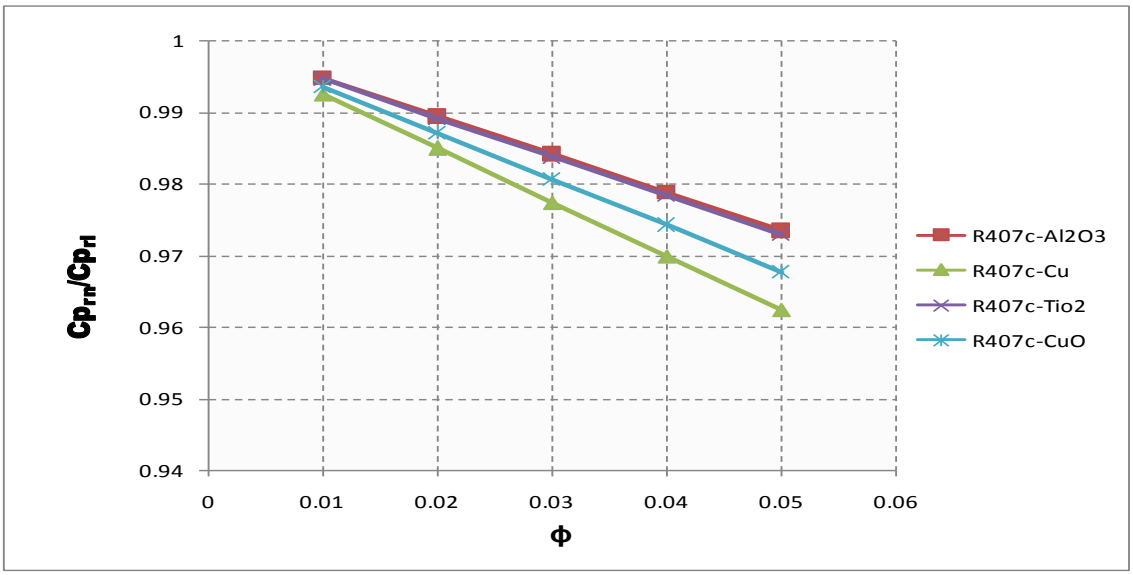

Fig.5.27 Variation of Specific heat ratio with volume fraction (ϕ) of R407c using different nanoparticles

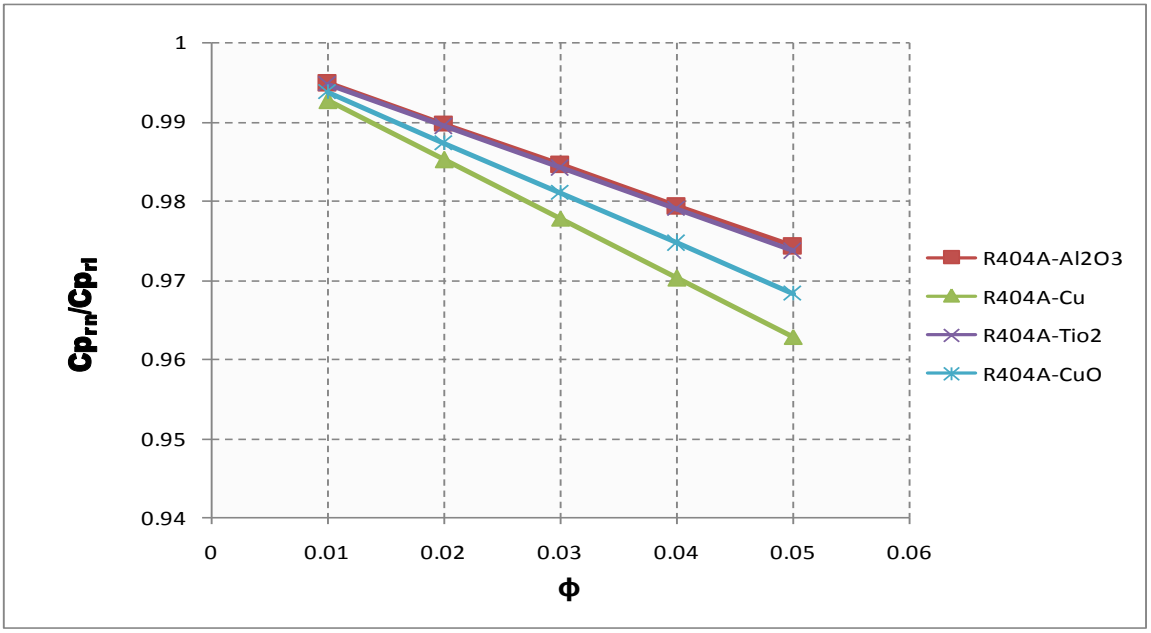

Fig.5.28 Variation of Specific heat ratio with volume fraction (ϕ) of R404A using different nanoparticles

Specific heat ratio shown in Fig 5.28, 5.27 and 5.29 is defined as the ratio of specific heat of nanorefrigerant (nanoparticle mixed with pure refrigerant) to the specific heat of pure refrigerant

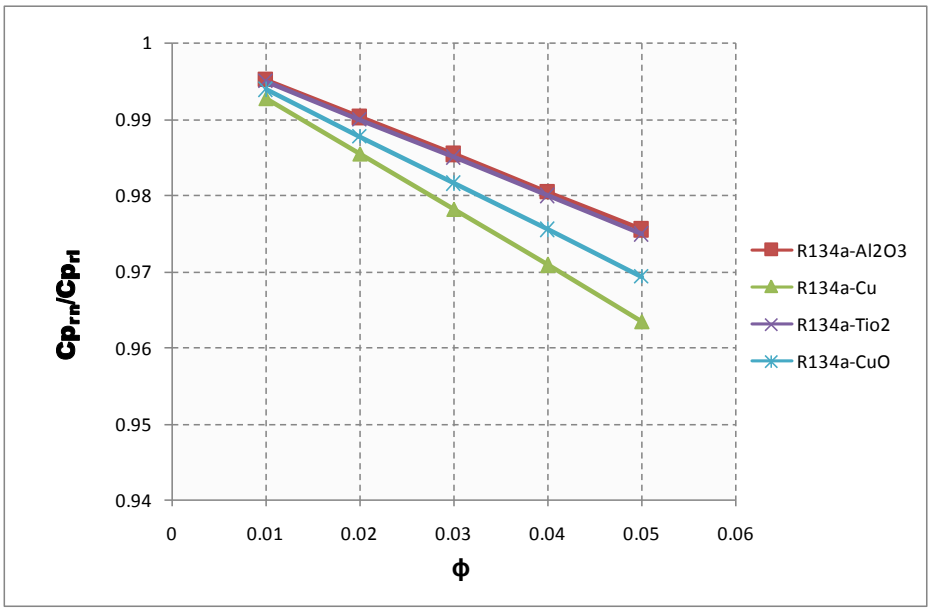

Fig.5.29 Variation of Specific heat ratio with volume fraction (ϕ) of R134a using different nanoparticles

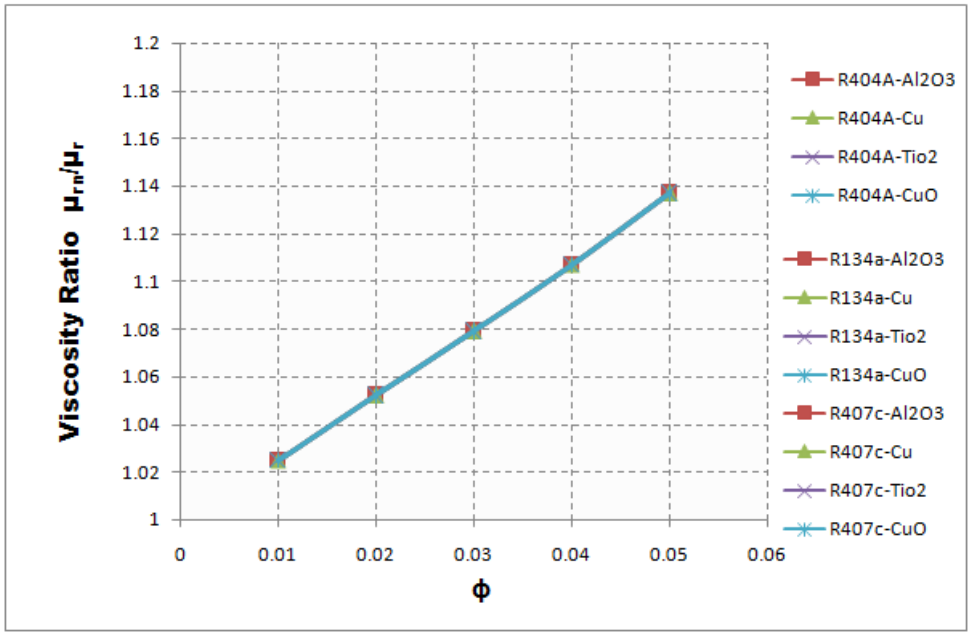

Fig.5.30 Variation of Viscosity ratio with volume fraction (ϕ) of all nanorefrigerant

Viscosity ratio shown in Fig 5.30 is defined as the ratio of Viscosity of nanorefrigerant (nanoparticle mixed with pure refrigerant) to the Viscosity of pure refrigerant

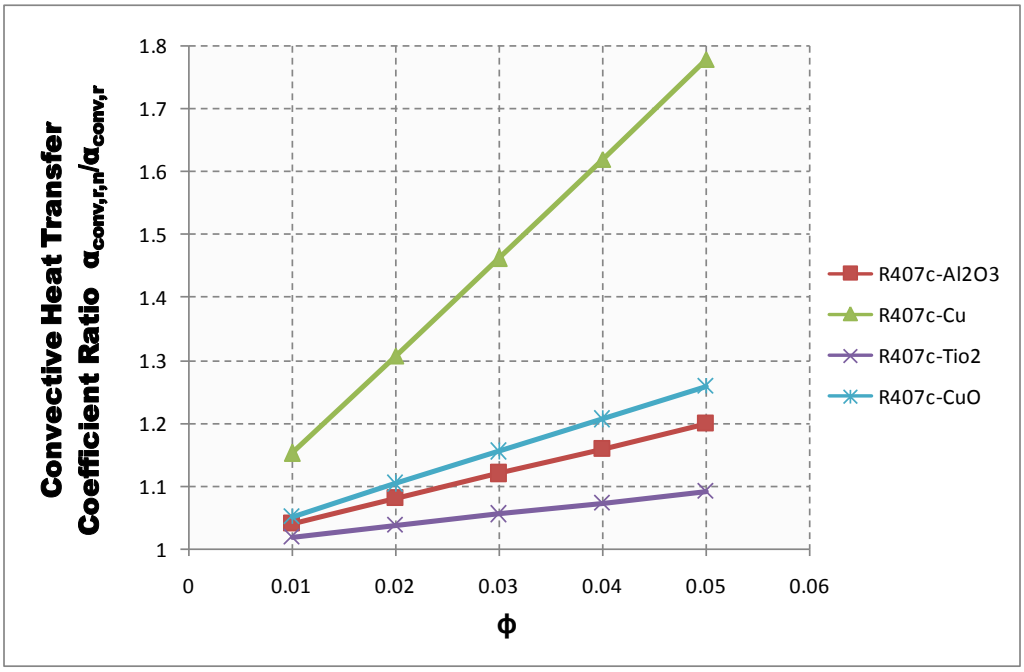

Fig.5.31 Variation of Convective heat transfer coefficient ratio with volume fraction (ϕ) of R407c using different nanoparticles

Convective heat transfer coefficient ratio shown in Fig 5.31, 5.32 and 5.33 is defined as the ratio of Convective heat transfer coefficient of nanorefrigerant (nanoparticle mixed with pure refrigerant) to the Convective heat transfer coefficient of pure refrigerant.

Heat transfer Enhancement Factor shown in Fig 5.34, 5.35 and 5.36 is defined as the ratio of heat transfer coefficient of nanorefrigerant (nanoparticle mixed with pure refrigerant) to the heat transfer coefficient of pure refrigerant

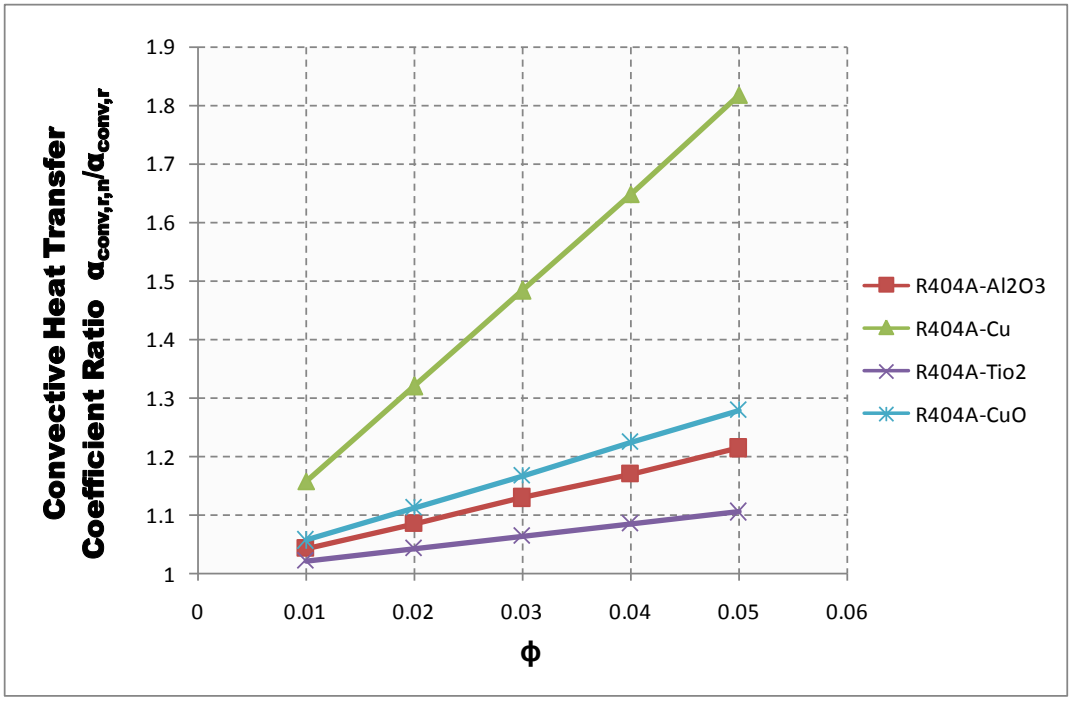

Fig.5.32 Variation of Convective heat transfer coefficient ratio with volume fraction (ϕ) of R404A using different nanoparticles

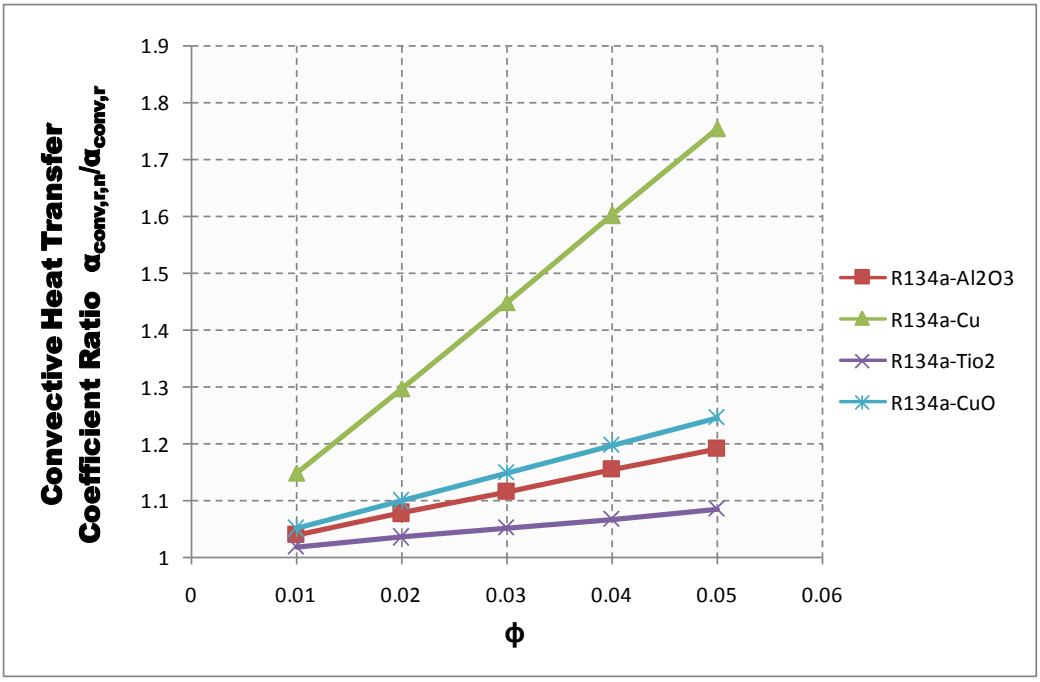

Fig.5.33 Variation of Convective heat transfer coefficient ratio with volume fraction (ϕ) of R134a using different nanoparticles

Fig 5.31 to 5.33 shows the convective heat transfer coefficient Ratio increases by increasing the concentration of nanoparticle. And copper nanoparticle based nanorefrigerant have highest convective heat transfer coefficient ratio than other particle its value ranges from 1 to 1.7.

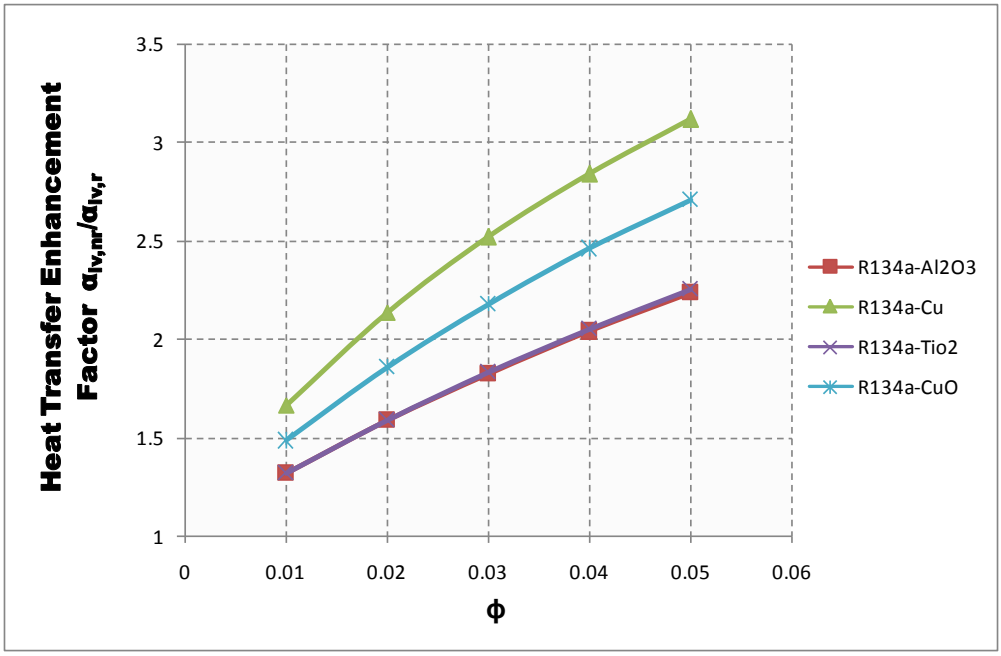

Fig.5.34 Variation of Heat transfer Enhancement Factor with volume fraction (ϕ) of R134a using different nanoparticles

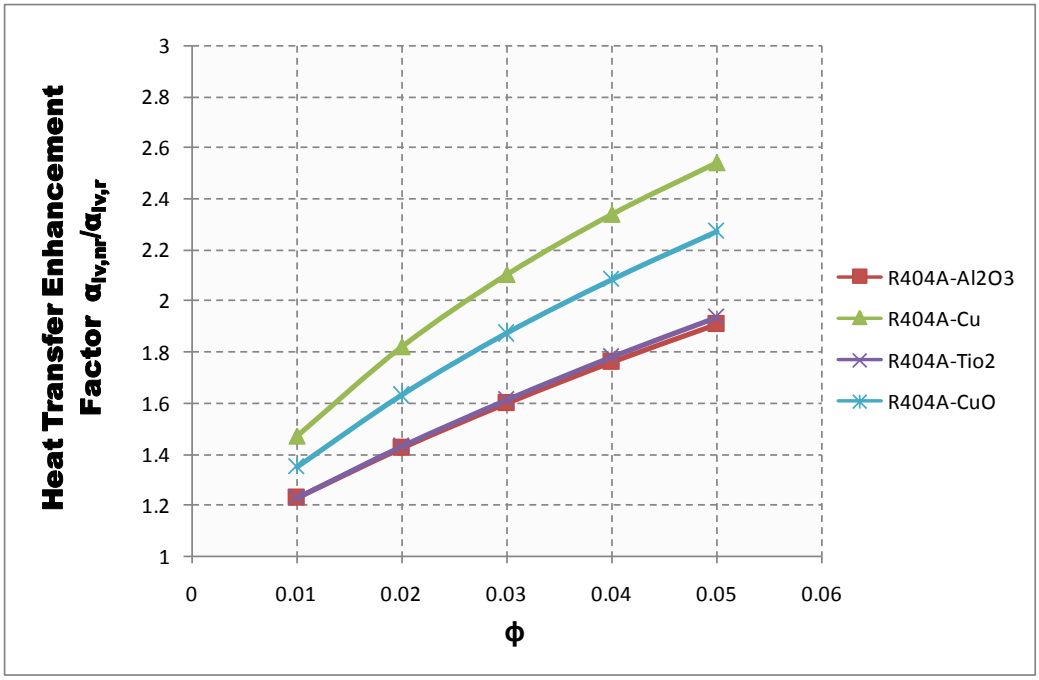

Fig.5.35 Variation of Heat transfer Enhancement Factor with volume fraction (ϕ) of R404A using different nanoparticles

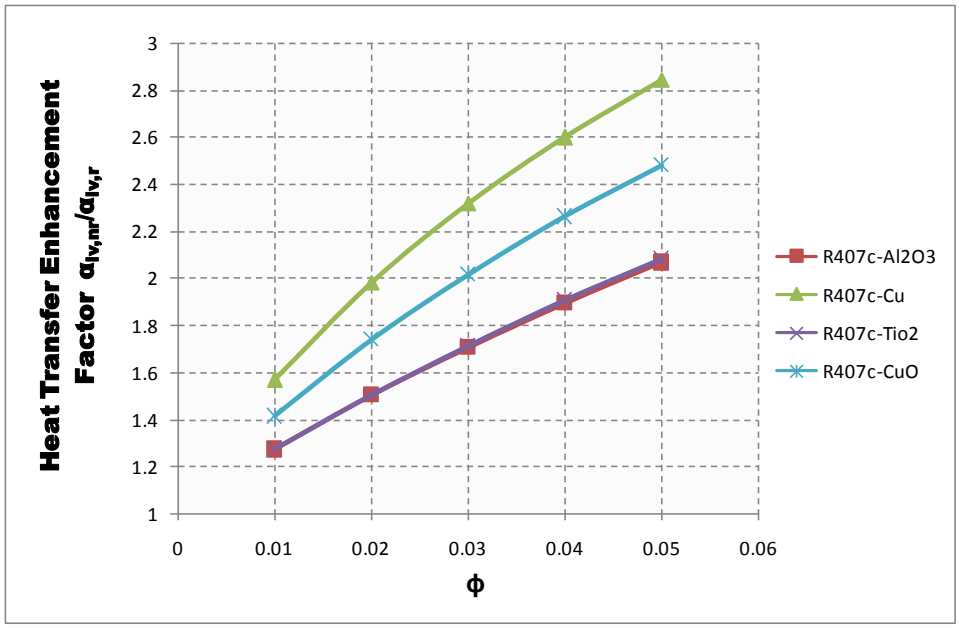

Fig.5.36 Variation of Heat transfer Enhancement Factor with volume fraction (ϕ) of R407c using different nanoparticles

Fig 5.34 to Fig. 5.36 show the heat transfer enhancement factor of nanorefrigerant with different nanoparticle its value ranges from 1.2 to 3.2. As it can be seen that R134 a with cu nanoparticle have highest EF approx 3.2 at 5 vol %. EF increases with increasing vol %.

5.4.2(b) Effect of nanoparticle volume fraction (ϕ) on the 1st law of thermodynamics (C.O.P.) of VCRS

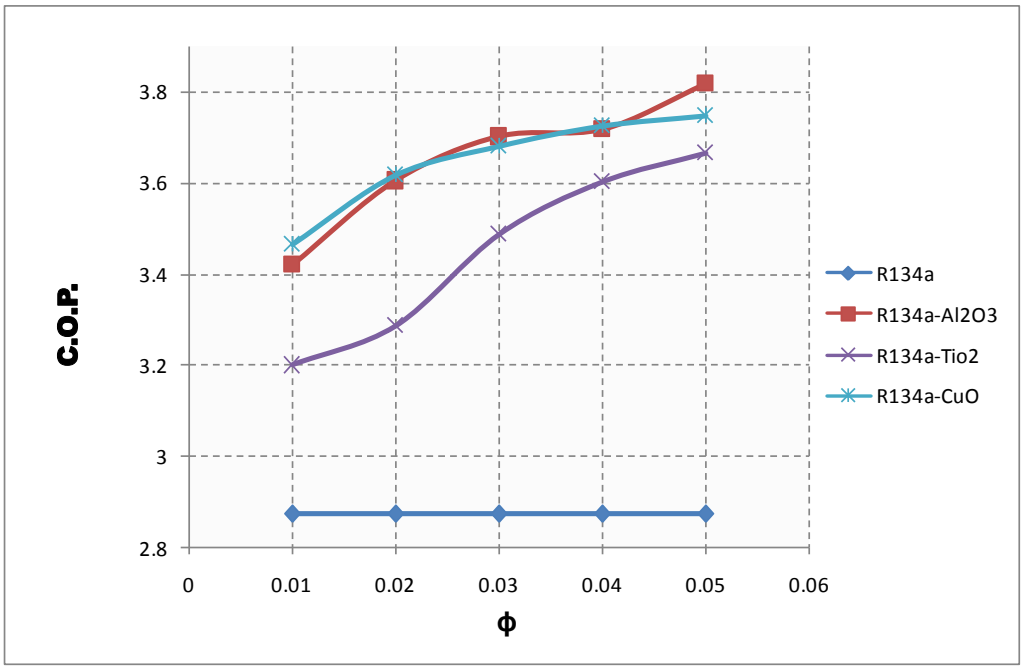

Fig.5.37 Variation of C.O.P with volume fraction (ϕ) of VCRS with R134a using different nanoparticles

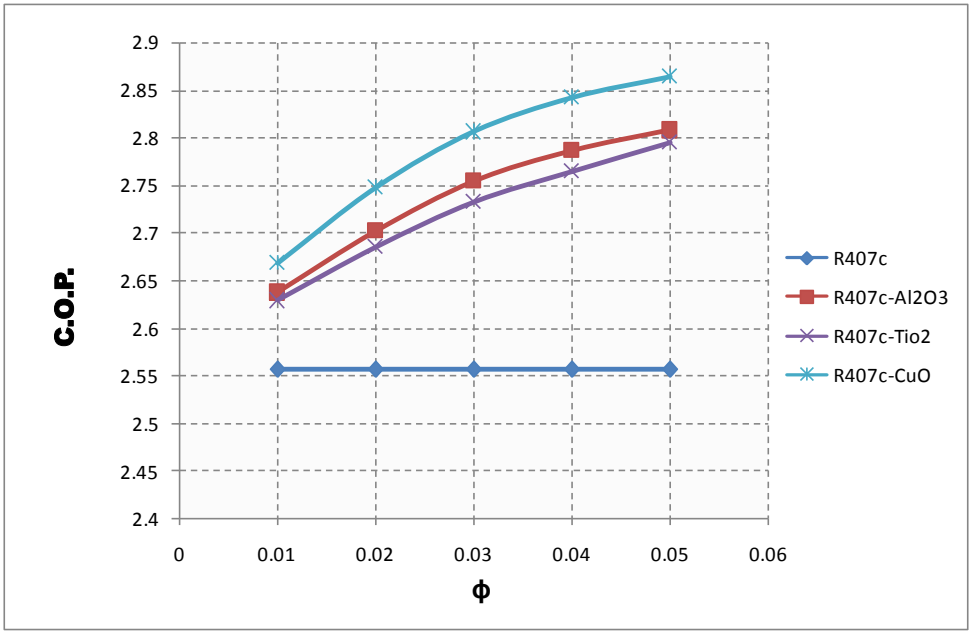

Fig.5.38 Variation of C.O.P with volume fraction (ϕ) of VCRS with R407c using different nanoparticles

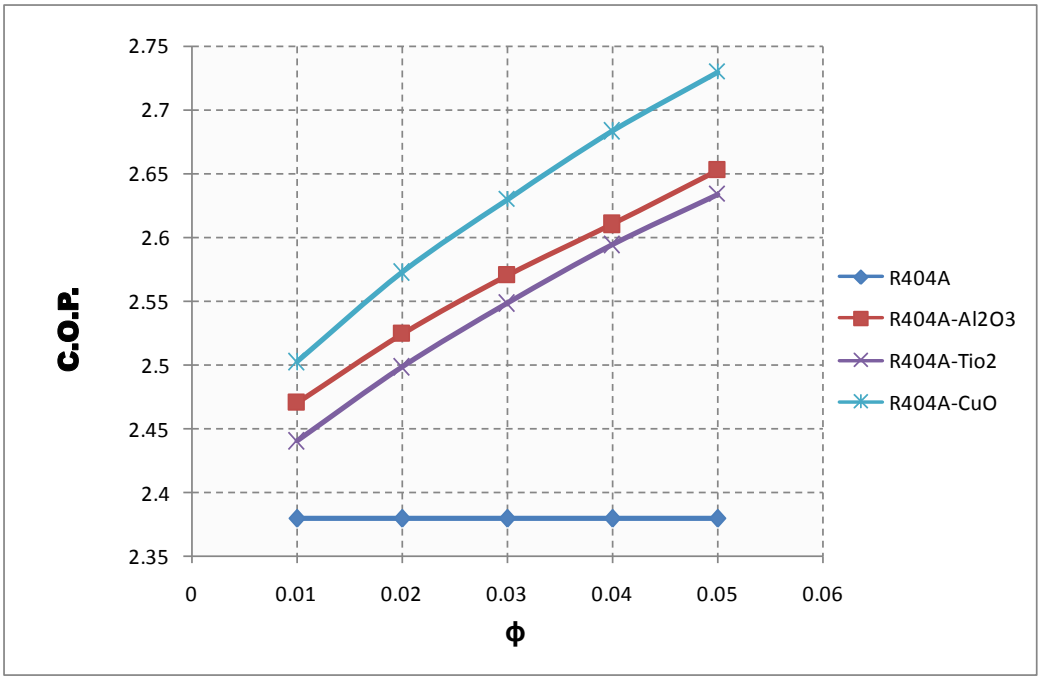

Fig.5.39 Variation of C.O.P with volume fraction (ϕ) of VCRS with R404A using different nanoparticles

Fig 5.37 to Fig 5.39 shows that 1st law of thermodynamics enhancement of VCRS can be achieved by using nanorefrigerant as a working fluid in VCRS. Fig show that the maximum enhancement theoretically achieved about 35 % with combination of R134a with Al_2O_3 nanoparticle at 5 vol % based nanorefrigerant. C.O.P. enhancements of VCRS with different combination of nanorefrigerant are given in table 5.7 below.

Refrigerant		R134a		R404A		R407c	
Nanoparticle	Volume Fraction (ϕ)	C.O.P.	% Enhancement	C.O.P.	% Enhancement	C.O.P.	% Enhancement
	0	2.82	-	2.379	-	2.556	-
Al2O3	0.01	3.421	21.3%	2.47	3.8%	2.637	3.2%
	0.02	3.604	27.8%	2.524	6.1%	2.702	5.7%
	0.03	3.701	31.2%	2.536	6.6%	2.755	7.8%
	0.04	3.717	31.8%	2.558	7.5%	2.787	9.0%
	0.05	3.817	35.4%	2.653	11.5%	2.808	9.9%
Tio2	0.01	3.287	16.6%	2.44	2.6%	2.629	2.9%
	0.02	3.488	23.7%	2.498	5.0%	2.685	5.0%
	0.03	3.603	27.8%	2.548	7.1%	2.733	6.9%
	0.04	3.666	30.0%	2.594	9.0%	2.765	8.2%
	0.05	3.691	30.9%	2.634	10.7%	2.795	9.4%
CuO	0.01	3.464	22.8%	2.502	5.2%	2.669	4.4%
	0.02	3.616	28.2%	2.572	8.1%	2.748	7.5%
	0.03	3.681	30.5%	2.63	10.6%	2.806	9.8%
	0.04	3.725	32.1%	2.683	12.8%	2.842	11.2%
	0.05	3.748	32.9%	2.73	14.8%	2.864	12.1%

Table 5.7 Show Enhancement in C.O.P using different nanorefrigerant of VCRS

5.4.2(c) Effect of nanoparticle volume fraction (ϕ) on the Exergy destruction ratio of VCRS

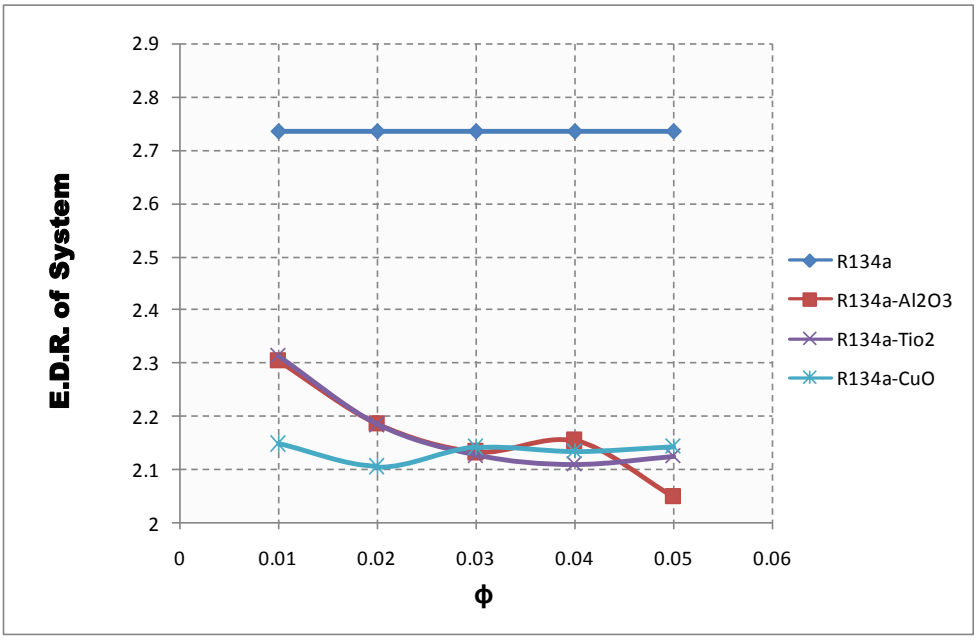

Fig.5.40 Variation of Exergy destruction ratio with volume fraction (ϕ) of VCRS with R134a using different nanoparticles

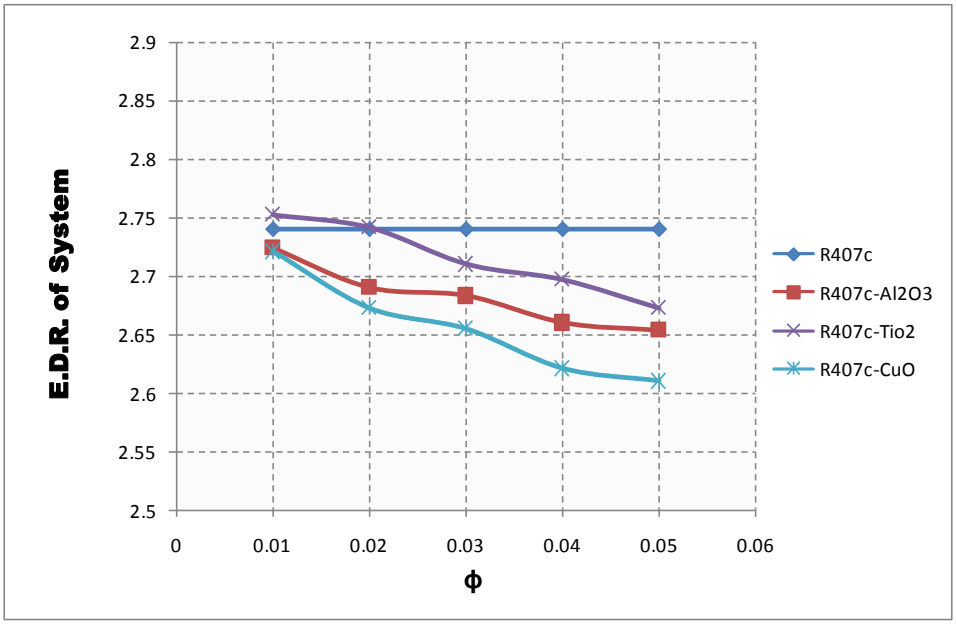

Fig.5.41 Variation of Exergy Destruction ratio with volume fraction (ϕ) of VCRS with R407c using different nanoparticles

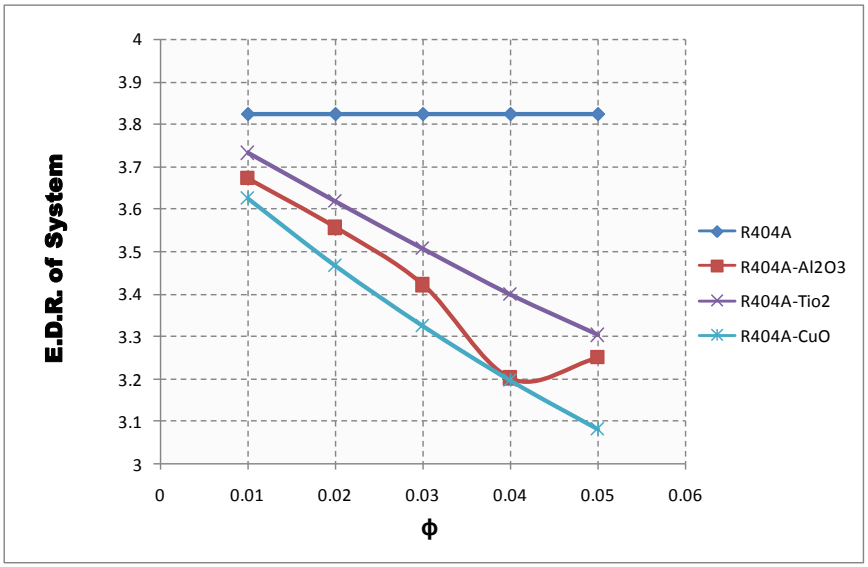

Fig.5.42 Variation of Exergy destruction ratio with volume fraction (ϕ) of VCRS with R404A using different nanoparticles

Fig 5.40 to Fig 5.42 shows that the E.D Ratio of VCRS will reduce by using nanofluid (nanoparticle based nanorefrigerant)

5.4.2(d) Effect of nanoparticle volume fraction (ϕ) on the 2nd law efficiency of VCRS

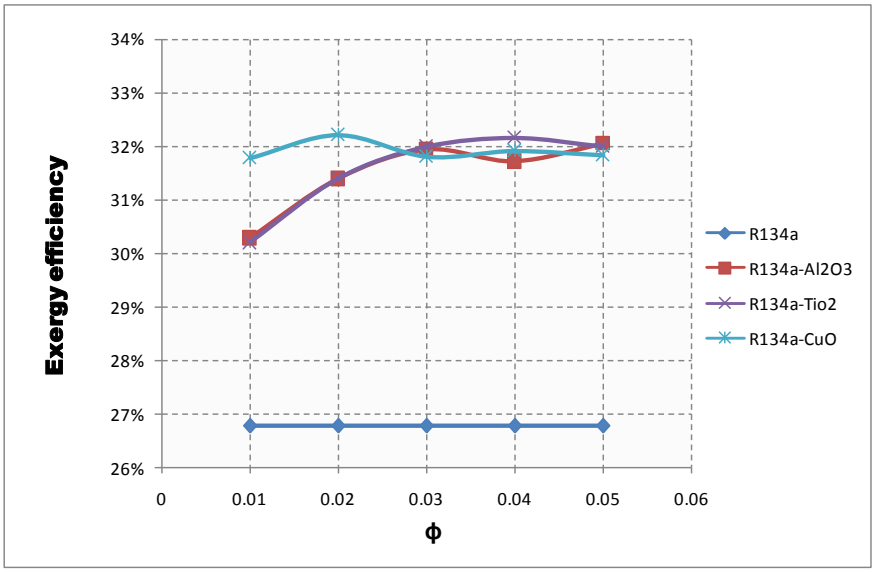

Fig.5.43 Variation of Exergy Efficiency with volume fraction (ϕ) of VCRS with R134a using different nanoparticles

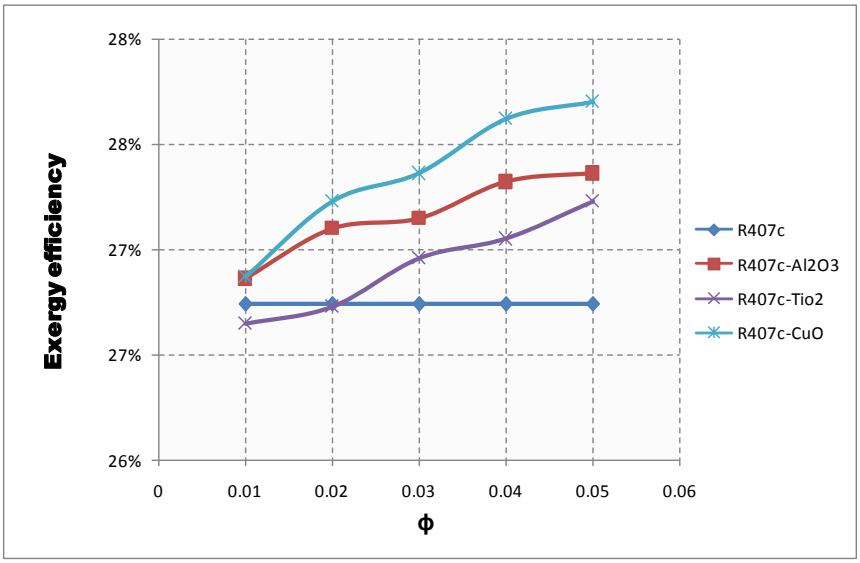

Fig.5.44 Variation of Exergy Efficiency with volume fraction (ϕ) of VCRS with R407c using different nanoparticles

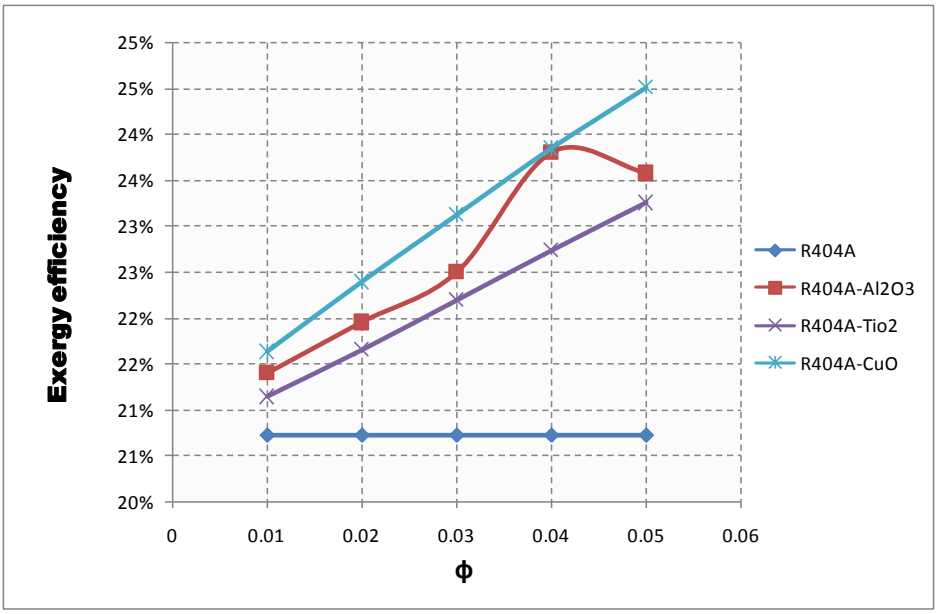

Fig.5.45 Variation of Exergy Efficiency with volume fraction (ϕ) of VCRS with R404A using different nanoparticles

Fig 5.43 to Fig 5.45 shows that 2nd Law efficiency will increase by using nanorefrigerant.

It can seen that the 2nd law efficiency of vapour compression refrigeration system using nanorefrigerant R134a/CuO is much higher than the other nanorefrigerant having value approx 32%.

5.5 Theoretical result of Nanofluid

A computational program has been developed to solve non linear equation of vapour compression refrigeration cycle for case (ii) mentioned in abstract. Considering same geometric parameter of the VCRS model theoretical analysis has been done using EES software for nanofluid (nanoparticle mixed with R718) flowing in secondary circuit and eco friendly refrigerant in primary circuit of VCRS and results are given below.

For Al_2O_3 at 5 vol %		
Refrigerant	C.O.P.	Improvement C.O.P.
R134a	3.406	17.98%
R404A	3.0635	16.00%
R407c	3.110488	17.20%
R-152a	3.4102	18.00%
R-600	3.3402	17.20%
R-600a	3.466	19.90%
R-125	3.033016	14.80%
R-290	3.54312	19.70%

Table 5.8 Show Enhancement in C.O.P using Al_2O_3 at 5 vol % nanofluid in secondary circuit

CHAPTER 6

CONCLUSION & FUTURE SCOPE OF WORK

6.1Conclusions

The research work presented in this thesis work following conclusion have been drawn.

1. Use of nanoparticles enhances thermal performance of vapour compression refrigeration system from 8 to 35 % using nanorefrigerant in primary circuit
2. Use of nanoparticles enhances the thermal performance of vapour compression refrigeration system from 7 to 19 % using nanofluid in secondary circuit.
3. Maximum enhancement in performance was observed using R134a/Al_2O_3 nanorefrigerant in primary circuit and water in secondary circuit of VCRS.
4. Lowest enhancement in performance was observed using R404Aa/TiO_2 nanorefrigerant in primary circuit and water in secondary circuit of VCRS.

6.2 Future Scope Of Work

1. Exergo economics to be done for vapour compression refrigeration system.
2. The proposed system model should be commercialized.

CHAPTER 7

REFERENCES

[1] Choi, S. U. S. (1995). Enhancing thermal conductivity of fluids with nanoparticles, in *Developments and Applications of Non-Newtonian Flows* D. A. Singer and H. P Wang, Eds., American Society of Mechanical Engineers, New York, FED–31/MD-66:99–105.

[2] Maxwell, J. C. (1873). *Treatise on Electricity and Magnetism*. Clarendon Press, Oxford.

[3] Kimoto, K., Y. Kamilaya, M. Nonoyama, and R. Uyeda (1963). An electron microscope study on fine metal particles prepared by evaporation in argon gas at low pressure, *Jpn. J. Appl. Phys.*, 2: 702.

[4] Jwo et.al, (2009) Effect of nano lubricant on the performance of Hydrocarbon refrigerant system. J. Vac. Sci. Techno. B, Vol.27, No. 3, pp. 1473-1477

[5] Hao Peng et.al., (2010) Nucleate pool boiling heat transfer characteristics of refrigerant/oil mixture with diamond nano parti cles. International Journal of Refrigeration, Vol.33, pp. 347-358.

[6] Henderson et al. (2010) Experimental analysis on the flow boiling heat transfer of R134a based nanofluids in a horizontal tube. IJHMT , Vol. 53, pp. 944-951.

[7] Bobbo S. et.al, (2010) Influence of nanoparticles dispersion in POE oils on lubricity and R134a solubility. International Journal of Refrigeration, Vol.33, pp. 1180-1186.

[8] Shengshan Bi, Performance of a Domestic Refrigerator using TiO2-R600a nano-refrigerant as working fluid, Int J of Energy Conservation and Management, Vol. 52, 2011, 733-737.

[9] Lee K, Hwang YJ, Cheong S, Kwon L, Kim S, Lee J. Performance evaluation of nano-lubricants of fullerene nanoparticles in refrigeration mineral oil. Current Applied Phys 2009; 9:128–31.

[10] Wang RX, Xie HB. A refrigerating system using HFC134a and mineral lubricant appended with N- TiO_2 (R) as working Fluids. In: Proceedings of the 4th international symposium on HAVC, Tsinghua University; 2003.

[11] S.Z. Heris, S.G. Etemad, M.N. Esfahany, Experimental investigation of oxide nanofluids laminar flow convective heat transfer, Int. Commun. Heat and Mass Transfer. 33 (2006) 529535.

[12] Y. He, Y. Jin, H. Chen, Y. Ding, D. Cang, H. Lu, Heat transfer and flow behavior of aqueous suspensions of TiO_2 nanoparticles (nanofluids) flowing upward through a vertical pipe, Int. J. Heat Mass Transf. 50 (2007) 2272-2281.

[13] D.P. Kulkarni, P.K. Namburu, H.E. Bargar, D.K. Das, Convective heat transfer and fluid dynamic characteristics of SiO2-ethylene glycol/water nanofluid, Heat Transf. Eng. 29 (12) (2008) 1027-1035.

[14] K.S. Hwang, S.P. Jang, S. U. S. Choi, Flow and convective heat transfer characteristics of water-based Al_2O_3 nanofluids in fully developed laminar flow regime, Int. J. Heat Mass Transf. 52 (2009) 193-199.

[15] A. Sharma, S. Chakraborty, Semi-analytical solution of the extended Graetz problem for combined electro osmotically and pressure-driven microchannel flows with stepchange in wall temperature, Int. J. Heat Mass Transf. 51 (2008) 4875-4885.

[16] W. Yu, D.M. France, D.S. Smith, D. Singh, E.V. Timofeeva, J.L. Routbort, Heat transfer to a silicon carbide/water nanofluid, Int. J. Heat Mass Transf 52 (2009) 3606-3612.

[17] S.Torii, W.J. Yang, Heat transfer augmentation of aqueous suspensions of nanodiamonds in turbulent pipe flow, J. Heat Transf. 131 (2009) 043203-1 - 043203-5.

[18] U. Rea, T. McKrell, L.W. Hu, J. Buongiorno, Laminar convective heat transfer and viscous pressure loss of alumina-water and zirconia-water nanofluids, Int. J. Heat Mass Transf. 52 (2009) 2042-2048.

[19] Murshed S. M. S., K. C. Leong, and C. Yang (2005). Enhanced thermal conductivity of TiO_2-water based nanofluids, *Int. J. Therm. Sci.*, 44: 367–373.

[20] Hamilton, R. L., and O. K. Crosser (1962). Thermal conductivity of heterogeneous two component systems, *I & EC Fundam.*, 1(3): 187–191

[21] Xuan, Y., and Q. Li (2003). Investigation on convective heat transfer and flow features of nanofluids, *J. Heat Transfer*, 125: 151–155.

[22] I.M. Mahbubul , A.Saadah Thermal performance analysis of Al_2O_3 R134a nanorefrigerant , international journal of heat and mass transfer 85 (2015) 1034-1040

[23] Faulkner, D. J., D. R. Rector, J. J. Davidson, and R. Shekarriz (2004). Enhanced heat transfer through the use of nanofluids in forced convection, Paper IMECE2004-

62147, presented at the 2004 ASME International Mechanical Engineering Congress and RD&D Expo, Anaheim, CA, Nov. 13–19.

[24] Wen, D., and Y. Ding (2004). Experimental investigation into convective heat transfer of nanofluids at the entrance region under laminar flow conditions, *Int. J. Heat Mass Transfer*, 47: 5181–5188.

[25]. Lee K, Hwang YJ, Cheong S, Kwon L, Kim S, Lee J. Performance evaluation of nano-lubricants of fullerene nanoparticles in refrigeration mineral oil. Current Applied Phys 2009; 9:128–31.

[26] Joaquin Navarro, Francisco, Angel, 2013. Experimental analysis of internal heat exchanger influence on vapour compression system performance working with R1234yf as drop in replacement of R134a. Applied thermal Engineering, 59, 153-161.

[27] A. Zukauskas, Heat transfer from tubes in cross flow, Advances in Heat Transfer, vol. 8, A Press, New York, 1972.

[28] J.C. Chen, Correlation for boiling heat transfer to saturated fluids in convective flow, I and EC Process Designs 5 (1966) 322–329.

[29] K.stephan, M. Abdelsalam, Heat transfer correlation for forced convection boiling , Heat and mass transfer 23 (1) 1980 73-87

[30] F.W. Dittus, L.M.K. Boelter, Publications on Engineering, vol. 2, University of California, Berkeley, 1930. p. 443.

[31] C. Sitprasert , P.Dechaumphai , A thermal conductivity model for nanofluid including effect of temperature –dependent interfacial layer, Res 11 (6) (2009) 1465-1476

[32] H. Brinkman, The viscosity of concentrated suspensions and solution J chem. Physics 20 (1952).

[33] B.C. Pak , Y.I.Cho, hydrodynamics and heat transfer study of dispersed fluid with submicron metallic oxide particle Exp. Heat transfer 11 (2) (1998) 151-170

[34] Hamilton, R.L., Crosser, O.K., 1962. Thermal conductivity of heterogeneous two-component systems. Industrial and Engineering *Chemistry Fundamentals*, Vol. 1, No. 3, pp. 187–191.

[35] Jensen, M.K., Jackman, D.L., 1984. Prediction of nucleate pool boiling heat transfer coefficients of refrigerant–oil mixtures. *Journal of Heat Transfer*, Vol. 106, pp. 184–190.

[36] Kedzierski, M.A., Kaul, M.P., (1993). Horizontal nucleate flow boiling heat transfer coefficient measurements and visual observations for R12, R134a, and R134a/ester lubricant mixtures. In: *Proceedings of the 6th International Symposium on Transport Phenomena in Thermal Engineering*, Vol. 1, pp. 111–116

[37] Baustian, J.J., Pate, M.B., Bergles, A.E., (1988). Measuring the concentration of a flowing oil–refrigerant mixture: instrument test facility and initial results. *ASHRAE Transactions*, Vol. 94, No. 1, pp167–177.